

Spring 4-2018

## Global Formulation and Control of a Class of Nonholonomic Systems

Muhammad Rehan  
*Embry-Riddle Aeronautical University*

Follow this and additional works at: <https://commons.erau.edu/edt>



Part of the [Engineering Commons](#), and the [Physics Commons](#)

---

### Scholarly Commons Citation

Rehan, Muhammad, "Global Formulation and Control of a Class of Nonholonomic Systems" (2018).  
*Doctoral Dissertations and Master's Theses*. 401.  
<https://commons.erau.edu/edt/401>

This Dissertation - Open Access is brought to you for free and open access by Scholarly Commons. It has been accepted for inclusion in Doctoral Dissertations and Master's Theses by an authorized administrator of Scholarly Commons. For more information, please contact [commons@erau.edu](mailto:commons@erau.edu).

**GLOBAL FORMULATION AND CONTROL OF A CLASS OF  
NONHOLONOMIC SYSTEMS**

By

Muhammad Rehan

A Dissertation submitted in Partial Fulfillment of the Requirements for the Degree  
of  
Doctor of Philosophy in Engineering Physics

Embry-Riddle Aeronautical University

Department of Physical Sciences

Daytona Beach, FL 32114

April 13th, 2018

Copyright by Muhammad Rehan 2018

All Rights Reserved

GLOBAL FORMULATION AND CONTROL OF A CLASS OF  
NONHOLONOMIC SYSTEMS


By


Muhammad Rehan


This Dissertation was prepared under the direction of the candidate's Dissertation Committee Chair, Dr. Mahmut Reyhanoglu and has been approved by the members of the Dissertation committee. It was submitted to the College of Arts and Sciences and was accepted in partial fulfillment of the requirements for the


Degree of  
Doctor of Philosophy in Engineering Physics

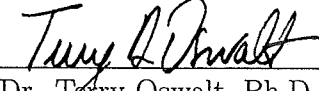
  
Mahmut Reyhanoglu, Ph.D  
Committee Chair


  
Dr. William MacKunis, Ph.D  
Committee Member


  
Dr. Yechiel Crispin, Ph.D  
Committee Member

  
Dr. John Hughes, Ph.D  
Committee Member

  
Dr. Matthew Zettergren  
EP Graduate Program Coordinator

  
Dr. Terry Oswalt, Ph.D  
Department Chair, Physical Sciences

  
Dr. Michael Hickey, Ph.D  
Dean of Research and Graduate Studies

  
Dr. Karen Frances Gaines, Ph.D  
Dean, College of Arts and Sciences

\_\_\_\_\_  
Date

## Acknowledgments

I am grateful to my advisor, Dr. Mahmut Reyhanoglu, for his generous support, technical insight, academic guidance and instruction throughout my doctoral study. I would also like to thank Dr. William MacKunis for the passion and enthusiasm he showed in both teaching and research. I also want to say thanks to all of my friends especially Derek Hoffman, Krishna Bhavithavya and Natalie Ramos Pedroza, whose company made every moment memorable.

I am also thankful to Physical Science Department for the support provided for my course work and research. I also want to acknowledge supportive role of the administrative staff at physical science department especially Donna Fermont and Susan Adams, who helped me with all possible means as and when needed.

I have no words to say thanks to my parents whose love, inspiration and prayers helped me in accomplishing one of important milestone of my life. I am also grateful to my siblings who supported me in the best possible way with immense love and affection .

I am really thankful to my wife, Sadia, for her lovely support and understanding that made my work very pleasant and enjoyable. I can't express intensity of the love that I have for my kids Hamza and Haadiya and the time I spent with them is one of the best moments of my life. I wish them a healthy and successful life ahead and hope that they will do something special in their life that will benefit humanity.

# Contents

<b>Acknowledgements</b>	<b>vi</b>
<b>Abstract</b>	<b>vii</b>
<b>1 Introduction</b>	<b>1</b>
<b>2 Mathematical Background</b>	<b>4</b>
2.1 Vectors and matrices . . . . .	4
2.2 Vector spaces . . . . .	4
2.3 Vector operations . . . . .	5
2.4 Continuously differentiable function . . . . .	5
2.5 Embedded manifold . . . . .	6
2.6 Tangent space and tangent bundle . . . . .	6
2.7 Orthogonal matrices . . . . .	7
2.8 Homogeneous matrices . . . . .	7
2.9 Lie bracket and it's properties . . . . .	8
2.9.1 Lie algebra . . . . .	9
2.10 Controllability and accessibility . . . . .	10
2.10.1 Controllability . . . . .	10
2.10.2 Accessibility . . . . .	11
<b>3 Knife-edge Moving on a Smooth Surface</b>	<b>15</b>
3.1 Introduction . . . . .	15
3.2 Kinematics of a knife-edge . . . . .	17
3.3 Controllability and motion planning for the knife-edge kinematics . .	20
3.4 Knife-edge moving on a flat plane . . . . .	21
3.4.1 Motion planning . . . . .	22
3.4.2 An example controlled maneuver . . . . .	24
3.5 Knife-edge moving on the surface of a sphere . . . . .	24
3.5.1 Control equations and controllability . . . . .	26
3.5.2 Motion planning . . . . .	27
3.5.3 An example controlled maneuver . . . . .	29
3.6 Knife-edge moving on the surface of a hyperboloid . . . . .	32

3.6.1	Motion planning . . . . .	32
3.6.2	Simulation . . . . .	35
3.7	Knife-edge moving on the surface of a torus . . . . .	37
3.7.1	Motion planning . . . . .	38
3.7.2	Simulation . . . . .	40
3.8	Conclusions and extensions . . . . .	43
<b>4</b>	<b>Control of Rolling Disk Motion on an Arbitrary Smooth Surface</b>	<b>44</b>
4.1	Introduction . . . . .	44
4.2	Dynamics of a rolling disk . . . . .	45
4.3	Controllability and motion planning . . . . .	48
4.4	Disk rolling on a flat surface . . . . .	49
4.4.1	Controllability . . . . .	51
4.4.2	Motion planning . . . . .	51
4.4.3	An example controlled maneuver . . . . .	52
4.5	Disk rolling on a spherical surface . . . . .	54
4.5.1	Controllability . . . . .	55
4.5.2	Motion planning . . . . .	56
4.5.3	An example controlled maneuver . . . . .	56
4.6	Conclusions . . . . .	59
<b>5</b>	<b>Global Formulation and Motion Planning for a Sphere Rolling on a Smooth Surface</b>	<b>60</b>
5.1	Introduction . . . . .	60
5.2	Kinematics of a sphere rolling on a smooth surface . . . . .	62
5.3	Sphere rolling on a flat plane . . . . .	64
5.3.1	Motion planning . . . . .	65
5.3.2	An example controlled maneuver . . . . .	68
5.4	Kinematics of a sphere rolling on a stationary sphere . . . . .	69
5.4.1	Motion planning . . . . .	72
5.4.2	An example controlled maneuver . . . . .	75
5.5	Conclusion and future work . . . . .	77

## Abstract

This thesis study motion of a class of non-holonomic systems using geometric mechanics, that provide us an efficient way to formulate and analyze the dynamics and their temporal evolution on the configuration manifold. The kinematics equations of the system, viewed as a rigid body, are constrained by the requirement that the system maintain contact with the surface. They describe the constrained translation of the point of contact on the surface. In this thesis, we have considered three different examples with nonholonomic constraint i-e knife edge or pizza cutter, a circular disk rolling without slipping, and rolling sphere. For each example, the kinematics equations of the system are defined without the use of local coordinates, such that the model is globally defined on the manifold without singularities or ambiguities. Simulation results are included that show effectiveness of the proposed control laws.



# List of Figures

2.1	Commutative iff $[f,g]=0$ . . . . .	9
2.2	A Lie bracket motion. . . . .	14
3.1	A moving frame for a knife edge on a smooth surface in $\mathbb{R}^3$ . . . . .	17
3.2	Position of the knife edge moving on a flat surface. . . . .	25
3.3	Direction of the knife edge moving on a flat surface. . . . .	25
3.4	Control effort for the knife edge moving on a flat surface. . . . .	26
3.5	Position of the knife edge moving on a flat surface. . . . .	30
3.6	Direction of the knife edge moving on a flat surface. . . . .	31
3.7	Control effort for the knife edge moving on a flat surface. . . . .	31
3.8	Hyperboloid as a ruled surface. . . . .	33
3.9	Knife-edge trajectory. . . . .	35
3.10	Time response of $x$ . . . . .	36
3.11	Time response of $\gamma$ . . . . .	36
3.12	Time responses of $V$ and $\omega$ . . . . .	37
3.13	The trajectory of the knife edge. . . . .	41
3.14	Position $x$ . . . . .	41
3.15	Direction vectors $\gamma$ and $\sigma$ . . . . .	42
3.16	Speed $V$ and turn rate $\omega$ . . . . .	42
4.1	Disk rolling on a smooth surface. . . . .	47
4.2	Rolling in the direction of $\gamma$ . . . . .	50
4.3	Steering about the surface normal $n$ . . . . .	50
4.4	Position $x$ (flat surface case). . . . .	53
4.5	Vectors $\gamma$ and $\sigma$ (flat surface case). . . . .	53
4.6	Controls $(u_1, u_2)$ and angular velocities $(\omega_r, \omega_s)$ (flat surface case). . . . .	54
4.7	Disk rolling on a spherical surface. . . . .	55
4.8	Position $x$ (spherical surface case). . . . .	57
4.9	Vectors $\gamma$ and $\sigma$ (spherical surface case). . . . .	58
4.10	Controls $(u_1, u_2)$ and angular velocities $(\omega_r, \omega_s)$ (spherical surface case). . . . .	58
5.1	Sphere rolling on a flat surface. . . . .	64
5.2	Slip maneuver; the position changes but the attitude remains the same. . . . .	66
5.3	Twist maneuver; the attitude changes but the position remains the same. . . . .	66

5.4	Position $x$ (flat surface case). . . . .	69
5.5	Controls $\omega_1$ and $\omega_2$ (flat surface case). . . . .	70
5.6	The path of the contact point of the rolling sphere (flat surface case). . . . .	70
5.7	Sphere rolling on a stationary sphere. . . . .	71
5.8	Position $x$ (spherical surface case). . . . .	75
5.9	Basis vectors of the actuation plane (spherical surface case). . . . .	76
5.10	Controls $\omega_1$ and $\omega_2$ (spherical surface case). . . . .	76
5.11	The path of the contact point of the rolling sphere (spherical surface case). . . . .	77

# List of Tables

# Chapter 1

## Introduction

The robots are becoming more intelligent than ever and they are capable of performing tasks with great accuracy and speed. There is a growing use robots in industrial applications, space robotics and medical science. For example, a mobile robot can move very precisely over the surface of asteroids and collect a sample of the material. Similarly, now a days, intelligent machines are able to perform robotic surgeries and they offer several advantages including greater precision in tissue cutting, lesser time, improved reproducibility and ultimately better comfort for the patients. In addition to that, the doctors have access to the high definition images of the patient in real time and so that they can monitor the robotic surgeries remotely. The design of a robotic system is proposed in (Ebrahimi et al, 2015) that is capable of performing ophthalmic surgeries.

Depending upon the mechanical design of the robot, the system may have motion constraints. We can categorize these constraints into two types. The first type is holonomic constraints, that arise from configuration and allow motion with physical restrictions. For example, a particle constrained to lie on a plane or a particle suspended from a taut string in three dimensional space. The holonomic constraints are integrable and such system can be characterized by a smaller number of generalized coordinates. The second type of constraints are nonholonomic constraints. Such constraints are non-integrable and it is impossible to reduce number of generalized coordinates. In this thesis, we have considered kinematics of three basic nonholonomic systems including motion of knife edge, rolling disk and a sphere rolling on an arbitrary smooth surface.

The knife-edge is assumed to have a single point of contact with the friction-less surface such that its velocity vector always lies in the tangent plane at the point of contact and the normal vector of the tangent plane is always aligned with the axis of the knife-edge. The knife-edge can turn around its axis at the point of contact or it can slide only in the direction of the velocity vector. Then we talked about nonholonomic motion of disk rolling on an arbitrary smooth surface. A thin uniform circular disk is considered as a rigid body that can roll on a the surface without slipping. The disk remains upright during the motion and can be steered about the

surface normal. The problem has a large number of application in wheeled mobile robotics, for example, precise motion control of a unicycle/bicycle/cars on an arbitrary smooth surface. Furthermore, we also studied the kinematics of a sphere rolling on a smooth surface, without slipping or twisting. The problem is mostly discussed in literature as Chaplygin's sphere after the name of Sergey A. Chaplygin. The velocity of rolling sphere on a smooth surface, always lie in the tangent space at the given position.

Nonholonomic system can be transformed from one state to another state but the final state always depends on the path taken by the system between the two states. For example if we roll the ball on flat surface between an initial and final position using different paths, the attitude of the ball at the final position may differ for different paths. Similarly, if the ball is rolled in different closed path trajectories, every time the ball will reach back to the starting point and it may have different orientation. Therefore, control of both position and attitude, for such systems, is a challenging task.

The literature on such nonholonomic control problems is large, both in terms of theoretical results and studies of specific physical examples in the context of robot manipulation, mobile robots, wheeled vehicles, and space robotics. An excellent reference that provides a geometric and control theoretical view of nonholonomic systems is the book by (Bloch, 2003). A few representative control works include the study of controllability and stabilizability in (Bloch et al, 1992, 1991); motion planning in (Murray et al, 1994; Reyhanoglu, 1994); and feedback stabilization and tracking in (Astolfi, 1996; Jiang et al, 1999, 1995; Sordalen et al, 1995). All of this literature is based on the use of mathematical models, most often arising from principles of mechanics and geometry, that are expressed in terms of local coordinates for the configuration vector. This use of local coordinates is a significant limitation in some physical examples, where non-local or even global results are desired. Our formulation in this thesis considers arbitrary smooth manifolds embedded in  $\mathbb{R}^3$ . We view the knife-edge as a rigid body but our formulation differs from the formulations using Lie group manifolds see e.g., (Leonard et al, 1995; Morin et al, 2003) and references therein.

Similarly, nonholonomic motion of the rolling sphere is explained in (Johnson, 2007). Geometric aspects for the control of position and orientation of the sphere rolling on a plane is discussed in (Bicchi et al, 1995). The dynamics of a spherical robot are discussed in (Camicia et al, 2000), wherein a linear control law for the longitudinal dynamics of the robot is proposed. In (Murray et al, 1993), steering of nonholonomic systems using sinusoids is discussed. The rolling motion of a homogeneous ball on an arbitrary surface is studied in (Borisov et al, 2002). In (Shen et al, 2008), internal rotors and sliders are proposed as the mechanism for the control of spherical robots. The work in (Morin et al, 2008) considers a rolling sphere actuated by a moving plate and develops a control algorithm for the stabilization of admissible reference trajectories. In (Borisov et al, 2012), dynamics and control of a non-symmetric sphere (with rotors) on a plane are discussed and the controllability for the system is shown.

Moreover, the influence of rolling friction on the control of the sphere is discussed. The work in (Muralidharan et al, 2015) derives the dynamics of a spherical robot on a plane in a geometric framework and studies strong accessibility and small-time local controllability for the system. A smooth global tracking controller is proposed for the position trajectories. In (Kleinstauber et al, 2006), the motion of the rolling sphere on a flat plane is studied and the ideas of slip and twist maneuvers are presented. In the slip maneuver, the sphere moves from a given position to the desired position without changing the attitude. While in the twist maneuver, the sphere rolls in a closed path trajectory to produce a desired twist about the surface normal.

These problems are widely studied but mostly the formulation is done with local coordinates using principles of mechanics and geometry. The use of local coordinates has significant limitation in some physical examples, where nonlocal or even global results are desired. The formulation for the same problems considers arbitrary smooth manifolds embedded in  $\mathbb{R}^3$ .

Control of nonholonomic systems can be accomplished using open loop control and the system can be steered from any initial configuration to any prescribed configuration. The motion planning solely uses kinematics of the system. Although, a feedback control can be designed for a nonholonomic system, but due to the fundamental restriction which prohibits existence of continuous state feedback controller. However, a discontinuous feedback control law can be designed that can stabilize a prescribed configuration. Discontinuous feedback control law for the nonholonomic systems have been proposed in (Bloch et al, 1992, 1991).

In this thesis, we are interested to study of nonholonomic systems subjected to motion constraints. First we need to formulate kinematics/dynamics of the systems without any use of local coordinates, so that the mathematical model remains valid everywhere on the configuration manifold and have no singularities or ambiguities. And later, comments are made for the motion planning of the nonholonomic systems on a variety of smooth surfaces like flat plane, sphere, hyperboloid and torus. The geometric mechanics provide us an efficient way to formulate and analyze the dynamics and their temporal evolution on the configuration manifold.

# Chapter 2

## Mathematical Background

We summarize the mathematical background that is used subsequent sections. Important results in linear algebra are introduced for finite dimensional vectors and matrices. A summary is given of manifold concepts and related differential geometric concepts are introduced; a summary of results for embedded manifolds is given. Further mathematical background can be found in Lee et al (2017), where additional details on manifolds are provided.

### 2.1 Vectors and matrices

A vector  $x$  is an  $n$ -tuple of real numbers. Vector addition and scalar multiplication are defined as usual. A matrix  $A$  is an  $n \times m$  ordered array of real numbers. Matrix addition, for compatible matrices, and scalar multiplication are defined as usual. The transpose of a  $n \times m$  matrix  $A$  is an  $m \times n$  matrix, denoted by  $A^T$ , obtained by interchange of the rows and columns. The  $n \times n$  identity matrix is denoted by  $I_{n \times n}$ . The  $n \times m$  zero matrix composed of zero elements is denoted by  $0_{n \times m}$  or more often by  $0$ . Vector spaces in this thesis should be understood as being defined over the real field.

### 2.2 Vector spaces

As usual,  $\mathbb{R}^n$  denotes the set of all ordered  $n$ -tuples of real numbers, with the usual definition of vector addition and scalar multiplication. Thus,  $\mathbb{R}^n$  is a real vector space. Also,  $\mathbb{R}^{n \times m}$  denotes the set of all  $n \times m$  real matrices consisting of  $n$  rows and  $m$  columns. With the usual definition of matrix addition and scalar multiplication of a matrix,  $\mathbb{R}^{n \times m}$  is a real vector space. Unless indicated otherwise, we view an  $n$ -tuple of real numbers as a column vector and we view a matrix as an array of real numbers. The common notions of span, linear independence, basis, and subspace are fundamental. The dimension of a vector space is the number of elements in a basis.

## 2.3 Vector operations

The usual Euclidean inner product or dot product of two vectors  $x, y \in \mathbb{R}^n$  is the real number

$$x \cdot y = x^T y = y^T x,$$

and the Euclidean norm on the real vector space  $\mathbb{R}^n$  is the non-negative real number

$$\|x\| = \sqrt{x^T x}$$

Vectors  $x, y \in \mathbb{R}^n$  that satisfy  $x \cdot y = 0$  are said to be orthogonal or normal.

The skew-symmetric matrix representing the cross product operator on  $\mathbb{R}^3$  given by

$$S(x) = \begin{bmatrix} 0 & -x_3 & x_2 \\ x_3 & 0 & -x_1 \\ -x_2 & x_1 & 0 \end{bmatrix}$$

which satisfy  $S(x)y = x \times y$  and  $S(x)^T = -S(x)$ .

The standard basis vectors in  $\mathbb{R}^n$  are denoted by  $e_1, \dots, e_n$ , where  $e_i \in \mathbb{R}^n$  denotes the n-tuple with 1 in the i-th place and zeros elsewhere. Note that each of the standard basis vectors has unit norm and they are mutually orthogonal, that is, they form a set of orthonormal vectors. In particular, in  $\mathbb{R}^2$  the standard basis vectors are  $e_1 = [1, 0]^T, e_2 = [0, 1]^T$ ; in  $\mathbb{R}^3$  the standard basis vectors are  $e_1 = [1, 0, 0]^T, e_2 = [0, 1, 0]^T, e_3 = [0, 0, 1]^T$ .

We make use of several categories of Euclidean frames. A Euclidean frame may be fixed or stationary with respect to a background in the material world; such frames are said to be inertial. We refer to such frames as fixed frames or inertial frames. In some cases, we introduce Euclidean frames that are attached to a rigid body, that is the frame translates and rotates with the body; such frames are said to be body-fixed frames. In some cases, it is convenient to introduce a reference Euclidean frame that is neither stationary nor body-fixed but is physically meaningful as a reference. In situations where several Euclidean frames are introduced, it is important to maintain their distinction. We do not introduce any special notation that identifies a specific frame or frames, but rather we hope that this is always clear from the context.

## 2.4 Continuously differentiable function

Let  $h : A \rightarrow \mathbb{R}$  be a scalar function defined on an open subset  $A$  of  $\mathbb{R}^n$ . The value of  $h$  at  $x = (x_1, \dots, x_n) \in A$  is denoted by  $h(x) = h(x_1, \dots, x_n)$ . The function  $h$  is called a  $C^k$  ( $k$  times continuously differentiable) function if it possesses continuous partial derivatives of all orders  $\leq k$  on  $A$ . Here  $k \in \mathbb{Z}^+$ , i.e.,  $k$  is a positive integer. If  $h$  is  $C^k$  for all  $k$  then  $h$  is said to be a smooth or  $C^\infty$  function.



## 2.5 Embedded manifold

A differentiable manifold, as a submersion or embedded manifold in  $\mathbb{R}^n$ , is described by

$$M = \{x \in \mathbb{R}^3 : \phi_i(x) = 0, i = 1, \dots, l\}$$

where  $\phi_i : \mathbb{R}^3 \rightarrow \mathbb{R}^1, i = 1, \dots, l$  are scalar differentiable functions with the property that the vectors  $\frac{\partial \phi_i(x)}{\partial x} \neq 0, x \in M, i = 1, \dots, l$  are linearly independent vectors in  $\mathbb{R}^n$  for each  $x \in M$ . Thus, necessarily  $1 \leq l \leq n$ . We say that the manifold  $M$  has dimension  $n - l$  and codimension  $l$ .

For example  $\mathbb{S}^1$  and  $\mathbb{S}^2$  are the unit sphere manifolds embedded in  $\mathbb{R}^2$  and  $\mathbb{R}^3$ , respectively, i.e.

$$\mathbb{S}^1 = \{x \in \mathbb{R}^2 : x^T x = 1\}$$

$$\mathbb{S}^2 = \{x \in \mathbb{R}^3 : x^T x = 1\}$$

Consequently, we can represent a vector in an embedded manifold  $M \subset \mathbb{R}^n$  as a vector in  $\mathbb{R}^n$  so long as the equality conditions defining the embedded manifold are satisfied. Such representations for a point in  $M$  have the geometric advantage that they are global in the sense that they are defined everywhere that the manifold  $M$  is defined.

Manifolds are fundamental to our subsequent development, and subsequent references to a smooth manifold or simply a manifold imply that the manifold is differentiable. A differentiable manifold  $M$  is also assumed to have an inner product, typically the inner product that arises from the finite-dimensional vector space within which it is embedded.

## 2.6 Tangent space and tangent bundle

Tangent space of  $M$  at  $x \in M$  is a subspace of  $\mathbb{R}^n$  that is the set of all tangent vectors to  $M$  at  $x \in M$ . It is denoted as  $T_x M$ . Let  $\xi \in T_x M$  is a tangent to  $M$  at  $x \in M$ . For a manifold  $M$  as given above, it can be shown that the tangent space

$$T_x M = \{\xi \in \mathbb{R}^n : (\frac{\partial \phi_i(x)}{\partial x} \cdot \xi) = 0, i = 1, \dots, m\}$$

so that the tangent space consists of the set of vectors in  $\mathbb{R}^n$  that are orthogonal to all of the gradients of the functions that define the manifold. The dimension of the tangent space is  $n - m$ .

The tangent bundle of  $M$  is  $TM = \bigcup_{x \in M} T_x M$ , the union of tangent spaces. A vector field  $\tau$  on  $M$  is a smooth map, which assigns to each point on  $x \in M$  a tangent vector  $\tau(x) \in T_x M$ .

## 2.7 Orthogonal matrices

We use the notation  $GL(n)$  for the set of all  $n \times n$  real nonsingular matrices. Since  $GL(n)$  is a subset of  $\mathbb{R}^{n \times n}$ , the inner product and the norm for matrices in  $GL(n)$  are defined. It can be shown that  $GL(n)$  has the properties of a group, formally introduced shortly, where matrix multiplication is the group operation. An important subset of  $GL(3)$  is the set of real  $3 \times 3$  orthogonal matrices, that is, matrices whose inverses are equal to their transposes. In other words, a matrix  $R \in \mathbb{R}^{3 \times 3}$  is orthogonal if  $RR^T = I_{3 \times 3}$ ,  $R^T R = I_{3 \times 3}$ . Orthogonal matrices have the property that their columns, as vectors in  $\mathbb{R}^3$ , are orthonormal and their rows, as vectors in  $\mathbb{R}^3$ , are orthonormal. An orthogonal matrix can be viewed as an invertible linear transformation on  $\mathbb{R}^3$ . The set of  $3 \times 3$  orthogonal matrices, with determinant  $+1$ , is denoted subsequently as  $SO(3)$ , referred to as the special orthogonal group or the group of rotations.

## 2.8 Homogeneous matrices

An important subset of  $GL(4)$  is the set of real  $4 \times 4$  matrices with the following partitioned matrix structure

$$\begin{bmatrix} R & x \\ 0 & 1 \end{bmatrix}$$

where  $R \in SO(3)$  is a  $3 \times 3$  orthogonal matrix with determinant  $+1$  and  $x \in \mathbb{R}^3$  is a column vector. Here, the 0 is a row vector in  $\mathbb{R}^3$  and 1 is a real number in  $\mathbb{R}^1$ . Such matrices are said to be homogeneous matrices. A homogeneous matrix can also be viewed as a linear transformation on  $\mathbb{R}^4$ . The set of  $4 \times 4$  homogeneous matrices is denoted subsequently as  $SE(3)$ , and the homogeneous matrix above is sometimes denoted by  $(R, x) \in SE(3)$ . It has important properties that we subsequently describe. The set of all real  $4 \times 4$  homogeneous matrices is closed under matrix multiplication. To illustrate, the matrix product of two homogeneous matrices is a homogeneous matrix since

$$\begin{bmatrix} R_2 & x_2 \\ 0 & 1 \end{bmatrix} \begin{bmatrix} R_1 & x_1 \\ 0 & 1 \end{bmatrix} = \begin{bmatrix} R_2 R_1 & x_2 + R_2 x_1 \\ 0 & 1 \end{bmatrix}$$

Each homogeneous matrix has an inverse given by

$$\begin{bmatrix} R & x \\ 0 & 1 \end{bmatrix}^{-1} = \begin{bmatrix} R^T & -R^T x \\ 0 & 1 \end{bmatrix}$$

which is also a homogeneous matrix. The identity matrix  $I_{4 \times 4}$  is a homogeneous matrix. Consequently, the set of all homogeneous matrices is closed under matrix multiplication and is a group. The matrix product represents the composition of the two linear transformations represented by the individual homogeneous matrices. As a set,  $SE(3)$  can be identified with  $SO(3) \times \mathbb{R}^3$ ; however the calculation above indicates that

the group composition on  $SE(3)$  is given by  $(R_2, x_2)(R_1, x_1) = (R_2R_1, x_2 + R_2x_1)$ , as opposed to the natural composition on  $SO(3) \times \mathbb{R}^3$ ,  $(R_2, x_2)(R_1, x_1) = (R_2R_1, x_2 + x_1)$ . The homogeneous matrix representation of  $SE(3)$  provides a convenient way of encoding the semidirect product structure in terms of matrix multiplication on  $GL(4)$ . We can identify a vector  $x \in \mathbb{R}^3$  with the vector  $(x, 1) \in \mathbb{R}^4$ .

The group action of a homogeneous matrix in  $SE(3)$  acting on  $\mathbb{R}^3$  can be expressed as

$$\begin{bmatrix} R & x_2 \\ 0 & 1 \end{bmatrix} \begin{bmatrix} x_1 \\ 1 \end{bmatrix} = \begin{bmatrix} x_2 + Rx_1 \\ 1 \end{bmatrix}$$

that represents the action  $x_1 \rightarrow x_2 + Rx_1$  of a homogeneous matrix in  $GL(4)$  on a vector in  $\mathbb{R}^3$ . In geometric terms, the element  $(R, x_2) \in SE(3)$  acts on  $x_1 \in \mathbb{R}^3$  by first rotating the vector  $x_1$  by  $R$ , followed by a translation by  $x_2$ .

## 2.9 Lie bracket and it's properties

A nonlinear system can be considered as a collection of dynamical systems (vector fields) parametrized by a parameter called control. It is natural to expect that basic properties of such system depend on interconnection between the different dynamical systems correspond to different controls. The dynamical systems are represented by vector fields as this allows algebraic operations on them such as taking linear combinations and a taking a product called Lie bracket. It is the Lie product which allows studying interconnections between different dynamical systems in a coordinate independent way.

The Lie bracket of two vector fields is another vector field. Let  $X \subset \mathbb{R}^n$ , and let  $f$  and  $g$  be vector fields on  $X$ . The Lie bracket of  $f$  and  $g$  is another vector field on  $X$  defined as follows

$$[f, g](x) = \frac{\partial g}{\partial x}(x)f(x) - \frac{\partial f}{\partial x}(x)g(x)$$

where  $\partial f / \partial x$  and  $\partial g / \partial x$  denote the Jacobi matrices of  $f$  and  $g$ .

**Example** For the vector fields  $f = (1, 0)^T$  and  $g = (0, x)^T$  on  $\mathbb{R}^n$ . The Lie bracket  $[f, g] = (0, 1)^T$  adds a new direction to the space spanned by  $f$  and  $g$  at the origin.

Let  $f = b$  be a constant vector field and  $g = Ax$  be a linear vector field. Then  $[f, g] = [b, Ax] = Ab$ .

**Proposition 2.1:** *The Lie bracket of two constant vector fields is zero. The Lie bracket of a constant vector field with a linear vector field is a constant vector field. Finally, the Lie bracket of two linear fields is a linear vector field.*

The basic geometric properties of Lie bracket are stated in the following propositions. The first one says that vanishing of Lie bracket  $[f, g]$  is equivalent to the fact that starting from a point  $p$  and going along trajectory of  $f$  for time  $t$  and then along trajectory  $g$  for time  $s$  gives always the same result  $s$  with the order of taking  $f$  and

$g$  reversed.

The Lie bracket of vector fields  $f$  and  $g$  is equal identically to zero if and only if their flows commute. i.e

$$[f, g] \equiv 0 \iff \gamma_t^f \circ \gamma_s^g(p) = \gamma_s^g \circ \gamma_t^f(p) \quad \forall s, t \in \mathbb{R}, \forall p \in X$$

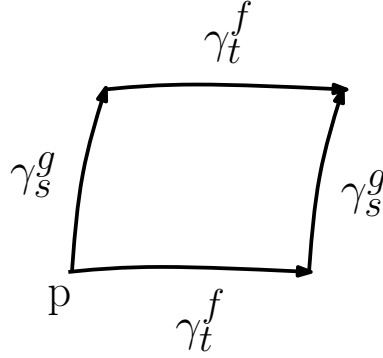


FIGURE 2.1: Commutative iff  $[f, g] = 0$ .

Given vector fields  $f, g, h \in \mathbb{R}^n$  and smooth functions  $\alpha, \beta : \mathbb{R}^n \rightarrow \mathbb{R}$ , the Lie bracket satisfies the following properties:

**Skew-symmetry**

$$[f, g] = -[g, f]$$

**Jacobi-Identity**

$$[f, [g, h]] + [h, [f, g]] + [g, [h, f]] = 0$$

**Chain rule**

$$[\alpha f, \beta g] = \alpha \beta [f, g] + \alpha (L_f \beta) g - \beta (L_g \alpha) f$$

where  $L_f \beta$  and  $L_g \alpha$  stand for the Lie derivatives of  $\beta$  and  $\alpha$  along the vector fields  $f$  and  $g$  respectively.

### 2.9.1 Lie algebra

A vector space  $V$  (over  $\mathbb{R}$ ) is a Lie algebra if there exists a bilinear operation  $V \times V \rightarrow V$ , denoted  $[\cdot, \cdot]$ , satisfying (i) skew-symmetry and (ii) the Jacobi identity.

The set of smooth vector fields on  $\mathbb{R}^n$  with the Lie bracket is a Lie algebra. Let  $g_1, \dots, g_m$  be a set of smooth vector fields,  $\Delta$  the distribution defined by  $g_1, \dots, g_m$  and,  $\bar{\Delta}$  the involutive closure of  $\Delta$ . Then,  $\bar{\Delta}$  is a Lie algebra (in fact the smallest Lie algebra containing  $g_1, \dots, g_m$ ). It is called the Lie algebra generated by  $g_1, \dots, g_m$  and is often denoted  $(\}_{\infty, \dots, \}_{\uparrow}$ . Elements of  $(\}_{\infty, \dots, \}_{\uparrow}$  are obtained by taking all linear combinations of elements of  $g_1, \dots, g_m$ , taking Lie brackets of these, taking all

linear combinations of these, and so on. We define the rank of  $L(\{_\infty, \dots, \}_{\uparrow})$  at a point  $q \in \mathbb{R}^n$  to be the dimension of  $\bar{\Delta}_q$  as a distribution.

## 2.10 Controllability and accessibility

A finite-dimensional nonlinear control system on a smooth  $n$ -manifold  $M$  is a differential equation of the form

$$\dot{x} = f(x, u)$$

where  $x \in M$ ,  $u(t)$  is a time-dependent map from the nonnegative reals  $\mathbb{R}^+$  to a constraint set  $\Omega \subset \mathbb{R}^m$ , and  $f$  is taken to be  $C^\infty$  (smooth) from  $M \times \mathbb{R}^m$  into  $TM$  such that for each fixed  $u$ ,  $f$  is a vector field on  $M$ . The map  $u$  is assumed to be piecewise smooth or piecewise analytic. Such a map  $u$  is said to be admissible. The manifold  $M$  is said to be the state space or the phase space of the system.

In this thesis, we will restrict our discussion to affine nonlinear control systems, which have the form

$$\dot{x} = f(x) + \sum_{i=1}^m g_i(x)u_i, \quad (2.1)$$

where  $f$  and the  $g_i, i = 1, \dots, m$ , are smooth vector fields on  $M$ . We usually suppose that the constraint set  $\Omega$  contains an open set of the origin in  $\mathbb{R}^m$ . Thus  $u \equiv 0$  is an admissible control resulting in trajectories generated by the vector field  $f$ . Hence the vector field  $f$  is usually called the **drift vector field**, and the  $g_i$  are called the **control vector fields**.

In the analysis of controlled dynamic systems, there are two basic goals : One goal is being able to drive the given system from one part of the state space (the phase space for a mechanical system) to another, and a second goal is being able to stabilize a given system about a given equilibrium or equilibrium manifold.

For the first goal, one is interested in the first instance in **controllability**, the question of whether one can drive the system from one point to another with the given class of controls, but one does not concern oneself with the path taken. On the other hand, one might want to prescribe a given path. This is the problem of **path planning**. Or one might want to choose a path that is optimal in some sense.

### 2.10.1 Controllability

We begin by making precise the general notion of controllability that was discussed informally in the previous section. We assume in this section that the set of admissible controls contains the set of piecewise constant controls with values in  $\Omega$ .

**Definition 2.1:** The system (2.1) is said to be controllable if for any two points  $x_0$  and  $x_f$  in  $M$  there exists an admissible control  $u(t)$  defined on some time interval  $[0, T]$  such that the system (2.1) with initial condition  $x_0$  reaches the point  $x_f$  in time  $T$ .

Controllability is a basic concept in control theory, and much work has been done on deriving useful sufficient conditions to ensure it. A related property, called (local) **accessibility**, is often much easier to prove.

### 2.10.2 Accessibility

. To define accessibility we first need the notion of a reachable set. This notion will depend on the choice of a positive time  $T$ . The reachable set from a given point at time  $T$  will be defined to be, essentially, the set of points that may be reached by the system by traveling on trajectories from the initial point in a time at most  $T$ . In particular, if  $q \in M$  is of the form  $x(t)$  for some trajectory with initial condition  $x(0) = p$  and for some  $t$  with  $0 \leq t \leq T$ , then  $q$  will be said to be reachable from  $p$  in time  $T$ . More precisely:

**Definition 2.2:** Given  $x_0 \in M$  we define  $R(x_0, t)$  to be the set of all  $x \in M$  for which there exists an admissible control  $u$  such that there is a trajectory of (2.1) with  $x(0) = x_0, x(t) = x$ . The reachable set from  $x_0$  at time  $T$  is defined to be

$$R_T(x_0) = \bigcup_{0 \leq t \leq T} R(x_0, t)$$

**Definition 2.3:** The **accessibility algebra**  $C$  of (2.1) is the smallest Lie algebra of vector fields on  $M$  that contains the vector fields  $f$  and  $g_1, \dots, g_m$ .

Note that the accessibility algebra is just the span of all possible Lie brackets of  $f$  and the  $g_i$ .

**Definition 2.4:** We define the **accessibility distribution**  $C$  of (2.1) to be the distribution generated by the vector fields in  $C$ ; i.e.,  $C(x)$  is the span of the vector fields  $X$  in  $C$  at  $x$ .

**Definition 2.5:** The system (2.1) on  $M$  is said to be **accessible** from  $p \in M$  if for every  $T > 0$ ,  $R_T(p)$  contains a nonempty open set. Roughly speaking, this means that there is some point  $q$  (not necessarily even close to a desired objective point) that is reachable from  $p$  in time no more than  $T$  and that points close to  $q$  are also reachable from  $p$  in time no more than  $T$ .

Accessibility, while relatively easy to prove, is far from proving controllability.

**Theorem 2.1:** Consider the system (2.1) and assume that the vector fields are  $C^\infty$ . If  $\dim C(x_0) = n$  (i.e., the accessibility algebra spans the tangent space to  $M$  at  $x_0$ ), then for any  $T > 0$ , the set  $R_T(x_0)$  has a nonempty interior; i.e., the system has the accessibility property from  $x_0$ .

When the hypotheses of this theorem, namely  $\dim C(x_0) = n$ , hold, we say that the **accessibility rank condition** holds at  $x_0$ .

Note that while this spanning condition is an intuitively reasonable condition, the resulting theorem is quite weak, since it is far from implying controllability. The problem is that one cannot move backward along the drift vector field  $f$ . If  $f$  is absent,

this is a strong condition.

**Controllability Rank Condition.** Another case of interest where accessibility implies controllability is a linear system of the form

$$\dot{x} = Ax + f(x) + \sum_{i=1}^m b_i(x)u_i = Ax + Bu, \quad (2.2)$$

where  $x \in \mathbb{R}^n$ , and  $A \in \mathbb{R}^n \times \mathbb{R}^n$  and  $B \in \mathbb{R}^n \times \mathbb{R}^m$  are constant matrices,  $b_i$  being the columns of  $B$ .

The Lie bracket of the drift vector field  $Ax$  with  $b_i$  is readily checked to be the constant vector field  $Ab_i$ . Bracketing the latter field with  $Ax$  and so on tells us that  $C$  is spanned by  $Ax, b_i, Ab_i, \dots, A^{n-1}b_i, i = 1, \dots, m$ .

Thus, the accessibility rank condition at the origin is equivalent to the classical controllability rank condition

$$\text{rank}[B, AB, \dots, A^{n-1}B] = n.$$

In fact, the following theorem holds.

**Theorem 2.2:** *The system (2.2) is controllable if and only if the controllability rank condition holds.*

Note that in this case accessibility is equivalent to controllability but that the drift vector field is involved.

In this linear setting if the system is not controllable, the reachable subspace  $R$  of the system (the space reachable from the origin) is given by the range of  $[B, AB, \dots, A^{n-1}B]$ .

**Strong Accessibility.** In the preceding discussion, note that the term  $\text{span}Ax$  is not present in the controllability rank condition. This motivates a slightly stronger definition of accessibility in the nonlinear setting, where the  $g_i$  (over which we have direct control) play a more prominent role in the rank condition:

**Definition 2.6:** The system (2.1) is said to be **strongly accessible** from  $x_0$  if the set  $R(x_0, T)$  contains a nonempty open set for any  $T$  sufficiently small.

Thus this means that points that we can reach in exactly time  $t$  contain a nonempty open set.

**Definition 2.7:** Let  $C$  be the accessibility algebra of (2.1). Define  $C_0$  to be the smallest subalgebra containing  $g_1, \dots, g_n$  and such that  $[f, X] \in C_0$  for all  $X \in C_0$ .

**Definition 2.8:** We define the **strong accessibility distribution**  $C_0$  of (2.1) to be the distribution generated by the vector fields in  $C_0$ .

If  $\dim C_0(x_0) = n$ , then the system (2.1) can be shown to be strongly accessible at  $x_0$ .

**Example.** The Euler equations for the rigid body are given by

$$\dot{\Omega}_1 = \frac{I_2 - I_3}{I_1} \Omega_2 \Omega_3 + a_1 u_1$$

$$\begin{aligned}\dot{\Omega}_2 &= \frac{I_3 - I_1}{I_2} \Omega_3 \Omega_1 + a_2 u_2 \\ \dot{\Omega}_3 &= \frac{I_1 - I_2}{I_3} \Omega_2 \Omega_3\end{aligned}$$

where the  $a_i$  are nonzero constants. Writing the system in the standard affine form

$$\dot{\Omega} = f(\Omega) + u_1 g_1(\Omega) + u_2 g_2(\Omega)$$

we find that  $[g_2, [g_1, f]](\Omega) = [0, 0, a_1 a_2 (I_1 I_2) / I_3]^T$ . The vectors  $[a_1, 0, 0]^T$ ,  $[a_2, 0, 0]^T$ , and  $[0, 0, a_1 a_2 (I_1 I_2) / I_3]^T$  are contained in  $C_0(0)$ , and hence if  $I_1 \neq I_2$ , the system is strongly accessible from  $\Omega = 0$ . Further,  $I_1 \neq I_2$  is also necessary, for if  $I_1 = I_2$ , then  $\dot{\Omega} = 0$ .

We will now restrict our attention to control systems of the form

$$\dot{q} = \sum_{i=1}^m g_i(q) u_i, \quad (2.3)$$

where  $q \in \mathbb{R}^n$ ,  $u \in U \subset \mathbb{R}^m$ . This system is said to be drift-free, meaning to say that when the controls are set to zero the state of the system does not drift. We assume that the  $g_j$  are smooth, linearly independent vector fields on  $\mathbb{R}^n$  and that their flows are defined for all time (i.e., the  $g_j$  are complete). We wish to determine conditions under which we can steer from  $q_0 \in \mathbb{R}^n$  to an arbitrary  $q_f \in \mathbb{R}^n$  by appropriate choice of  $u(\cdot)$ .

A system (2.3) is controllable if for any  $q_0, q_f \in \mathbb{R}^n$  there exists a  $T > 0$  and  $u : [0, T] \rightarrow U$  such that (2.3) satisfies  $q(0) = q_0$  and  $q(T) = q_f$ . A system is said to be **small-time locally controllable** at  $q_0$  if we can reach nearby points in arbitrarily small amounts of time and stay near to  $q_0$  at all times. Given an open set  $V \subseteq \mathbb{R}^n$ , define  $R^V(q_0, T)$  to be the set of states  $q$  such that there exists  $u : [0, T] \rightarrow U$  that steers (2.3) from  $q(0) = q_0$  to  $q(T) = q_f$  and satisfies  $q(t) \in V$  for  $0 \leq t \leq T$ . We also define

$$R^V(q_0, \leq T) = \bigcup_{0 \leq \tau \leq T} R^V(q_0, \tau)$$

to be the set of states reachable up to time  $T$ . A system is small-time locally controllable (locally controllable for brevity) if  $R^V(q_0, T)$  contains a neighborhood of  $q_0$  for all neighborhoods  $V$  of  $q_0$  and  $T > 0$ . Let  $\Delta = L(\{g_1, \dots, g_m\})$  be the Lie algebra generated by  $g_1, \dots, g_m$ . It is referred to as the **controllability Lie algebra**. For the system given in (2.3) using an input sequence of the following

$$\begin{aligned}u_1 &= +1 & u_2 &= 0 & \text{for } 0 \leq t < \epsilon \\ u_1 &= 0 & u_2 &= +1 & \text{for } \epsilon \leq t < 2\epsilon\end{aligned}$$



$$u_1 = -1 \quad u_2 = 0 \quad \text{for} \quad 2\epsilon \leq t < 3\epsilon$$

$$u_1 = 0 \quad u_2 = -1 \quad \text{for} \quad 3\epsilon \leq t < 4\epsilon$$

That implies that the points attainable from  $p$  by means of the vector fields  $g_1$  and  $g_2$  lie not only in the direction  $g_1$  and  $g_2$ , but also in the direction of the Lie bracket  $[g_1, g_2](p)$ . This fact will be of basic importance for studying controllability properties of nonlinear control system.

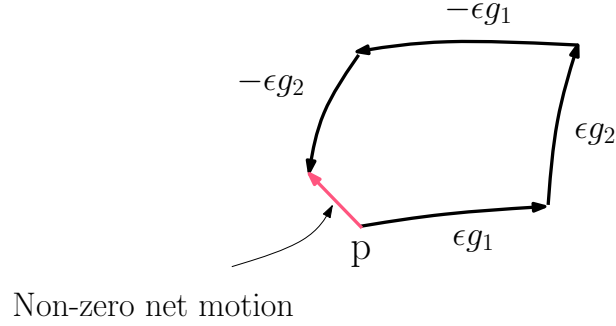


FIGURE 2.2: A Lie bracket motion.

we get motion in the direction of the Lie bracket  $[g_1, g_2]$ . If we were to iterate on this sequence, it should be possible to generate motion along directions given by all the other Lie products associated with the  $g_i$ . Thus, it is not surprising that it is possible to steer the system along all of the directions represented in  $L(\{\infty, \dots, \}_{\uparrow})$ . This is made precise by the following theorem, which was originally proved by W.-L. Chow (in somewhat different form) in the 1940s.

**Theorem 2.3:** *The control system (2.3) is locally controllable at  $q \in \mathbb{R}^n$  if  $\bar{\Delta}_q = T_q \mathbb{R}^n$ .*

In principle, we now have a recipe for solving the motion planning problem for systems which meet the controllability rank condition.

## Chapter 3

# Knife-edge Moving on a Smooth Surface

This chapter studies a new formulation for the kinematics of a knife-edge moving on an arbitrary smooth surface in  $\mathbb{R}^3$ . The kinematics equations for a knife-edge, viewed as a rigid body, are constrained by the requirement that the knife-edge maintain contact with the surface. They describe the constrained translation of the point of contact of the knife-edge on the surface and the constrained attitude of the knife-edge as a rigid body. These equations for the knife-edge kinematics in  $\mathbb{R}^3$  are expressed in a geometric form, without the use of local coordinates; they are globally defined without singularities or ambiguities. The kinematics equations can be expressed in several simplified forms and written as a drift-free nonlinear control system. Comments are made about interesting motion planning and path planning problems. The kinematics equations are specialized for two specific surfaces defined in  $\mathbb{R}^3$ , namely a flat plane and the surface of a sphere. Results for the flat plane are compared with standard results obtained using local coordinates; results for the sphere, in contrast, require full attention to the three-dimensional geometry.

### 3.1 Introduction

A knife-edge, viewed as a rigid body, can slide on a smooth surface without friction; the knife-edge is assumed to have a single point of contact with the surface. The motion of the point of contact of the knife-edge is constrained so that its velocity vector is always in the direction of the axis of the knife-edge. This constraint on the direction of the velocity vector is an example of a nonholonomic or non-integrable constraint. If the motion of the knife-edge is controlled by the axial velocity of the knife-edge and the turn rate of the knife-edge, the result is one of the simplest examples of a nonholonomic control system. This is in fact an example of a nonholonomic control system, expressed in a kinematics form Jiang et al (1995). This knife-edge control system has been extensively studied in (Neimark et al, 1972; Osborne et al,

2005; Salinic et al, 2013), where it is referred to as a Čaplygin sleigh; all of these results are based on simplified planar models of the knife-edge kinematics expressed in terms of local coordinates.

We also recognize that this model of a knife-edge has been used, on occasion, to describe the kinematics of a flight vehicle where the angle of attack and side slip angle are maintained to be zero so that the control inputs are the axial flight velocity and the turn rate of the flight vehicle. The requirement that the motion of the flight vehicle is constrained to a surface can arise naturally from mission specifications. This interpretation is not pursued further.

The literature on such nonholonomic control problems is large, both in terms of theoretical results and studies of specific physical examples in the context of robot manipulation, mobile robots, wheeled vehicles, and space robotics. An excellent reference that provides a geometric and control theoretical view of nonholonomic systems is the book by Bloch (2003). A few representative control works include the study of controllability and stabilizability in Bloch et al (1992, 1991); motion planning in Murray et al (1994); Reyhanoglu (1994); and feedback stabilization and tracking in Astolfi (1996); Jiang et al (1999, 1995); Sordalen et al (1995). All of this literature is based on the use of mathematical models, most often arising from principles of mechanics and geometry, that are expressed in terms of local coordinates for the configuration vector. This use of local coordinates is a significant limitation in some physical examples, where non-local or even global results are desired. Our formulation in this paper considers arbitrary smooth manifolds embedded in  $\mathbb{R}^3$ . We view the knife-edge as a rigid body but our formulation differs from the formulations using Lie group manifolds (see e.g., Leonard et al (1995); Morin et al (2003) and references therein).

This chapter makes two contributions by studying a new formulation that describes the motion of a knife-edge moving on a smooth surface. The two contributions, developed and explained in the context of the controlled motion of a knife-edge, are: (1) the knife-edge, viewed as a rigid body, translates and rotates while maintaining a point of contact with an arbitrary smooth surface in three-dimensions and (2) we express the results without the use of local coordinates in a geometric form where the mathematical models are globally defined without singularities or ambiguities.

We first develop the kinematics equations for a rigid knife-edge that translates and rotates while maintaining point contact with an arbitrary smooth surface. These kinematics equations are expressed in several equivalent forms and it is shown that they can be expressed as a drift-free nonlinear control system defined on a configuration manifold. Comments are made about nonlinear controllability and about the formulation of motion and path planning problems for the controlled knife edge. Then the equations of motion are specialized for two specific surfaces. In the first case, the smooth surface is a flat plane in  $\mathbb{R}^3$ ; in the second case, the smooth surface is the surface of a sphere in  $\mathbb{R}^3$ . Controllability and motion planning results are described in each case.

We are motivated to study the knife-edge kinematics, subject to constrained mo-

tion on a surface (especially a surface with nontrivial curvature), to illustrate the geometric formulation of nonholonomic kinematics and their use in nonlinear control. The development in this paper follows the results in Lee et al (2009) and the book Lee et al (2017); similar formulations are suggested in problems given on page 87 and pages 483-484 of Lee et al (2017).

## 3.2 Kinematics of a knife-edge

A Euclidean frame in  $\mathbb{R}^3$  is introduced with standard basis vectors  $e_1, e_2, e_3$  in  $\mathbb{R}^3$ . A fixed surface is defined by the two-dimensional manifold

$$M = \{x \in \mathbb{R}^3 : \phi(x) = 0\},$$

where  $\phi : \mathbb{R}^3 \rightarrow \mathbb{R}^1$  is a differentiable function that satisfies  $\frac{\partial \phi(x)}{\partial x} \neq 0, x \in M$ . The manifold is assumed to be connected.

The knife-edge is assumed to be a rigid body that maintains contact with the surface at a single point, the contact point. The knife-edge can translate with respect to the surface only in a direction that is defined by the heading of the knife-edge; the knife-edge can also rotate only about a direction that is normal to the surface at the contact point.

Let  $x \in M \subset \mathbb{R}^3$  denote the position vector of the contact point of the knife-edge in the Euclidean frame; let  $\gamma \in \mathbb{S}^2 \subset \mathbb{R}^3$  denote the heading direction vector of the knife-edge as shown in Figure 3.1. As usual  $\mathbb{S}^2$  denotes the unit sphere, a smooth manifold embedded in  $\mathbb{R}^3$ .

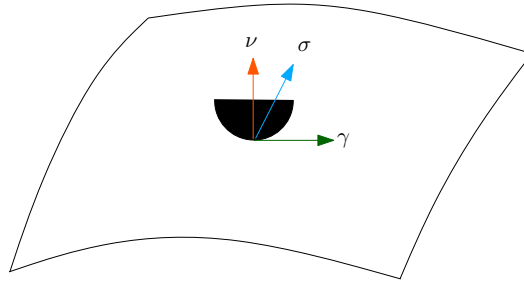


FIGURE 3.1: A moving frame for a knife edge on a smooth surface in  $\mathbb{R}^3$ .

A nonholonomic constraint is important in characterizing the motion of a knife-edge on a smooth manifold. The nonholonomic constraint, in this case, is that the velocity vector  $\dot{x}$  of the point of contact of the knife-edge is always in the heading direction  $\gamma \in \mathbb{S}^2$  of the knife-edge and the heading direction satisfies  $\gamma \in T_x M$ . Let  $\nu \in \mathbb{S}^2$  be the unit normal of the surface at the point of contact. A right hand Euclidean frame, fixed to the knife-edge with origin located at the point of contact,

is defined by introducing the unit vector  $\sigma = \nu \times \gamma \in \mathbb{S}^2$ . It follows that  $\sigma \in T_x M$ . (see Figure 3.1.)

The control inputs are the scalar  $V \in \mathbb{R}^1$  that denotes the magnitude of the velocity vector of the point of contact of the knife-edge, referred to as the speed of the knife-edge, and the scalar  $\omega \in \mathbb{R}^1$  that denotes the turn rate of the knife-edge about the normal vector  $\nu \in \mathbb{S}^2$ .

**Proposition 3.1:** *The kinematics of a knife edge controlled by its speed  $V$  along the heading direction  $\gamma$  and its turn rate  $\omega$  about the normal axis  $\nu = n(x)$  are given by*

$$\dot{x} = V\gamma, \quad (3.1)$$

$$\dot{\gamma} = \omega S(n(x))\gamma - V(\gamma^T N(x)\gamma)n(x), \quad (3.2)$$

where  $n(x) = \frac{\partial \phi(x)}{\partial x} / \left\| \frac{\partial \phi(x)}{\partial x} \right\|$  and  $N(x) = \frac{\partial n(x)}{\partial x}$ .

**Proof:** The knife edge can move only in the heading direction; thus it satisfies the nonholonomic constraint given by (3.1). Since  $\gamma \in \mathbb{S}^2$  is allowed to rotate with the angular velocity vector  $\omega n(x)$ , its time rate of change in the tangent plane  $T_x M$  is given by  $S(\omega n(x))\gamma$ . The time rate of change along the normal to the tangent plane  $T_x M$  due to the translational motion is of the form  $Vh(x, \gamma)n(x)$ . Therefore,  $\dot{\gamma}$  can be expressed as

$$\dot{\gamma} = \omega S(n(x))\gamma + Vh(x, \gamma)n(x),$$

where  $h(x, \gamma)$  is a scalar function to be determined using the geometric properties of the configuration manifold  $Q$ . Clearly,  $\nu^T \dot{\gamma} = Vh(x, \gamma)$ . Since

$$\nu^T \gamma = 0 \Rightarrow \nu^T \dot{\gamma} + \dot{\nu}^T \gamma = 0,$$

it follows that

$$\nu^T \dot{\gamma} = -\gamma^T \dot{\nu} = -V\gamma^T N(x)\gamma.$$

Therefore,  $h(x, \gamma) = -\gamma^T N(x)\gamma$ , and thus the equation (3.2) follows.  $\blacksquare$

The equations (3.1) and (3.2) describe the coupled translational and rotational kinematics of the knife-edge moving on an arbitrary smooth surface. Since  $Q$  is a three-dimensional configuration manifold, there are three degrees of freedom and there are two scalar control input variables.

Here  $S : \mathbb{R}^3 \rightarrow \mathbb{R}^{3 \times 3}$  is the skew-symmetric matrix representing the cross product operator on  $\mathbb{R}^3$  given by

$$S(x) = \begin{bmatrix} 0 & -x_3 & x_2 \\ x_3 & 0 & -x_1 \\ -x_2 & x_1 & 0 \end{bmatrix},$$

and the  $3 \times 3$  matrix function  $N(x) = \frac{\partial n(x)}{\partial x}$ . The first term on the right hand side of

(3.2) lies in the tangent plane  $T_x M$  while the second term is normal to the tangent plane  $T_x M$ .

The configuration vector is  $(x, \gamma) \in M \times \mathbb{S}^2$  and

$$Q = \{(x, \gamma) \in M \times \mathbb{S}^2 : \gamma \in T_x M\} \quad (3.3)$$

is the configuration manifold.

Suppose that the control inputs  $V$  and  $\omega$  are given time functions. Let the initial conditions satisfy  $(x(0), \gamma(0)) \in Q$ ; the unique solution of (3.1) and (3.2) can be shown to satisfy  $(\dot{x}, \dot{\gamma}) \in T_{(x, \gamma)} Q$  so that  $(x(t), \gamma(t)) \in Q$ ,  $t \geq 0$ .

Consequently, these equations (3.1) and (3.2) describe the coupled translational and rotational kinematics of the knife-edge moving on an arbitrary smooth surface. They define the global evolution of  $(x, \gamma) \in Q$  in the sense that for any control inputs  $(V, \omega) : [0, \infty) \rightarrow \mathbb{R}^2$ , the motion of the knife-edge is defined by a flow on  $Q$ ; there are no singularities or ambiguities in the characterization of the flow on  $Q$ . Since  $Q$  is a three-dimensional configuration manifold, there are three degrees of freedom and there are two scalar control input variables.

To fully describe the rotational kinematics of the knife-edge as a rigid body, we characterize the previously introduced attitude vectors  $\sigma = S(n(x))\gamma$  and  $\nu = n(x)$  of the knife-edge. In fact, these three unit vectors  $\{\gamma, \sigma, \nu\}$  determine a rotation matrix in  $SO(3)$  for the attitude of the rigid body knife-edge.

Alternatively, the translational and rotational kinematics for the knife-edge can be written in terms of  $x \in M$  and  $\sigma \in \mathbb{S}^2$  on the configuration manifold

$$Q = \{(x, \sigma) \in \mathbb{R}^3 \times \mathbb{S}^2 : \sigma \in T_x M\}.$$

Using the fact that  $\gamma = S(\sigma)n(x)$ , it can be shown that equations (3.1) and (3.2) are equivalent to the coupled translational and rotational kinematics equations

$$\dot{x} = -VS(n(x))\sigma, \quad (3.4)$$

$$\dot{\sigma} = \omega S(n(x))\sigma + V(\sigma^T N(x)S(n(x))\sigma)n(x). \quad (3.5)$$

The following initial value property can be shown to be valid based on the definition of the configuration manifold and the kinematics equations (3.4) and (3.5). Suppose that the control inputs  $V$  and  $\omega$  are given time functions. Let the initial conditions satisfy  $(x(0), \sigma(0)) \in Q$ ; the unique solution of (3.4) and (3.5) can be shown to satisfy  $(\dot{x}, \dot{\sigma}) \in T_{(x, \sigma)} Q$  so that  $(x(t), \sigma(t)) \in Q$ ,  $t \geq 0$ . Consequently, these equations (3.4) and (3.5) describe the coupled translational and rotational kinematics of the knife-edge moving on an arbitrary smooth surface. The full attitude of the knife edge is completed by  $\gamma = S(\sigma)n(x)$  and  $\nu = n(x)$ .

The kinematics of the knife-edge can be represented by either equations (3.1) and (3.2) or by equations (3.4) and (3.5). These equations have similar forms and either can be used as the basis for control of the knife-edge kinematics using the knife-edge

speed and turn rate as control inputs.

### 3.3 Controllability and motion planning for the knife-edge kinematics

It is convenient to write equations (3.1) and (3.2) and equations (3.4) and (3.5) in a standard nonlinear control form. Each of these set of equations can be expressed in the form of a driftless control-affine nonlinear system as

$$\dot{q} = g_1(q)V + g_2(q)\omega, \quad (3.6)$$

where  $g_1(q)$  and  $g_2(q)$  are control vector fields defined on the configuration manifold  $Q$ .

In the case of equations (3.1) and (3.2), the configuration vector is  $q = (x, \gamma) \in Q$  and the control vector fields are

$$g_1(q) = \begin{bmatrix} \gamma \\ -\gamma^T N(x) \gamma n(x) \end{bmatrix}, \quad g_2(q) = \begin{bmatrix} 0 \\ S(n(x)) \gamma \end{bmatrix}.$$

In the case of equations (3.4) and (3.5), the configuration vector is  $q = (x, \sigma) \in Q$  and the control vector fields are

$$g_1(q) = \begin{bmatrix} -S(n(x))\sigma \\ \sigma^T N(x) S(n(x)) \sigma n(x) \end{bmatrix}, \quad g_2(q) = \begin{bmatrix} 0 \\ S(n(x)) \sigma \end{bmatrix}.$$

These equations are in a standard drift-free affine form to which standard nonlinear control results can be applied.

In particular, equation (3.6) is controllable on  $Q$ , according to Chow's theorem, if

$$\text{rank} \begin{bmatrix} g_1 & g_2 & [g_1, g_2] \end{bmatrix} (q) = \dim(Q) = 3, \quad \forall q \in Q.$$

That is, the knife edge can be maneuvered so that it moves from any initial point on  $Q$  to any prescribed final point on  $Q$  if the Lie bracket  $[g_1, g_2]$  is linearly independent of the two control vector fields on  $Q$ .

There are many possible approaches to motion planning that have been proposed in the literature. Several possible construction approaches involve the use the spanning brackets, sums of sinusoidals, or switchings of the control. Here we propose a motion planning approach that makes use of the geometry of the knife-edge problem.

For example, let  $t_f \geq 0$  and consider the problem of determining the control inputs, namely the forward speed and the turn rate  $(V, \omega) : [0, t_f] \rightarrow \mathbb{R}^2$ , that transfers the initial configuration  $q^0 = (x^0, \gamma^0) \in Q$  at time 0 to the the final configuration  $q^f = (x^f, \gamma^f) \in Q$  at time  $t_f$ . This implies that the initial position and initial attitude of the knife-edge satisfy  $x^0 \in M$ ,  $\gamma^0 \in T_{x^0}M$  and  $\sigma^0 = S(n(x^0))\gamma^0$ ,  $\nu_0 = n(x^0)$ ; the

final position and final attitude of the knife-edge at completion of the maneuver satisfy  $x^f \in M$ ,  $\gamma^f \in T_{x^f}M$  and  $\sigma^f = S(n(x^f))\gamma^f$ ,  $\nu_f = n(x^f)$ .

A natural approach for the knife-edge maneuver problem is to construct a smooth path in  $M$  that connects  $x^0 \in M$  and  $x^f \in M$ . We select the path this is the intersection of  $M$  and a transversal plane and connects  $x^0 \in M$  and  $x^f \in M$ . This path defines an initial heading direction  $\gamma^1 \in T_{x^0}M$  and a final heading direction  $\gamma^2 \in T_{x^f}M$ . The motion planning problem then involves the following procedure:

**Step 1:** Set  $V = 0$ , choose the turn rate  $\omega$  to rotate the initial heading direction  $\gamma^0$  to the heading direction  $\gamma^1$  required to move along the determined path.

**Step 2:** Set  $\omega = 0$ , choose the speed  $V$  of the knife edge to translate the knife-edge along the determined path.

**Step 3:** Set  $V = 0$ , choose the turn rate  $\omega$  to rotate the heading direction  $\gamma^2$  at the end of the path to the desired terminal heading direction  $\gamma^f$ .

The changes in the attitude vectors  $\sigma$  and  $\nu$  of the knife-edge during a maneuver can be determined from the prior expressions that show how they depend on  $(x, \gamma) \in Q$ . There are many ways to implement this planning approach; illustrations are given in the following sections.

### 3.4 Knife-edge moving on a flat plane

Here, we assume that the constraint surface is a flat plane in  $\mathbb{R}^3$  and the constraint manifold is

$$M = \{x \in \mathbb{R}^3 : e_3^T x = 0\}$$

and the configuration manifold is

$$Q = \{(x, \gamma) \in \mathbb{R}^3 \times \mathbb{S}^2 : e_3^T \gamma = 0\}.$$

The vector function for the scaled normal vector is  $n(x) = e_3$ , so that the matrix function  $N(x) = 0$ .

The kinematics of the knife-edge moving on the flat plane are given by

$$\dot{x} = V\gamma, \tag{3.7}$$

$$\dot{\gamma} = \omega S(e_3)\gamma, \tag{3.8}$$

or equivalently by

$$\dot{x} = -VS(e_3)\sigma, \tag{3.9}$$

$$\dot{\sigma} = \omega S(e_3)\sigma. \tag{3.10}$$



If we introduce the attitude angle  $\theta$  of the knife-edge, then

$$x = \begin{bmatrix} x_1 \\ x_2 \\ 0 \end{bmatrix}, \quad \gamma = \begin{bmatrix} \cos \theta \\ \sin \theta \\ 0 \end{bmatrix}$$

In this way we obtain the standard form for the equations of motion of the knife-edge on a flat plane expressed in local coordinates:

$$\begin{aligned} \dot{x}_1 &= V \cos \theta, \\ \dot{x}_2 &= V \sin \theta, \\ \dot{\theta} &= \omega. \end{aligned}$$

These kinematics equations for a knife-edge on a flat plane have been extensively studied. However, they are limited by the ambiguity that is introduced by the use of an angle. This motivates our use of the prior equations.

Based on equations (3.7) and (3.8), the control vector fields are given by

$$g_1(q) = \begin{bmatrix} \gamma \\ 0 \end{bmatrix}, \quad g_2(q) = \begin{bmatrix} 0 \\ S(e_3)\gamma \end{bmatrix}.$$

The following Lie bracket is computed:

$$[g_1, g_2](q) = \begin{bmatrix} -S(e_3)\gamma \\ 0 \end{bmatrix}.$$

It can be shown that

$$\text{rank} \begin{bmatrix} g_1 & g_2 & [g_1, g_2] \end{bmatrix} (q) = 3, \quad \forall q \in Q.$$

Therefore, the knife-edge is controllable on the flat plane and it can be maneuvered so that it moves from any initial point on  $Q$  to any prescribed final point on  $Q$ .

### 3.4.1 Motion planning

We follow the strategy described previously to describe a solution to the motion planning problem. In particular, the path connecting  $x^0 \in M$  to  $x^f \in M$  is taken as the straight line path between these two points, which necessarily lies in the flat plane.

Suppose that  $0 \leq t_1 \leq t_2 \leq t_f$ . Assume that  $x^0 \neq x^f$  and let  $\gamma^1$  denote the unit vector in the direction of  $x^f - x^0$ , given by

$$\gamma^1 = \frac{x^f - x^0}{\|x^f - x^0\|}.$$

Define the three scalars

$$\begin{aligned}\omega_1 &= \frac{1}{t_1} \tan^{-1} \left( \frac{e_3^T S(\gamma^0) \gamma^1}{\gamma^{0T} \gamma^1} \right), \\ V_2 &= \frac{\|x^f - x^0\|}{t_2 - t_1}, \\ \omega_3 &= \frac{1}{t_f - t_2} \tan^{-1} \left( \frac{e_3^T S(\gamma^1) \gamma^f}{\gamma^{1T} \gamma^f} \right).\end{aligned}$$

A solution of the maneuver problem is given as follows:

**Step 1:** Set  $V = 0$ ,  $\omega = \omega_1$ ,  $0 \leq t < t_1$ . This step can be shown to rotate the knife edge about the normal attitude vector  $e_3$  from  $\gamma^0$  at time 0 to  $\gamma^1$  at time  $t_1$ .

**Step 2:** Set  $V = V_2$ ,  $\omega = 0$ ,  $t_1 \leq t < t_2$ . This step can be shown to translate the knife edge in the constant direction of the heading attitude vector  $\gamma^1$  from  $x^0$  at time  $t_1$  to  $x^f$  at time  $t_2$ .

**Step 3:** Set  $V = 0$ ,  $\omega = \omega_3$ ,  $t_2 \leq t \leq t_f$ . This step can be shown to rotate the knife edge about the normal attitude vector  $e_3$  from  $\gamma^1$  at time  $t_2$  to  $\gamma^f$  at time  $t_f$ .

Note that if  $x^0 = x^f$ , then we set  $t_2 = t_1 = 0$  and start from Step 3 with  $\gamma^1 = \gamma^0$ .

In this case the first and third steps involve only rotations while the second step involves only translation along a manifold geodesic, namely a straight line segment.

The translational and rotational motion of the rigid knife-edge corresponding to the above steps can be expressed as

$$\begin{aligned}x(t) &= \begin{cases} x^0, & t \in [0, t_1) \\ x^0 + \gamma^1 V_2 (t - t_1), & t \in [t_1, t_2) \\ x^f, & t \in [t_2, t_f] \end{cases} \\ \gamma(t) &= \begin{cases} e^{S(e_3)\omega_1 t} \gamma^0, & t \in [0, t_1) \\ \gamma^1, & t \in [t_1, t_2) \\ e^{S(e_3)\omega_3(t-t_2)} \gamma^1, & t \in [t_2, t_f] \end{cases} \\ \sigma(t) &= \begin{cases} e^{S(e_3)\omega_1 t} \sigma^0, & t \in [0, t_1) \\ \sigma^1, & t \in [t_1, t_2) \\ e^{S(e_3)\omega_3(t-t_2)} \sigma^1, & t \in [t_2, t_f] \end{cases} \\ \nu(t) &= e_3, \quad t \in [0, t_f],\end{aligned}$$

where  $\sigma^0 = S(e_3)\gamma^0$  and  $\sigma^1 = S(e_3)\gamma^1$ .

### 3.4.2 An example controlled maneuver

We consider the following initial and final conditions for a knife-edge maneuver on the flat plane, assuming  $t_1 = 2$ ,  $t_2 = 4$ ,  $t_f = 6$ .

$$x^0 = (2, 2, 0), \quad \gamma^0 = (0, 1, 0),$$

$$x^f = (0, 0, 0), \quad \gamma^f = (1, 0, 0).$$

The control functions that solve this maneuver problem, according to the above prescription, can be expressed as

$$V(t) = \begin{cases} 0, & t \in [0, 2) \\ 1.414, & t \in [2, 4) \\ 0, & t \in [4, 6] \end{cases}$$

$$\omega(t) = \begin{cases} 1.178, & t \in [0, 2) \\ 0, & t \in [2, 4) \\ 1.178, & t \in [4, 6] \end{cases}$$

The complete description of the translational and rotational motion of the knife-edge, in completing this maneuver, is given as follows:

$$x(t) = \begin{cases} (2, 2, 0), & t \in [0, 2) \\ (2, 2, 0) - (1, 1, 0)(t - 2), & t \in [2, 4) \\ (0, 0, 0), & t \in [4, 6] \end{cases}$$

$$\gamma(t) = \begin{cases} (-\sin(1.178t), \cos(1.178t), 0), & t \in [0, 2) \\ (-1, -1, 0)/\sqrt{2}, & t \in [2, 4) \\ (-c_3 + s_3, -s_3 - c_3, 0)/\sqrt{2}, & t \in [4, 6] \end{cases}$$

$$\sigma(t) = \begin{cases} (-\cos(1.178t), -\sin(1.178t), 0), & t \in [0, 2) \\ (1, -1, 0)/\sqrt{2}, & t \in [2, 4) \\ (c_3 + s_3, s_3 - c_3, 0)/\sqrt{2}, & t \in [4, 6] \end{cases}$$

$$\nu(t) = e_3, \quad t \in [0, t_f],$$

where  $s_3 = \sin(1.178(t - 4))$  and  $c_3 = \cos(1.178(t - 4))$ .

## 3.5 Knife-edge moving on the surface of a sphere

Here, we assume that the knife-edge is constrained to the surface of a sphere, a compact manifold in  $\mathbb{R}^3$ , given by

$$M = \mathbb{S}_R^2 = \{x \in \mathbb{R}^3 : \|x\|^2 - R^2 = 0\}, \quad (3.11)$$

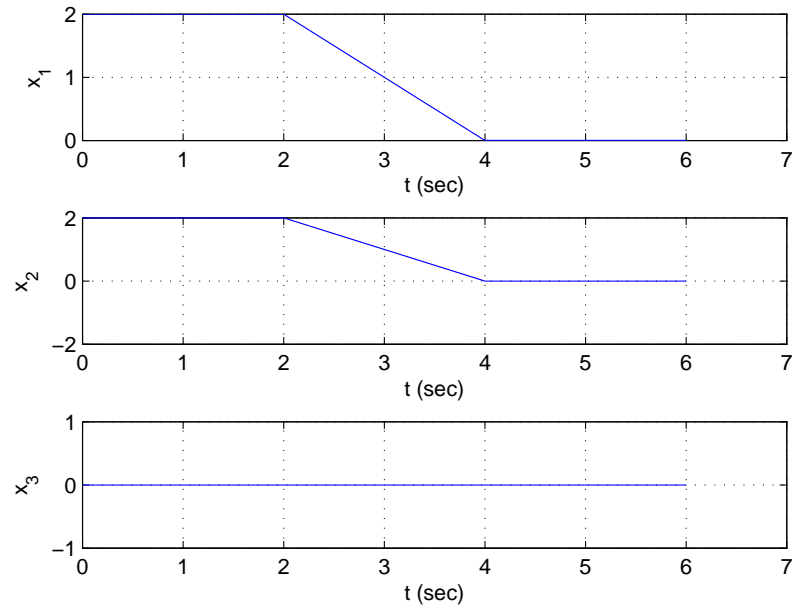


FIGURE 3.2: Position of the knife edge moving on a flat surface.

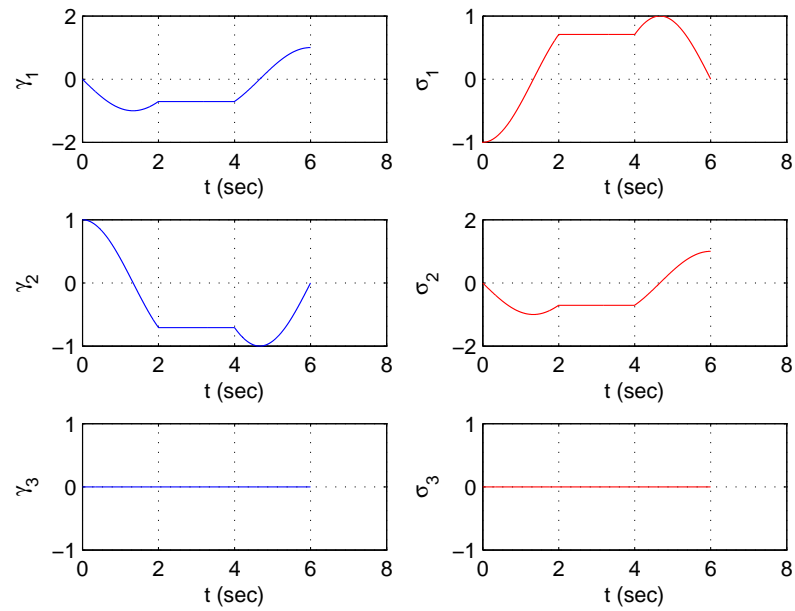


FIGURE 3.3: Direction of the knife edge moving on a flat surface.

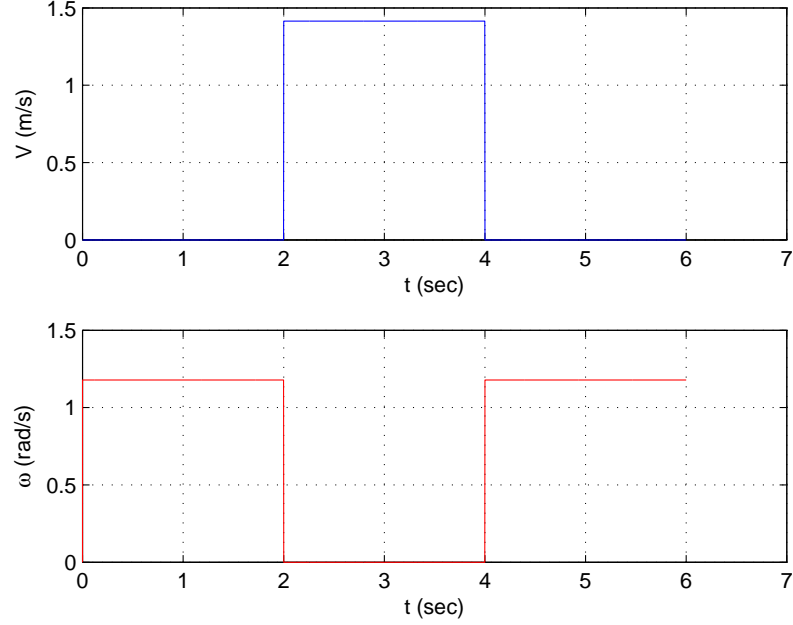


FIGURE 3.4: Control effort for the knife edge moving on a flat surface.

where  $R > 0$ . The configuration manifold is

$$Q = \{(x, \gamma) \in \mathbb{S}_R^2 \times \mathbb{S}^2 : \gamma \in T_x \mathbb{S}_R^2\}. \quad (3.12)$$

The vector function for the scaled normal vector is  $n(x) = \frac{x}{R}$ , so that the matrix function  $N(x) = \frac{I_{3 \times 3}}{R}$ .

### 3.5.1 Control equations and controllability

The kinematics of the knife-edge moving on a sphere are given by

$$\dot{x} = V\gamma, \quad (3.13)$$

$$\dot{\gamma} = \omega S\left(\frac{x}{R}\right)\gamma - \frac{V}{R^2}x, \quad (3.14)$$

or equivalently by

$$\dot{x} = -VS\left(\frac{x}{R}\right)\sigma, \quad (3.15)$$

$$\dot{\sigma} = \omega S\left(\frac{x}{R}\right)\sigma. \quad (3.16)$$

The equations of motion are globally defined on the configuration manifold and

they do not have any singularities or ambiguities.

The equations of motion can also be expressed in terms of an attitude angle in the tangent plane that described the direction of the knife-edge and a latitude angle and a longitude angle that describe the position vector of the knife-edge on the sphere. These equations, not given here, necessarily have singularities that limit their domain of definition.

Based on equations (3.13) and (3.14), the control vector fields given by

$$g_1(q) = \frac{1}{R^2} \begin{bmatrix} R^2 \gamma \\ -x \end{bmatrix},$$

$$g_2(q) = \frac{1}{R} \begin{bmatrix} 0 \\ S(x) \gamma \end{bmatrix}.$$

The following Lie bracket is computed:

$$[g_1, g_2](q) = \frac{1}{R} \begin{bmatrix} -S(x) \gamma \\ 0 \end{bmatrix}.$$

It can be shown that

$$\text{rank} \begin{bmatrix} g_1 & g_2 & [g_1, g_2] \end{bmatrix} (q) = 3, \forall q \in Q.$$

Therefore, the knife-edge is controllable on the surface of a sphere and it can be maneuvered so that it moves from any initial point on  $Q$  to any prescribed final point on  $Q$ .

### 3.5.2 Motion planning

We follow the strategy described previously to describe a solution to the motion planning problem. In particular, the path connecting  $x^0 \in M$  to  $x^f \in M$  is taken as the intersection of a plane containing  $x^0$ ,  $x^f$ , 0 and the sphere; this defines the arc of a great circle path between these two points, which necessarily lies in the surface of the sphere.

Suppose that  $0 \leq t_1 \leq t_2 \leq t_f$ . The initial and final configurations define the initial and final attitude vectors:

$$\sigma^0 = S\left(\frac{x^0}{R}\right) \gamma^0, \quad \sigma^f = S\left(\frac{x^f}{R}\right) \gamma^f,$$

$$\nu_0 = \frac{x^0}{R}, \quad \nu_f = \frac{x^f}{R}.$$

Assume that  $x^0$  and  $x^f$  are not parallel and let  $\sigma^1$  denote the unit vector (normal to

the plane formed by  $x^0$  and  $x^f$ ) given by

$$\sigma^1 = \frac{S(x^0)x^f}{\|S(x^0)x^f\|}.$$

Define the three scalars

$$\begin{aligned}\omega_1 &= \frac{1}{t_1} \tan^{-1} \left( \frac{R\sigma^{0T}x^f}{\sigma^{0T}\sigma^1\|S(x^0)x^f\|} \right), \\ V_2 &= \frac{R}{t_2 - t_1} \tan^{-1} \left( \frac{R^4 - (x^{0T}x^f)^2}{x^{0T}x^f\|S(x^0)x^f\|} \right), \\ \omega_3 &= \frac{1}{t_f - t_2} \tan^{-1} \left( \frac{R\sigma^{fT}x^0}{\sigma^{fT}\sigma^1\|S(x^0)x^f\|} \right).\end{aligned}$$

A solution of the maneuver problem is given as follows:

**Step 1:** Set  $V = 0$ ,  $\omega = \omega_1$ ,  $0 \leq t < t_1$ . This step can be shown to rotate the knife edge about the normal attitude vector  $\frac{x^0}{R}$  from  $\gamma^0$  at time 0 to  $\gamma^1$  at time  $t_1$ .

**Step 2:** Set  $V = V_2$ ,  $\omega = 0$ ,  $t_1 \leq t < t_2$ . This step can be shown to translate the knife edge in the direction of the attitude heading vector from  $x^0$  at time  $t_1$  to  $x^f$  at time  $t_2$ . The attitude heading vector of the knife-edge rotates about the attitude vector  $\sigma$  as required to maintain satisfaction of the nonholonomic constraint.

**Step 3:** Set  $V = 0$ ,  $\omega = \omega_3$ ,  $t_2 \leq t \leq t_f$ . This step can be shown to rotate the knife edge about the normal attitude vector  $\frac{x^f}{R}$  from  $\gamma^1$  at time  $t_2$  to  $\gamma^f$  at time  $t_f$ .

Note that if  $x^0$  is parallel to  $x^f$ , then we let  $\sigma^1 = \sigma^0$  at  $t_1 = 0$ , i.e., Step 1 is skipped. Moreover, if  $x^0 = x^f$ , then  $t_2 = t_1 = 0$ , i.e., both Step 1 and Step 2 are skipped.

In this case the first and third steps involve only rotations while the second step involves only translation along a manifold geodesic, namely the arc segment of a great circle.

The translational and rotational motion of the rigid knife-edge corresponding to

the above steps can be expressed as

$$\begin{aligned}
 x(t) &= \begin{cases} x^0, & t \in [0, t_1) \\ e^{S(\sigma^1)} \bar{V}_2(t - t_1) x^0, & t \in [t_1, t_2) \\ x^f, & t \in [t_2, t_f] \end{cases} \\
 \gamma(t) &= \begin{cases} e^{S(\frac{x^0}{R})} \omega_1 t \gamma^0, & t \in [0, t_1) \\ e^{S(\sigma^1)} \bar{V}_2(t - t_1) \gamma^1, & t \in [t_1, t_2) \\ e^{S(\frac{x^f}{R})} \omega_3(t - t_2) \gamma^2, & t \in [t_2, t_f] \end{cases} \\
 \sigma(t) &= \begin{cases} e^{S(\frac{x^0}{R})} \omega_1 t \sigma^0, & t \in [0, t_1) \\ \sigma^1, & t \in [t_1, t_2) \\ e^{S(\frac{x^f}{R})} \omega_3(t - t_2) \sigma^1, & t \in [t_2, t_f] \end{cases} \\
 \nu(t) &= \frac{x(t)}{R}, \quad t \in [0, t_f]
 \end{aligned}$$

where  $\bar{V}_2 = \frac{V_2}{R}$ ,  $= S(\sigma^1) \frac{x^0}{R}$ , and  $\gamma^2 = S(\sigma^1) \frac{x^f}{R}$ .

### 3.5.3 An example controlled maneuver

We consider the following initial and final conditions for a knife-edge maneuver on the surface of a sphere with radius  $R = 2$  and  $t_1 = 2$ ,  $t_2 = 4$ ,  $t_f = 6$ .

$$\begin{aligned}
 x^0 &= (0, 0, 2), \quad \gamma^0 = (0, 1, 0), \\
 x^f &= (-\sqrt{2}, \sqrt{2}, 0), \quad \gamma^f = \left(-\frac{1}{\sqrt{2}}, -\frac{1}{\sqrt{2}}, 0\right).
 \end{aligned}$$

The control functions that solve this maneuver problem, according to the above prescription, can be expressed as

$$V(t) = \begin{cases} 0, & t \in [0, 2) \\ \pi/2, & t \in [2, 4) \\ 0, & t \in [4, 6] \end{cases}$$

$$\omega(t) = \begin{cases} \pi/8, & t \in [0, 2) \\ 0, & t \in [2, 4) \\ \pi/4, & t \in [4, 6] \end{cases}$$



The complete description of the translational and rotational motion of the knife-edge, in completing this maneuver, is given as follows:

$$\begin{aligned}
 x(t) &= \begin{cases} (0, 0, 2), & t \in [0, 2) \\ (-\sqrt{2}s_2, \sqrt{2}s_2, 2c_2), & t \in [2, 4) \\ (-\sqrt{2}, \sqrt{2}, 0), & t \in [4, 6] \end{cases} \\
 \gamma(t) &= \begin{cases} (-\sin(\pi t/8), \cos(\pi t/8), 0), & t \in [0, 2) \\ (-c_2/\sqrt{2}, c_2/\sqrt{2}, -s_2), & t \in [2, 4) \\ (-s_3/\sqrt{2}, -s_3/\sqrt{2}, -c_3), & t \in [4, 6] \end{cases} \\
 \sigma(t) &= \begin{cases} (-\cos(\pi t/8), -\sin(\pi t/8), 0), & t \in [0, 2) \\ (-1, -1, 0)/\sqrt{2}, & t \in [2, 4) \\ (-c_3/\sqrt{2}, -c_3/\sqrt{2}, s_3), & t \in [4, 6] \end{cases} \\
 \nu(t) &= 0.5x(t), \quad t \in [0, t_f]
 \end{aligned}$$

where  $s_2 = \sin(\pi(t - 2)/4)$ ,  $c_2 = \cos(\pi(t - 2)/4)$ ,  $s_3 = \sin(\pi(t - 4)/4)$ , and  $c_3 = \cos(\pi(t - 4)/4)$ .

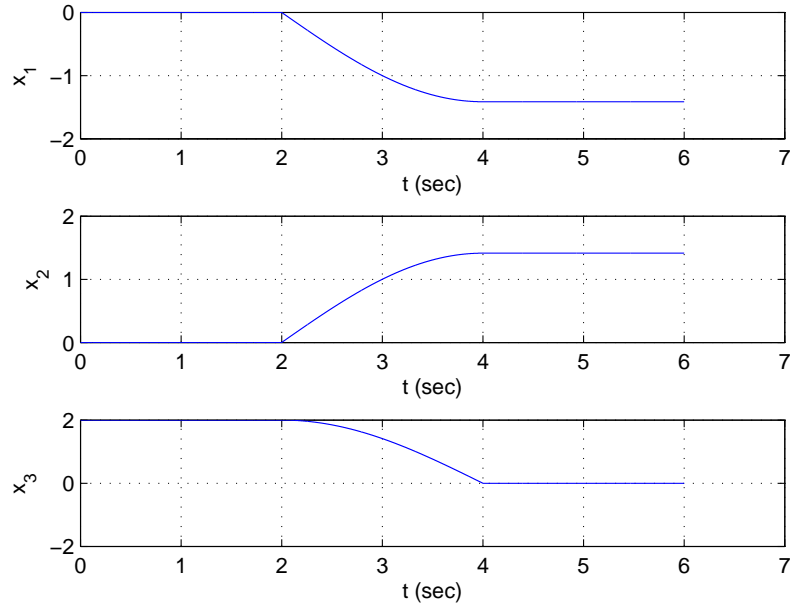


FIGURE 3.5: Position of the knife edge moving on a flat surface.

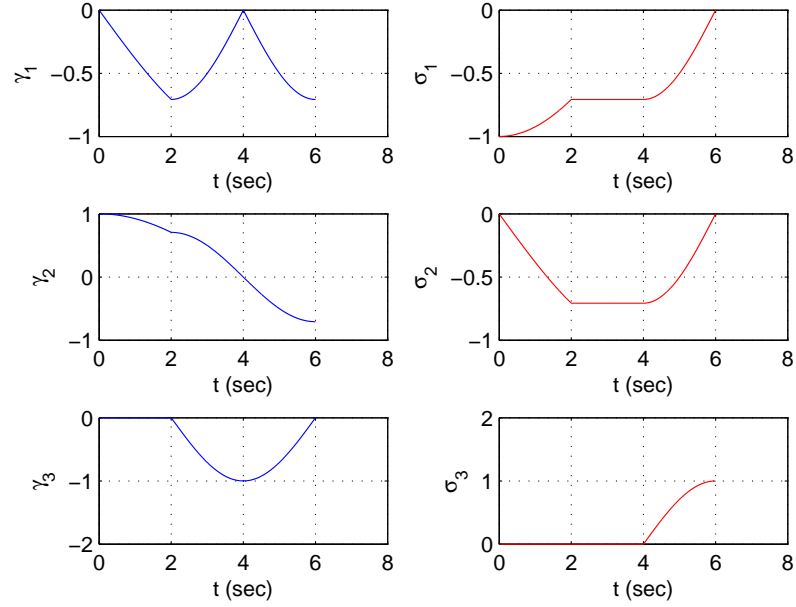


FIGURE 3.6: Direction of the knife edge moving on a flat surface.

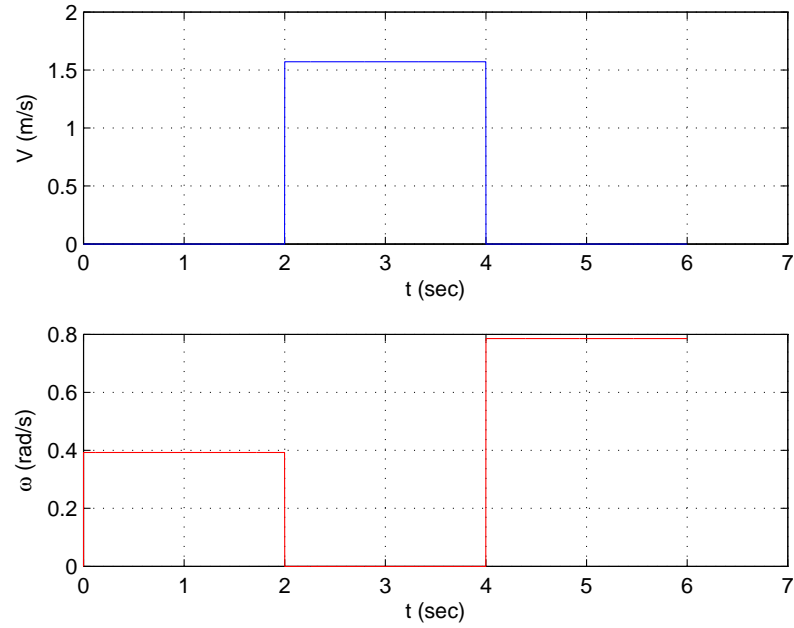


FIGURE 3.7: Control effort for the knife edge moving on a flat surface.

## 3.6 Knife-edge moving on the surface of a hyperboloid

In this section, we study the motion planning problem for a knife edge moving on the surface of a hyperboloid using our new formulation in (McClamroch et al, 2017). Assuming that the motion of the knife-edge is controlled by the axial velocity of the knife-edge and the turn rate of the knife-edge, we formulate the kinematics as a drift-free nonholonomic control system. We then make comments about nonlinear controllability and provide a solution of the path planning problem. Our main contributions in this paper are (i) the development of a motion planning algorithm for a knife edge moving on the surface of a hyperboloid and (ii) the demonstration of the effectiveness of the algorithm via simulation results.

Consider the surface of a hyperboloid defined by the two-dimensional manifold

$$M = \{x \in \mathbb{R}^3 : \phi(x) = x_1^2 + x_2^2 - x_3^2 - 1 = 0\}. \quad (3.17)$$

The explicit expressions for  $n(x)$  and  $N(x)$  are given by

$$n(x) = \frac{1}{\sqrt{1 + 2x_3^2}} \begin{bmatrix} x_1 \\ x_2 \\ -x_3 \end{bmatrix} \quad (3.18)$$

and

$$N(x) = \frac{1}{\sqrt{1 + 2x_3^2}} \begin{bmatrix} 1 & 0 & -\frac{2x_1x_3}{1+2x_3^2} \\ 0 & 1 & -\frac{2x_2x_3}{1+2x_3^2} \\ 0 & 0 & -\frac{1}{1+2x_3^2} \end{bmatrix}. \quad (3.19)$$

### 3.6.1 Motion planning

We first note that the hyperboloid given by (3.17) is a one-sheeted circular hyperboloid, which can be described as a surface of revolution obtained by rotating a hyperbola about the perpendicular bisector to the line between the foci. As can be seen in Figure 3.8, it is a ruled surface, i.e., it belongs to an important class of quadratic surfaces that can be generated by an infinite number of straight lines. That means, every point on the curved surface is also part of one or more straight lines lying on the surface. It is a doubly ruled surface, which means that there are two distinct set of straight lines that can generate the same hyperboloid (Hilbert et al, 1999).

We first note that at every point on the surface of the hyperboloid, the ruled

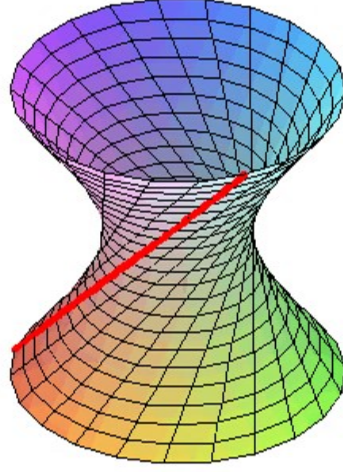


FIGURE 3.8: Hyperboloid as a ruled surface.

straight lines can be determined using the following parameterizations:

$$x_1 = \cos u \mp v \sin u, \quad (3.20)$$

$$x_2 = \sin u \pm v \cos u, \quad (3.21)$$

$$x_3 = \pm v. \quad (3.22)$$

Assume that the initial and final position and direction vectors are given by  $(x^0, \gamma^0)$  and  $(x^f, \gamma^f)$ , respectively. A natural approach for the knife-edge maneuver problem is to construct a path in  $M$  that connects  $x^0 \in M$  and  $x^f \in M$ . Let  $x^1$  and  $x^2$  denote two points on the unit circle corresponding to  $x_3 = 0$ , which lie on the ruled straight lines passing through  $x^0$  and  $x^f$ , respectively. We select the path as the concatenation of the ruled straight line that connects  $x^0$  to  $x^1$ , a circular arc that connects  $x^1$  to  $x^2$  on the unit circle, and the final ruled straight line that connects  $x^2$  to  $x^f$ .

Using (3.20)-(3.22),  $x^1$  and  $x^2$  can be computed as

$$u_1 = \tan^{-1} \frac{x_2^0 - x_1^0 x_3^0}{x_1^0 + x_2^0 x_3^0}, \quad x^1 = (\cos u_1, \sin u_1, 0),$$

$$u_2 = \tan^{-1} \frac{x_2^f - x_1^f x_3^f}{x_1^f + x_2^f x_3^f}, \quad x^2 = (\cos u_2, \sin u_2, 0).$$

Suppose that  $0 \leq t_1 \dots \leq t_6 \leq t_f$ . A solution of the maneuver problem can now be given as follows:

**Step 1:** Let  $\nu^0 = n(x^0)$  and compute

$$\gamma^1 = \frac{x^1 - x^0}{\|x^1 - x^0\|}, \omega_1 = \frac{1}{t_1} \tan^{-1} \frac{\nu^0 \cdot S(\gamma^0)\gamma^1}{\gamma^0 \cdot \gamma^1}$$

If  $\gamma^1 = \gamma^0$ , then set  $V = \omega = 0$ ,  $t_1 = 0$  and go to Step 3. Else set  $V = 0$ ,  $\omega = \omega_1$ ,  $0 \leq t < t_1$ . This step can be shown to rotate the knife edge about the normal vector  $\nu^0$  from  $\gamma^0$  at time 0 to  $\gamma^1$  at time  $t_1$ .

**Step 2:** If  $x^1 = x^0$ , then set  $V = \omega = 0$ ,  $t_2 = t_1$  and go to Step 3. Else compute

$$V_2 = \frac{1}{t_2 - t_1} \|x^1 - x^0\|$$

and set  $V = V_2, \omega = 0$ ,  $t_1 \leq t < t_2$ . This step can be shown to translate the knife edge in the direction of the heading vector  $\gamma^1$  from  $x^0$  at time  $t_1$  to  $x^1$  at time  $t_2$ .

**Step 3:** Let  $\nu^1 = n(x^1)$  and compute

$$\gamma^2 = S(e_3)\nu^1, \omega_3 = \frac{1}{t_3 - t_2} \tan^{-1} \frac{\nu^1 \cdot S(\gamma^1)\gamma^2}{\gamma^1 \cdot \gamma^2}$$

Then set  $V = 0$ ,  $\omega = \omega_3$ ,  $t_2 \leq t < t_3$ . This step can be shown to rotate the knife edge about the normal vector  $\nu^1$  from  $\gamma^1$  at time  $t_2$  to  $\gamma^2$  at time  $t_3$ .

**Step 4:** If  $x^2 = x^1$ , then set  $V = \omega = 0$ ,  $t_4 = t_3$  and go to Step 5. Else compute

$$V_4 = \frac{1}{t_4 - t_3} \tan^{-1} \frac{e_3 \cdot S(x^1)x^2}{x^1 \cdot x^2}$$

and set  $V = V_4, \omega = 0$ ,  $t_3 \leq t < t_4$ . This step can be shown to translate the knife edge along the circular arc from  $x^1$  at time  $t_3$  to  $x^2$  at time  $t_4$ .

**Step 5:** Let  $\nu^2 = n(x^2)$  and compute

$$\gamma^3 = \frac{x^f - x^2}{\|x^f - x^2\|}, \omega_5 = \frac{1}{t_5 - t_4} \tan^{-1} \frac{\nu^2 \cdot S(\gamma^2)\gamma^3}{\gamma^2 \cdot \gamma^3}.$$

Then set  $V = 0$ ,  $\omega = \omega_5$ ,  $t_4 \leq t < t_5$ . This step can be shown to rotate the knife edge about the normal vector  $\nu^2$  from  $\gamma^2$  at time  $t_4$  to  $\gamma^3$  at time  $t_5$ .

**Step 6:** If  $x^f = x^2$ , then set  $V = \omega = 0$ ,  $t_6 = t_5$  and go to Step 7. Else compute

$$V_6 = \frac{1}{t_6 - t_5} \|x^f - x^2\|$$

and set  $V = V_6, \omega = 0$ ,  $t_5 \leq t < t_6$ . This step can be shown to translate the knife edge in the direction of the heading vector  $\gamma^3$  from  $x^2$  at time  $t_5$  to  $x^f$  at time  $t_6$ .

**Step 7:** Let  $\nu^f = n(x^f)$  and compute

$$\omega_7 = \frac{1}{t_f - t_6} \tan^{-1} \frac{\nu^f \cdot S(\gamma^3) \gamma^f}{\gamma^3 \cdot \gamma^f}.$$

Then set  $V = 0$ ,  $\omega = \omega_7$ ,  $t_6 \leq t < t_7$ . This step can be shown to rotate the knife edge about the normal vector  $\nu^f$  from  $\gamma^3$  at time  $t_6$  to  $\gamma^f$  at time  $t_7$ .

### 3.6.2 Simulation

We now illustrate the ideas developed in the previous sections through computer simulations of a knife-edge moving on the surface of the hyperboloid with  $(t_1, t_2, \dots, t_f) = (2, 4, \dots, 14)$ . We implement the control algorithm described in Section 3.6.1 for the following initial and final conditions:

$$x_0 = (2.828, 3, 4), \quad \gamma_0 = (0, 0.8, 0.6),$$

$$x_f = (2.828, -3, -4), \quad \gamma_f = (0, 0.8, 0.6).$$

Figures 3.9-3.12 show the results of the simulation. The controlled knife-edge trajectory is shown in Figure 3.9. Figures 3.10 and 3.11 show the time responses of  $x$  and  $\gamma$ , respectively. The time responses of  $V$  and  $\omega$  are shown in Figure 3.12.

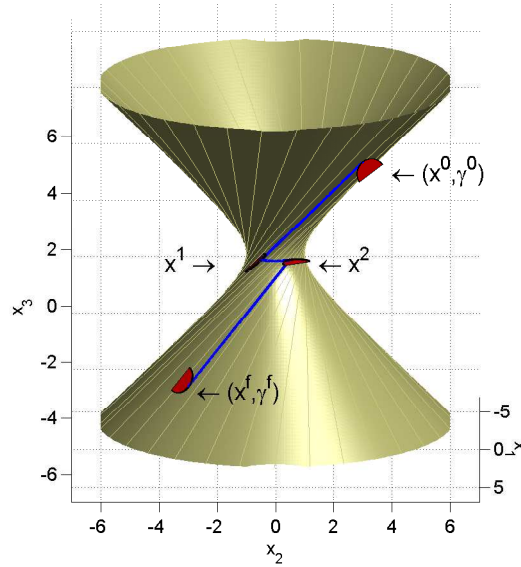
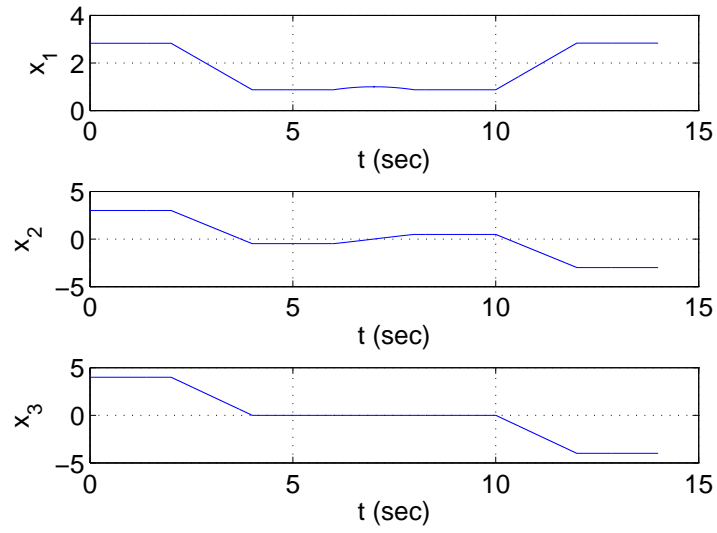
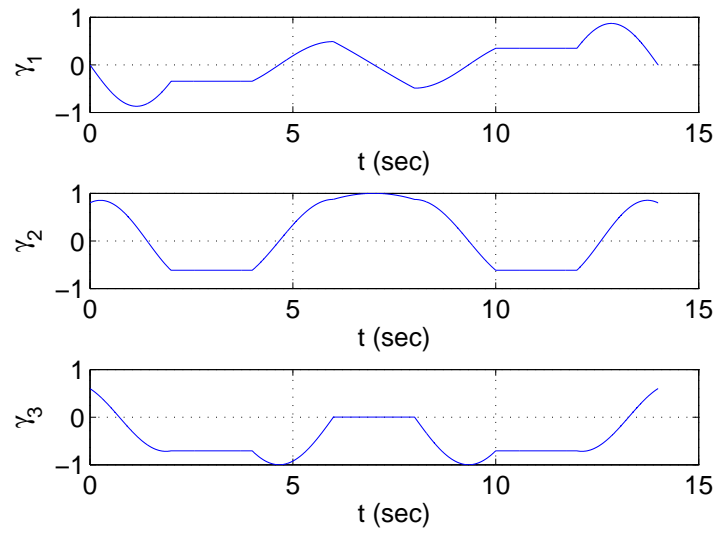
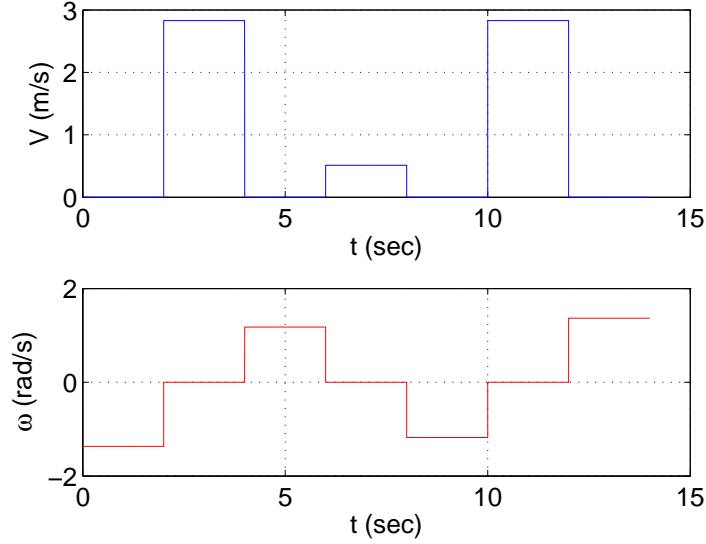


FIGURE 3.9: Knife-edge trajectory.

FIGURE 3.10: Time response of  $x$ .FIGURE 3.11: Time response of  $\gamma$ .

FIGURE 3.12: Time responses of  $V$  and  $\omega$ .

### 3.7 Knife-edge moving on the surface of a torus

Let  $x \in M \subset \mathbb{R}^3$  denote the position vector of the contact point of the knife-edge in the Euclidean frame and consider the surface of a torus, which is the surface of revolution generated by revolving a circle about an axis, coplanar with the circle, that does not touch the circle. It is assumed that the torus has major radius  $R > 0$ , which is the distance from the axis of the torus to the center of the circle, and minor axis  $0 < r < R$ , which is the radius of the revolved circle. The surface of the torus can be defined by the two-dimensional manifold

$$M = \left\{ x \in \mathbb{R}^3 : \phi(x) = \left( R - \sqrt{(x_1)^2 + (x_2)^2} \right)^2 + (x_3)^2 - r^2 = 0 \right\}. \quad (3.23)$$

The explicit expressions for  $n(x)$  and  $N(x)$  are given by

$$n(x) = \frac{1}{r\sqrt{(x_1)^2 + (x_2)^2}} \begin{bmatrix} x_1 \left( \sqrt{(x_1)^2 + (x_2)^2} - R \right) \\ x_2 \left( \sqrt{(x_1)^2 + (x_2)^2} - R \right) \\ x_3 \sqrt{(x_1)^2 + (x_2)^2} \end{bmatrix} \quad (3.24)$$



and

$$N(x) = \frac{1}{r} \begin{bmatrix} 1 - R(x_2)^2 \left( \sqrt{(x_1)^2 + (x_2)^2} \right)^{-3} & Rx_1x_2 \left( \sqrt{(x_1)^2 + (x_2)^2} \right)^{-3} & 0 \\ Rx_1x_2 \left( \sqrt{(x_1)^2 + (x_2)^2} \right)^{-3} & 1 - R(x_1)^2 \left( \sqrt{(x_1)^2 + (x_2)^2} \right)^{-3} & 0 \\ 0 & 0 & 1 \end{bmatrix}. \quad (3.25)$$

We can write the equations (3.1) and (3.2) in the form of a driftless-control-affine nonlinear system as

$$\dot{q} = g_1(q)V + g_2(q)w. \quad (3.26)$$

Here the configuration vector is  $q = (x, \gamma)$ , so the control vector fields are defined as

$$g_1(q) = \begin{bmatrix} \gamma \\ -(\gamma^T N(x) \gamma) n(x) \end{bmatrix},$$

$$g_2(q) = \begin{bmatrix} 0 \\ S(n(x))\gamma \end{bmatrix}.$$

It can be shown that

$$\text{rank} \begin{bmatrix} g_1 & g_2 & [g_1, g_2] \end{bmatrix} (q) = 3, \forall q \in Q.$$

Therefore, the knife-edge is controllable on the surface of the torus and it can be maneuvered so that it moves from any initial point on  $Q$  to any prescribed final point on  $Q$ .

### 3.7.1 Motion planning

We first note that the parametric equations for the surface of the torus are given by

$$x_1 = (R + r \cos v) \cos u, \quad (3.27)$$

$$x_2 = (R + r \cos v) \sin u, \quad (3.28)$$

$$x_3 = r \sin v, \quad (3.29)$$

where  $(u, v) \in \mathbb{R}^2$ .

Assume that the initial and final position and direction vectors are given by  $(x^0, \gamma^0)$  and  $(x^f, \gamma^f)$ , respectively. A natural approach for the knife-edge maneuver problem is to construct a path in  $M$  that connects  $x^0 \in M$  and  $x^f \in M$ . Let  $x^1 = (x_1^1, x_2^1, 0)$  and  $x^2 = (x_1^2, x_2^2, 0)$  denote two points on the surface of the torus such that  $x^1$  lies on the same small circle as  $x^0$  and  $x^2$  lies on the same small circle as  $x^f$ . Clearly,  $x^1$  and  $x^2$  lie on the large outer circle of radius  $R + r$ .

Using (3.27)-(3.29), we can compute the parameters  $u_0$  and  $u_f$  corresponding to

$x^0$  and  $x^f$ , respectively, as

$$u_0 = \tan^{-1} \left( \frac{x_2^0}{x_1^0} \right), \quad (3.30)$$

$$u_f = \tan^{-1} \left( \frac{x_2^f}{x_1^f} \right). \quad (3.31)$$

We can now determine the intermediate points  $x^1$  and  $x^2$  as

$$x^1 = (R + r)(\cos u_0, \sin u_0, 0), \quad (3.32)$$

$$x^2 = (R + r)(\cos u_f, \sin u_f, 0). \quad (3.33)$$

In what follows, we define  $\nu^i = n(x^i)$ .

Suppose that  $0 \leq t_1 \dots \leq t_6 \leq t_f$ . A solution of the maneuver problem can now be given as follows:

**Step 1:** Let  $\sigma^1 = S(\nu^0)\nu^1$  and  $\gamma^1 = S(\sigma^1)\nu^0$ . Then, compute

$$\omega_1 = \frac{1}{t_1} \tan^{-1} \frac{\nu^0 \cdot S(\gamma^0)\gamma^1}{\gamma^0 \cdot \gamma^1}. \quad (3.34)$$

If  $\gamma^1 = \gamma^0$ , then set  $V = \omega = 0$ ,  $t_1 = 0$  and go to Step 2. Else set  $V = 0$ ,  $\omega = \omega_1$ ,  $0 \leq t < t_1$ . This step can be shown to rotate the knife edge about the normal vector  $\nu^0$  from  $\gamma^0$  at time 0 to  $\gamma^1$  at time  $t_1$ .

**Step 2:** If  $x^1 = x^0$ , then set  $V = \omega = 0$ ,  $t_2 = t_1$  and go to Step 3. Else compute

$$V_2 = \frac{r}{t_2 - t_1} \tan^{-1} \left( \frac{\sigma^1 \cdot S(\nu^0)\nu^1}{\nu^0 \cdot \nu^1} \right), \quad (3.35)$$

and set  $V = V_2$ ,  $\omega = 0$ ,  $t_1 \leq t < t_2$ . This step can be shown to translate the knife edge along the small circular arc from  $x^0$  at time  $t_1$  to  $x^1$  at time  $t_2$ .

**Step 3:** Compute  $\gamma^2 = S(\sigma^1)\nu^1$  and

$$\begin{aligned} \sigma^3 &= \frac{S(x^1)x^2}{\|S(x^1)x^2\|}, \quad \gamma^3 = S(\sigma^3)\nu^1, \\ \omega_3 &= \frac{1}{t_3 - t_2} \tan^{-1} \left( \frac{\nu^1 \cdot S(\gamma^2)\gamma^3}{\gamma^2 \cdot \gamma^3} \right). \end{aligned} \quad (3.36)$$

Then set  $V = 0$ ,  $\omega = \omega_3$ ,  $t_2 \leq t < t_3$ . This step can be shown to rotate the knife edge about the normal vector  $\nu^1$  from  $\gamma^2$  at time  $t_2$  to  $\gamma^3$  at time  $t_3$ .

**Step 4:** If  $x^2 = x^1$ , then set  $V = \omega = 0$ ,  $t_4 = t_3$  and go to Step 5. Else compute

$$V_4 = \frac{R + r}{t_4 - t_3} \tan^{-1} \left( \frac{\sigma^3 \cdot S(x^1)x^2}{x^1 \cdot x^2} \right) \quad (3.37)$$

and set  $V = V_4, \omega = 0, t_3 \leq t < t_4$ . This step can be shown to translate the knife edge along the large circular arc from  $x^1$  at time  $t_3$  to  $x^2$  at time  $t_4$ .

**Step 5:** Compute  $\gamma^4 = S(\sigma^3)\nu^2$  and

$$\begin{aligned}\sigma^5 &= S(\nu^2)\nu^f, \quad \gamma^5 = S(\sigma^5)\nu^2, \\ \omega_5 &= \frac{1}{t_5 - t_4} \tan^{-1} \left( \frac{\nu^2 \cdot S(\gamma^4)\gamma^5}{\gamma^4 \cdot \gamma^5} \right).\end{aligned}\tag{3.38}$$

Then set  $V = 0, \omega = \omega_5, t_4 \leq t < t_5$ . This step can be shown to rotate the knife edge about the normal vector  $\nu^2$  from  $\gamma^4$  at time  $t_4$  to  $\gamma^5$  at time  $t_5$ .

**Step 6:** If  $x^f = x^2$ , then set  $V = \omega = 0, t_6 = t_5$  and go to Step 7. Else compute

$$\begin{aligned}\sigma^6 &= S(\nu^2)\nu^f, \quad \gamma^6 = S(\sigma^6)\nu^f, \\ V_6 &= \frac{r}{t_6 - t_5} \tan^{-1} \left( \frac{\sigma^6 \cdot S(\nu^2)\nu^f}{\nu^2 \cdot \nu^f} \right),\end{aligned}\tag{3.39}$$

and set  $V = V_6, \omega = 0, t_5 \leq t < t_6$ . This step can be shown to translate the knife edge along the small circular arc from  $x^2$  at time  $t_5$  to  $x^f$  at time  $t_6$ .

**Step 7:** Compute

$$\omega_7 = \frac{1}{t_f - t_6} \tan^{-1} \left( \frac{\nu^f \cdot S(\gamma^6)\gamma^f}{\gamma^6 \cdot \gamma^f} \right).\tag{3.40}$$

Then set  $V = 0, \omega = \omega_7, t_6 \leq t \leq t_f$ . This step can be shown to rotate the knife edge about the normal vector  $\nu^f$  from  $\gamma^6$  at time  $t_6$  to  $\gamma^f$  at time  $t_f$ .

### 3.7.2 Simulation

We now illustrate the ideas developed in the previous sections through computer simulations of a knife-edge moving on the surface of a torus with  $R = 5, r = 2$ , and  $(t_1, t_2, \dots, t_f) = (2, 4, \dots, 14)$ . We implement the control algorithm described in the previous section for the following initial and final conditions:

$$x^0 = (-3, 4, 2), \quad \gamma^0 = (0.7071, -0.7071, 0),$$

$$x^f = (5, 0, 2), \quad \gamma^f = (0.7071, -0.7071, 0).$$

Figures 3.13-3.16 show the results of the simulation. The controlled knife-edge trajectory is shown in Figure 3.13. Figures 3.14 and 3.15 show the time responses of position and direction vectors, respectively. The time responses of the speed and turn rate are shown in Figure 3.16.

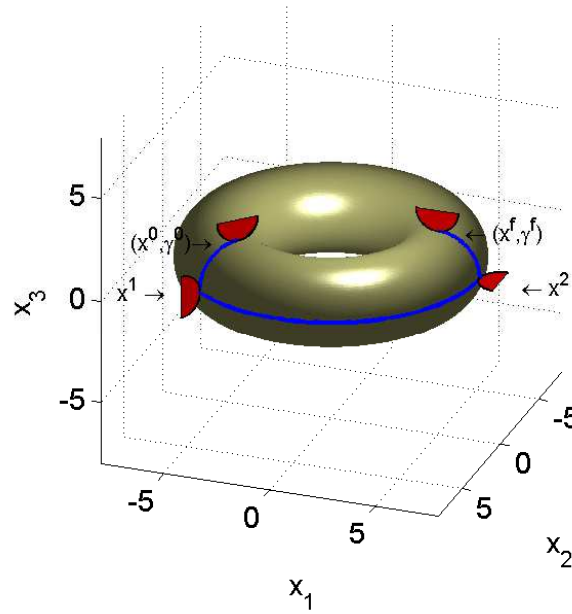
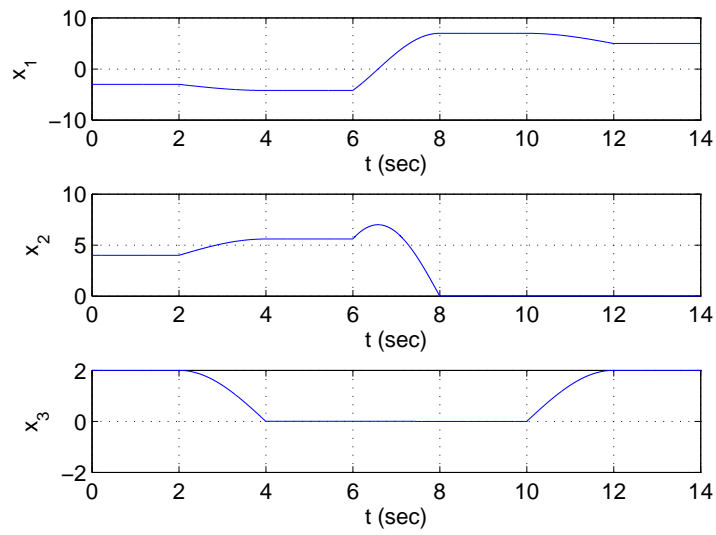
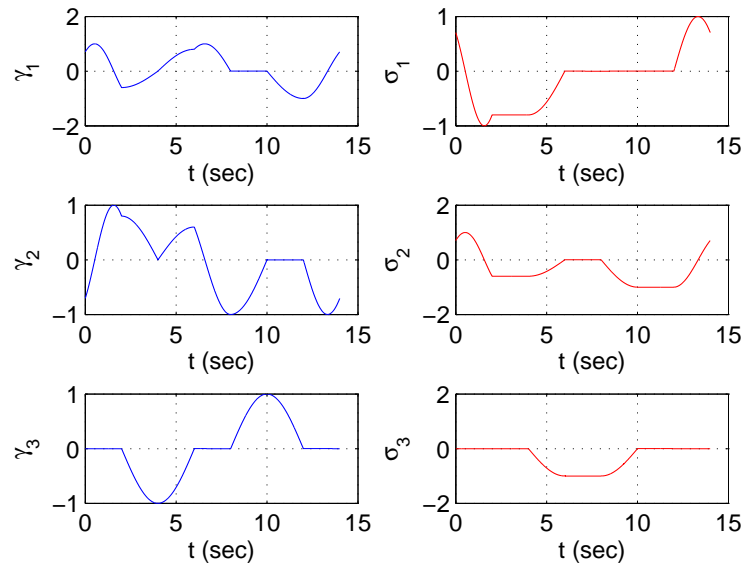
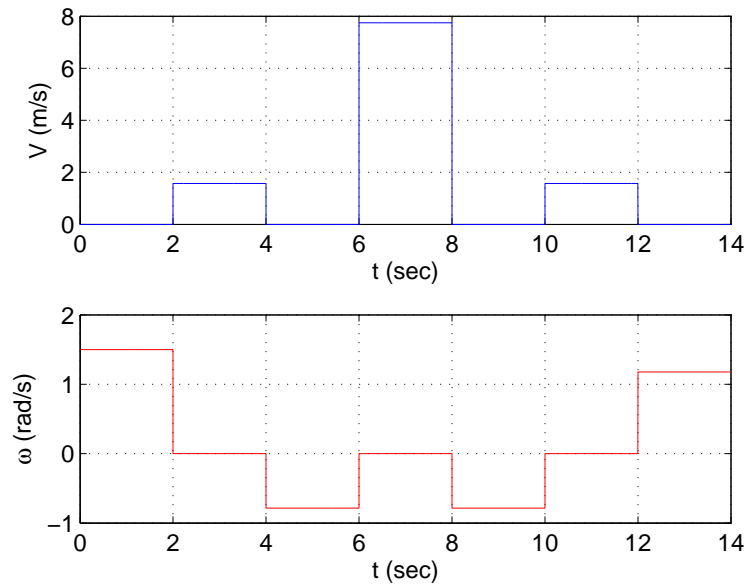


FIGURE 3.13: The trajectory of the knife edge.

FIGURE 3.14: Position  $x$ .

FIGURE 3.15: Direction vectors  $\gamma$  and  $\sigma$ .FIGURE 3.16: Speed  $V$  and turn rate  $\omega$ .

## 3.8 Conclusions and extensions

The focus in this chapter has been on the nonholonomic constraint equation and the associated knife-edge kinematics. The problem of controlling a knife-edge moving on a smooth surface embedded in  $\mathbb{R}^3$  has been studied. The results are based on new formulations of the translational and rotational kinematics equations, including the nonholonomic knife-edge constraint, that are globally defined on the surface and capture the rigid body motion of the knife-edge in three-dimensions.

The geometries of different surfaces allow development of analytical expressions for the knife-edge motions in the proposed maneuvers. It is possible to formulate the knife-edge dynamics, using methods of dynamic extension, and to develop associated control results for such nonholonomic dynamics. In other words, the development in Bloch et al (1992), expressed in terms of local coordinates, can be extended to a globally defined geometric formulation following the methods used in this chapter.

## Chapter 4

# Control of Rolling Disk Motion on an Arbitrary Smooth Surface

This chapter studies the motion of a vertical rolling disk on an arbitrary smooth surface in  $\mathbb{R}^3$ . The disk can roll without slipping about its axis and turn about the surface normal. A global formulation for the dynamics of the rolling disk is proposed without the use of local coordinates, and the model is globally defined on the manifold without singularities or ambiguities. The theoretical results are specialized for two different surfaces; a flat surface and a spherical surface. The proposed motion planning algorithm consists of three phases and each phase is a rest-to-rest maneuver, such that the rolling disk is stationary at both the start and the end of each phase. Simulation results are included that show effectiveness of the motion planning algorithm on the smooth surfaces.

### 4.1 Introduction

A (vertical) disk rolling on a flat surface is one of the basic and widely studied systems in classical mechanics. In these studies, the disk is treated as a rigid body that can roll on the surface without slipping. The disk remains upright during the motion and can be steered (turned) about the surface normal. If the motion of the rolling disk is controlled by the rolling and steering accelerations (which can be expressed in terms of rolling and steering torques through the respective moments of inertia), the control problem for the rolling disk can be formulated as a nonholonomic control problem. The nonholonomic constraints of a homogeneous vertical disk are explained in Bloch. (2003); Neimark et al (1972), where the kinematics of the system are given using local variables. Feedback control law for the trajectory tracking of a disk rolling on a horizontal plane is proposed in Yavin et al (1999).

The literature on nonholonomic control problems is large, both in terms of theoretical results and studies of specific physical examples in the context of robot manipulation, wheeled mobile robotic systems, and space robotic systems (see e.g., Li et al

(1990); Murray et al (1994); Osborne et al (2005); Young et al (2000)). A few representative control works include the study of controllability and stabilizability in Bloch et al (1992, 1991); motion planning in Ito (2015); Reyhanoglu (1994); and feedback stabilization and tracking in Astolfi (1996); Ishikawa et al (2008); Jiang et al (1999, 1995); Sordalen et al (1995). This literature is based on the use of mathematical models that are expressed in terms of local coordinates for the configuration vector. This use of local coordinates is a significant limitation in some physical examples, where non-local or even global results are desired. Formulations using Lie group manifolds can be found in Jurdjevic (1993); Leonard et al (1995); Morin et al (2003, 2008), and references therein.

In our recent work McClamroch et al (2017), we have studied the kinematics of a knife-edge on an arbitrary smooth surface (smooth embedded manifold) in  $\mathbb{R}^3$  using ideas from geometric mechanics. In McClamroch et al (2017), a nonlinear system model is derived that is globally defined on the manifold without singularities or ambiguities. The formulation describes the constrained translation of the point of contact of the knife-edge on the surface and the constrained attitude of the knife-edge as a rigid body. These equations for the knife-edge kinematics in  $\mathbb{R}^3$  are expressed in a geometric form, without the use of local coordinates; they are globally defined without singularities or ambiguities. The development in McClamroch et al (2017) follows the results in Lee et al (2009) and the book Lee et al (2017). This formulation has been applied to different smooth surfaces including a flat surface, a spherical surface, and the surface of a hyperboloid Rehan et al (2007).

In this article, we study the dynamics of a rolling disk on an arbitrary smooth surface (smooth embedded manifold) using tools from geometric mechanics. Assuming that the motion of the rolling disk is controlled by the rolling and steering accelerations, we formulate the dynamics as a nonholonomic control system. We then make comments about nonlinear controllability and provide a solution of the motion control problem. The theoretical results are specialized for two specific surfaces defined in  $\mathbb{R}^3$ , namely a flat surface and the surface of a stationary sphere. Our main contributions in this chapter are (i) the dynamic formulation and controllability analysis for a vertical disk rolling on the surface of an arbitrary smooth surface in  $\mathbb{R}^3$ , (ii) the development of a motion planning algorithm, and (iii) the demonstration of the effectiveness of the algorithm via simulation results.

## 4.2 Dynamics of a rolling disk

Consider a smooth connected manifold embedded in  $\mathbb{R}^3$  given by

$$M = \{x \in \mathbb{R}^3 : \phi(x) = 0\},$$

where  $\phi : \mathbb{R}^3 \rightarrow \mathbb{R}^1$  is a differentiable function that satisfies  $\frac{\partial \phi(x)}{\partial x} \neq 0, x \in M$ . The manifold is assumed to be connected. As usual, the notation  $T_x M$  denotes the



tangent plane of the manifold at  $x \in M$ , which is given by

$$T_x M = \left\{ \xi \in \mathbb{R}^n : \left( \frac{\partial \phi(x)}{\partial x} \cdot \xi \right) = 0 \right\}.$$

The disk is assumed to be a rigid body that maintains a single point of contact with the surface. Let  $x \in M \subset \mathbb{R}^3$  denote the position vector of the contact point of the rolling disk in the Euclidean frame and let  $\gamma \in \mathbb{S}^2 \subset \mathbb{R}^3$  be the heading direction vector of the rolling disk as shown in Figure 4.1. As usual  $\mathbb{S}^2$  denotes the unit sphere, a smooth manifold embedded in  $\mathbb{R}^3$ . The configuration vector is  $q = (x, \gamma) \in M \times \mathbb{S}^2$  and

$$Q = \{(x, \gamma) \in M \times \mathbb{S}^2 : \gamma \in T_x M\} \quad (4.1)$$

is the configuration manifold. Note that the rolling angle of the disk (Bloch, , 2003) is not included in the definition of the configuration space as it is not considered to be part of the control problem. This is consistent with the modeling of a unicycle or Hilare-type mobile robot (see e.g., Young et al (2000)).

Let  $n \in \mathbb{S}^2$  be the unit normal of the surface at the point of contact. A right hand Euclidean frame, fixed to the rolling disk with origin located at the point of contact, is defined by introducing the unit vector  $\sigma = n \times \gamma \in \mathbb{S}^2$  (see Figure 4.1). It follows that  $\sigma \in T_x M$ .

Let  $S : \mathbb{R}^3 \rightarrow \mathbb{R}^{3 \times 3}$  denote the skew-symmetric matrix representing the cross product operator on  $\mathbb{R}^3$  given by

$$S(x) = \begin{bmatrix} 0 & -x_3 & x_2 \\ x_3 & 0 & -x_1 \\ -x_2 & x_1 & 0 \end{bmatrix}.$$

The following result can now be stated:

**Proposition 4.1:** *The kinematics of a disk of radius  $r$  with rolling rate  $\omega_r$  about its axis parallel to  $\sigma$  and steering rate  $\omega$  about the normal axis  $n = n(x)$  are given by*

$$\dot{x} = r\omega_r \gamma, \quad (4.2)$$

$$\dot{\gamma} = \omega_s S(n(x)) \gamma - r\omega_r (\gamma^T N(x) \gamma) n(x), \quad (4.3)$$

where

$$n(x) = \frac{\partial \phi(x)}{\partial x} / \left\| \frac{\partial \phi(x)}{\partial x} \right\|$$

and

$$N(x) = \frac{\partial n(x)}{\partial x}.$$

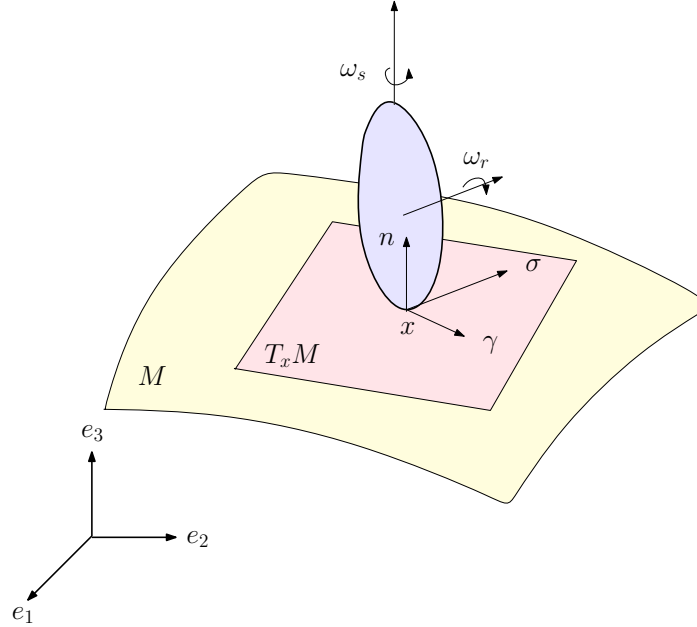


FIGURE 4.1: Disk rolling on a smooth surface.

**Proof:** The disk is assumed to roll without slipping so that it translates with a speed  $V = r\omega_r$  only in the heading direction; thus it satisfies the nonholonomic constraint given by (4.2). Since  $\gamma \in \mathbb{S}^2$  is allowed to rotate with the angular velocity vector  $\omega_s n(x)$ , its time rate of change in the tangent plane  $T_x M$  is given by  $S(\omega_s n(x))\gamma$ . The time rate of change along the normal to the tangent plane  $T_x M$  due to the translational motion is of the form  $r\omega_r h(x, \gamma)n(x)$ . Therefore,  $\dot{\gamma}$  can be expressed as

$$\dot{\gamma} = \omega_s S(n(x))\gamma + r\omega_r h(x, \gamma)n(x),$$

where  $h(x, \gamma)$  is a scalar function to be determined using the geometric properties of the configuration manifold  $Q$ . Clearly,  $n^T \dot{\gamma} = r\omega_r h(x, \gamma)$ . Since  $n^T \gamma = 0 \Rightarrow n^T \dot{\gamma} + \dot{n}^T \gamma = 0$ , it follows that  $n^T \dot{\gamma} = -\gamma^T \dot{n} = -r\omega_r \gamma^T N(x)\gamma$ . Therefore,  $h(x, \gamma) = -\gamma^T N(x)\gamma$ , and thus the equation (4.3) follows. ■

In what follows, we will consider the dynamic extension of (4.2), (4.3) given by

$$\dot{x} = r\omega_r \gamma, \tag{4.4}$$

$$\dot{\gamma} = \omega_s S(n(x))\gamma - r\omega_r (\gamma^T N(x)\gamma)n(x), \tag{4.5}$$

$$\dot{\omega}_r = u_1, \tag{4.6}$$

$$\dot{\omega}_s = u_2, \tag{4.7}$$

where the control inputs  $u_1$  and  $u_2$  correspond to the rolling and steering accelerations,

respectively, which can be expressed in terms of rolling and steering torques through the respective moments of inertia.

Note that the knife edge model in McClamroch et al (2017) is a drift-free system (where Chow's theorem is used straightforwardly to prove controllability), whereas the rolling disk model described by (4.4)-(4.7) is a nonlinear system with drift. As such, nonlinear controllability analysis and motion planning algorithm development become much more involved. The rolling disk model introduced here is consistent with the dynamic model of a unicycle or Hilare-type mobile robot (see e.g., Young et al (2000)). In other words, the dynamic extension given by (4.4)-(4.7) represents the dynamic equations of motion for such robots. The significance of our formulation above is that it provides a global description of the robot dynamics on any smooth surface, without singularities or ambiguities.

**Remark:** *For simplicity in presenting the main ideas, the effect of gravity has been ignored in the formulation above assuming that there is a physical mechanism based on electromagnetic or electrostatic principles that generate forces/torques that counteract the effect due to gravity. For example, it is possible to design an electromagnet-based rolling disk configured to adhere to and roll over a ferrous spherical surface.*

### 4.3 Controllability and motion planning

Let  $z = (x, \gamma, \omega_r, \omega_s)$  denote the state. Equations (4.4)-(4.7) define a drift vector field

$$f(z) = (r\omega_r\gamma, \omega_s S(n(x))\gamma - r\omega_r(\gamma^T N(x)\gamma)n(x), 0, 0)$$

and control vector fields  $g_1 = (0, 0, 1, 0)$ ,  $g_2 = (0, 0, 0, 1)$ , according to the standard control system form

$$\dot{z} = f(z) + \sum_{i=1}^2 g_i u_i. \quad (4.8)$$

Note that an equilibrium solution  $z^e$ , corresponding to  $u = 0$ , of equation (4.8) has the form  $z^e = (x^e, \gamma^e, 0, 0)$ ,  $(x^e, \gamma^e) \in Q$ ; i.e., an equilibrium solution corresponds to a motion of the system for which all the configuration variables remain constant. In the subsequent sections, it will be shown for the flat surface and spherical surface cases that the space spanned by the vectors

$$g_1, g_2, [g_1, f], [g_2, f], [g_2, [f, [g_1, f]]]$$

has dimension 5 at any equilibrium solution. Since the above spanning Lie brackets are all good and the bad brackets of order 1 and 3 are zero at the equilibrium solution  $z^e$ , Sussmann's sufficient conditions for small time local controllability Sussmann (1987) are satisfied. Clearly, the system is a real analytic system, and therefore there exist both time-invariant piecewise analytic feedback laws Sussmann et al (1979) and time-

periodic continuous feedback laws Coron (1995) which asymptotically stabilize  $z^e$ .

Let  $t_f \geq 0$  and consider the problem of determining the control inputs, namely the rolling acceleration and the steering acceleration  $(u_1, u_2) : [0, t_f] \rightarrow \mathbb{R}^2$ , that transfers the initial rest configuration  $q^0 = (x^0, \gamma^0) \in Q$  at time 0 to the final rest configuration  $q^f = (x^f, \gamma^f) \in Q$  at time  $t_f$ . The initial position and initial attitude of the rolling disk satisfy  $x^0 \in M$ ,  $\gamma^0 \in T_{x^0}M$  and  $\sigma^0 = S(n^0)\gamma^0$ ,  $n^0 = n(x^0)$ ; the final position and final attitude of the rolling disk at completion of the maneuver satisfy  $x^f \in M$ ,  $\gamma^f \in T_{x^f}M$  and  $\sigma^f = S(n^f)\gamma^f$ ,  $n^f = n(x^f)$ .

There are many possible approaches to motion planning problems that have been proposed in the literature. Several possible construction approaches involve the use of the spanning brackets, sums of sinusoids, or switchings of the control. Here we propose a rest-to-rest motion planning approach that makes use of the geometry of the rolling disk problem.

A natural approach for the rolling disk maneuver problem is to construct a smooth path in  $M$  that connects  $x^0 \in M$  and  $x^f \in M$ . As in our recent work McClamroch et al (2017), we select the path that is the intersection of  $M$  and a transversal plane, which connects  $x^0 \in M$  and  $x^f \in M$ . This path defines an initial heading direction  $\gamma^1 \in T_{x^0}M$  and a final heading direction  $\gamma^2 \in T_{x^f}M$ . The motion planning problem then involves the following procedure:

**Step 1:** Set  $u_1 = 0$ , choose the steering acceleration  $u_2$  to rotate the initial heading direction  $\gamma^0$  to the heading direction  $\gamma^1$  required to move along the determined path.

**Step 2:** Set  $u_2 = 0$ , choose the rolling acceleration  $u_1$  of the rolling disk to translate the disk along the determined path.

**Step 3:** Set  $u_1 = 0$ , choose the steering acceleration  $u_2$  to rotate the heading direction  $\gamma^2$  at the end of the path to the desired terminal heading direction  $\gamma^f$ .

Figures 4.2 and 4.3 illustrate one possible way to design the controls  $u_1$  and  $u_2$  to accomplish the above steps. Let  $T > 0$  and for  $i = 0, 1, 2$  define

$$u_{[iT, (i+1)T)}(\omega^*) = \begin{cases} \frac{2}{T}\omega^*, & t \in [iT, (i+\frac{1}{2})T) \\ -\frac{2}{T}\omega^*, & t \in [(i+\frac{1}{2})T, (i+1)T) \end{cases} \quad (4.9)$$

The control inputs in Figures 4.2 and 4.3 correspond to

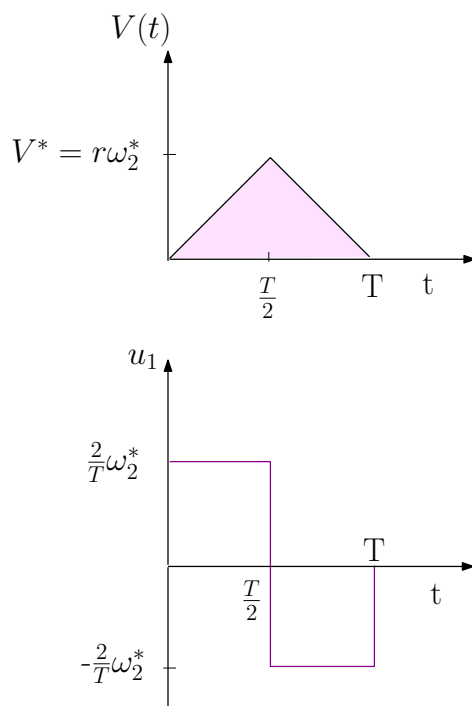
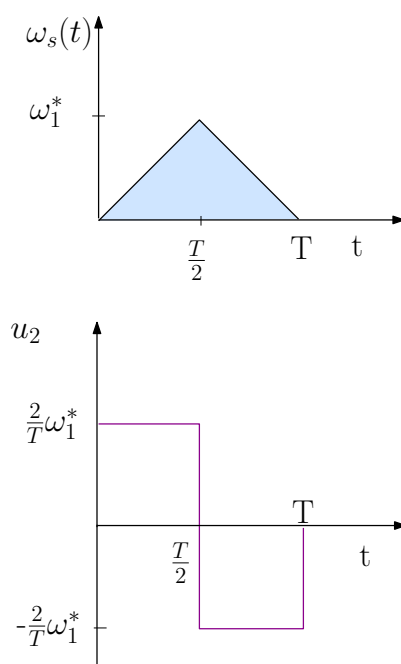
$$u_1 = u_{[0, T)}(\omega_r^*), \quad u_2 = u_{[0, T)}(\omega_s^*),$$

where  $\omega_r^*$  and  $\omega_s^*$  are to be determined from the initial and final configurations.

## 4.4 Disk rolling on a flat surface

Consider a disk rolling on a flat surface. The constraint manifold is given by

$$M = \{x \in \mathbb{R}^3 : e_3^T x = 0\}$$

FIGURE 4.2: Rolling in the direction of  $\gamma$ .FIGURE 4.3: Steering about the surface normal  $n$ .

and the configuration manifold is

$$Q = \{(x, \gamma) \in \mathbb{R}^3 \times \mathbb{S}^2 : e_3^T \gamma = 0\}.$$

The vector function for the scaled normal vector is  $n(x) = e_3$ , so that the matrix function  $N(x) = 0$ . The dynamics of the disk on the flat surface are given as

$$\dot{x} = r\omega_r\gamma, \tag{4.10}$$

$$\dot{\gamma} = \omega_s S(e_3)\gamma, \tag{4.11}$$

$$\dot{\omega}_r = u_1, \tag{4.12}$$

$$\dot{\omega}_s = u_2. \tag{4.13}$$

#### 4.4.1 Controllability

Based on equations (4.10)-(4.13), the drift vector field is given by  $f(z) = (r\omega_r\gamma, \omega_s S(e_3)\gamma, 0, 0)$  and the control vector fields are  $g_1 = (0, 0, 1, 0)$ ,  $g_2 = (0, 0, 0, 1)$ . The following Lie brackets can be computed:

$$\begin{aligned} [g_1, f] &= (r\gamma, 0, 0, 0), \quad [g_2, f] = (0, S(e_3)\gamma, 0, 0, 0), \\ [g_2, [f, [g_1, f]]] &= (rS(e_3)\gamma, 0, 0, 0). \end{aligned}$$

The space spanned by the vectors

$$g_1, g_2, [g_1, f], [g_2, f], [g_2, [f, [g_1, f]]]$$

has dimension 5 at any equilibrium solution  $z^e$ . Since the above spanning Lie brackets are all good and the bad brackets of order 1 and 3 are zero at  $z^e$ , Sussmann's sufficient conditions for small time local controllability Sussmann (1987) are satisfied. Again since the system is a real analytic system, there exist both time-invariant piecewise analytic feedback laws and time-periodic continuous feedback laws which asymptotically stabilize  $z^e$ .

#### 4.4.2 Motion planning

We follow the strategy described previously to develop a solution to the rest-to-rest motion planning problem. In particular, the path connecting  $x_0 \in M$  to  $x_f \in M$  is taken as the straight line path between these two points, which necessarily lies on the flat surface.

Without loss of generality, assume that  $x^f \neq x^0$  and  $\gamma^f \neq \gamma^0$ . Also, for simplicity, let  $t_i = iT$ ,  $i = 0, 1, 2$ ,  $T > 0$ , denote the time instants switching is performed. A solution of the maneuver problem can now be given as follows:

**Step 1:** Compute

$$\gamma^1 = \frac{x^f - x^0}{\|x^f - x^0\|}, \quad \omega_s^1 = \frac{2}{T} \tan^{-1} \left( \frac{e_3 \cdot S(\gamma^0) \gamma^1}{\gamma^0 \cdot \gamma^1} \right)$$

and set  $u_1 = 0$ ,  $u_2 = u_{[0,T]}(\omega_s^1)$  to rotate the disk about the normal vector  $e_3$  from  $\gamma^0$  at time 0 to  $\gamma^1$  at time  $T$ .

**Step 2:** Compute

$$\omega_r^2 = \frac{2}{Tr} \|x^f - x^0\|$$

and set  $u_1 = u_{[T,2T]}(\omega_r^2)$ ,  $u_2 = 0$  to roll the disk in the constant heading direction  $\gamma^1$  from  $x^0$  at time  $T$  to  $x^f$  at time  $2T$ .

**Step 3:** Compute

$$\omega_s^3 = \frac{2}{T} \tan^{-1} \left( \frac{e_3 \cdot S(\gamma^1) \gamma^f}{\gamma^1 \cdot \gamma^f} \right)$$

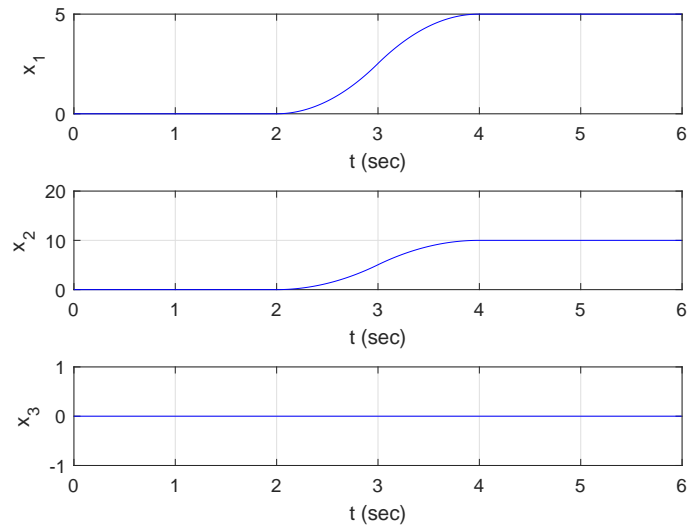
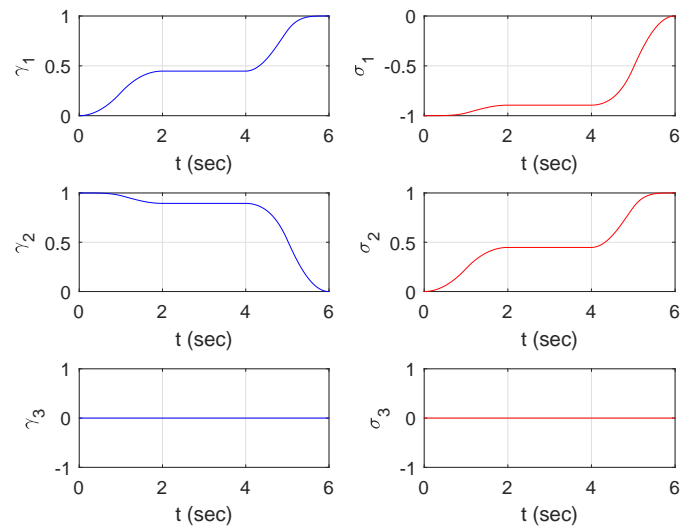
and set  $u_1 = 0$ ,  $u_2 = u_{[2T,3T]}(\omega_s^3)$  to rotate the disk about the normal vector  $e_3$  from  $\gamma^1$  at time  $2T$  to  $\gamma^f$  at time  $3T$ .

### 4.4.3 An example controlled maneuver

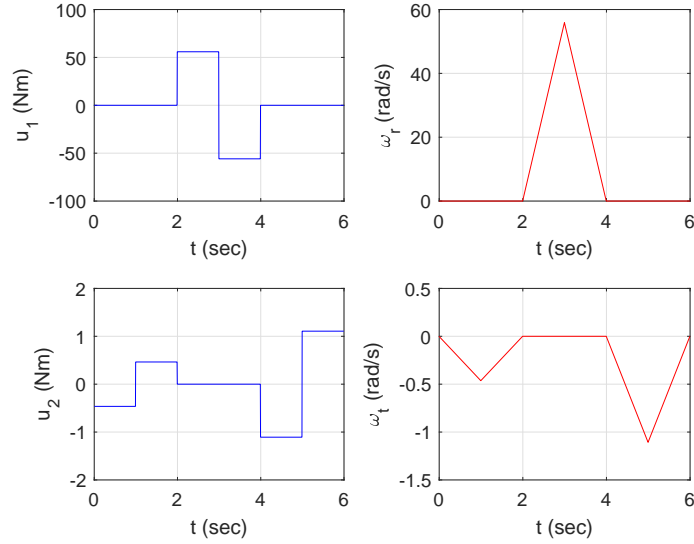
We now illustrate the ideas developed in the previous section through computer simulations of a disk of radius  $r = 0.2$  m on a flat surface with  $T = 2$  s. We implement the 3-Step algorithm described in the previous section for the following initial and final conditions:

$$\begin{aligned} x^0 &= (0, 0, 0), \quad \gamma^0 = (0, 1, 0), \\ x^f &= (5, 10, 0), \quad \gamma^f = (1, 0, 0). \end{aligned}$$

Figures 4.4-4.6 show the results of the simulation.

FIGURE 4.4: Position  $x$  (flat surface case).FIGURE 4.5: Vectors  $\gamma$  and  $\sigma$  (flat surface case).



FIGURE 4.6: Controls  $(u_1, u_2)$  and angular velocities  $(\omega_r, \omega_s)$  (flat surface case).

## 4.5 Disk rolling on a spherical surface

Consider a circular disk rolling on a (stationary) spherical surface as shown in Figure 4.7. Let  $r$  and  $R$  denote the radii of the disk and the spherical surface, respectively. The constraint manifold is given by

$$M = \mathbb{S}_R^2 = \{x \in \mathbb{R}^3 : \|x\|^2 - R^2 = 0\}$$

and the configuration manifold is

$$Q = \{(x, \gamma) \in \mathbb{S}_R^2 \times \mathbb{S}^2 : \gamma \in T_x \mathbb{S}_R^2\}.$$

The vector function for the scaled normal vector is  $n(x) = \frac{x}{R}$ , so that the matrix function  $N(x) = \frac{I_{3 \times 3}}{R}$ .

The dynamics of the disk on the spherical surface are given as

$$\dot{x} = r\omega_r\gamma, \tag{4.14}$$

$$\dot{\gamma} = \omega_s S\left(\frac{x}{R}\right)\gamma - \frac{r\omega_r}{R^2}x, \tag{4.15}$$

$$\dot{\omega}_r = u_1, \tag{4.16}$$

$$\dot{\omega}_s = u_2. \tag{4.17}$$

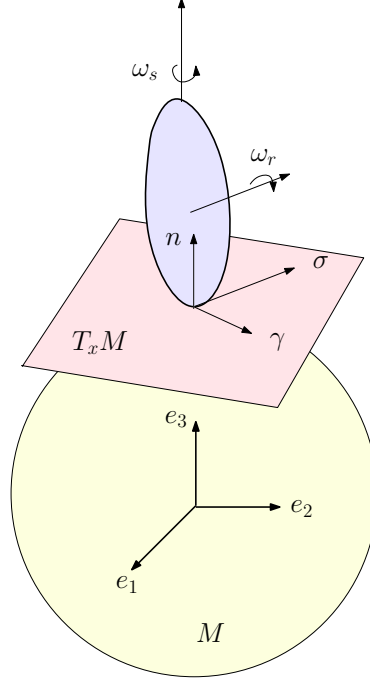


FIGURE 4.7: Disk rolling on a spherical surface.

### 4.5.1 Controllability

Based on equations (4.14)-(4.17), the drift vector field is given by

$$f(z) = \left( r\omega_r\gamma, \omega_s S\left(\frac{x}{R}\right)\gamma - \frac{r\omega_r}{R^2}x, 0, 0 \right)$$

and the control vector fields are  $g_1 = (0, 0, 1, 0)$ ,  $g_2 = (0, 0, 0, 1)$ . The following Lie brackets can be computed:

$$\begin{aligned} [g_1, f] &= \left( r\gamma, -\frac{rx}{R^2}, 0, 0 \right), \quad [g_2, f] = \left( 0, S\left(\frac{x}{R}\right)\gamma, 0, 0 \right), \\ [g_2, [f, [g_1, f]]] &= \left( rS\left(\frac{x}{R}\right)\gamma, 0, 0, 0 \right). \end{aligned}$$

The space spanned by the vectors

$$g_1, g_2, [g_1, f], [g_2, f], [g_2, [f, [g_1, f]]]$$

has dimension 5 at any equilibrium solution  $z^e$ . Since the above spanning Lie brackets are all good and the bad brackets of order 1 and 3 are zero at the equilibrium solution  $z^e$ , Sussmann's sufficient conditions for small time local controllability Sussmann (1987) are satisfied. Again since the system is a real analytic system, there exist both time-invariant piecewise analytic feedback laws and time-periodic continuous

feedback laws which asymptotically stabilize  $z^e$ .

### 4.5.2 Motion planning

We follow the strategy described previously to develop a solution to the rest-to-rest motion planning problem. In particular, the path connecting  $x_0 \in M$  to  $x_f \in M$  is taken as the geodesic path connecting these two points, which necessarily lies on the spherical surface.

Again, without loss of generality, assume that  $x^f \neq x^0$  and  $\gamma^f \neq \gamma^0$ . Also, for simplicity, let  $t_i = iT$ ,  $i = 0, 1, 2$ ,  $T > 0$ , denote the time instants switching is performed. A solution of the maneuver problem can now be given as follows:

**Step 1:** Compute

$$\begin{aligned}\sigma^1 &= S(n^0)n^f, \quad \gamma^1 = S(\sigma^1)n^0 \\ \omega_s^1 &= \frac{2}{T} \tan^{-1} \left( \frac{n^0 \cdot S(\gamma^0)\gamma^1}{\gamma^0 \cdot \gamma^1} \right)\end{aligned}$$

and set  $u_1 = 0$ ,  $u_2 = u_{[0,T)}(\omega_s^1)$  to rotate the disk about the normal vector  $\frac{x^0}{R}$  from  $\gamma^0$  at time 0 to  $\gamma^1$  at time  $T$ .

**Step 2:** Compute

$$\omega_r^2 = \frac{2R}{Tr} \tan^{-1} \left( \frac{\sigma^1 \cdot S(n^0)n^f}{n^0 \cdot n^f} \right)$$

and set  $u_1 = u_{[T,2T)}(\omega_r^2)$ ,  $u_2 = 0$  to roll the disk in the heading direction vector from  $x^0$  at time  $T$  to  $x^f$  at time  $2T$ . The heading vector of the disk rotates about the attitude vector  $\sigma$  as required to maintain satisfaction of the nonholonomic constraint. At time  $2T$ , the heading vector is  $\gamma^2 = S(\sigma^1)n^f$ .

**Step 3:** Compute

$$\omega_s^3 = \frac{2}{T} \tan^{-1} \left( \frac{n^f \cdot S(\gamma^2)\gamma^f}{\gamma^2 \cdot \gamma^f} \right),$$

and set  $u_1 = 0$ ,  $u_2 = u_{[2T,3T)}(\omega_s^3)$  to rotate the disk about the normal vector  $\frac{x^f}{R}$  from  $\gamma^2$  at time  $2T$  to  $\gamma^f$  at time  $3T$ .

### 4.5.3 An example controlled maneuver

We now illustrate the ideas developed in the previous section through computer simulations of a disk of radius  $r = 0.2$  m on a spherical surface with  $R = 2$  m. Again we set  $T = 2$  s. We implement the 3-Step algorithm described in the previous section

for the following initial and final conditions:

$$\begin{aligned} x^0 &= (0, 0, 2), \quad \gamma^0 = (1, 0, 0), \\ x^f &= (\sqrt{2}, -\sqrt{2}, 0), \quad \gamma^f = (1/\sqrt{2}, 1/\sqrt{2}, 0). \end{aligned}$$

Figures 4.8-4.10 show the results of the simulation.

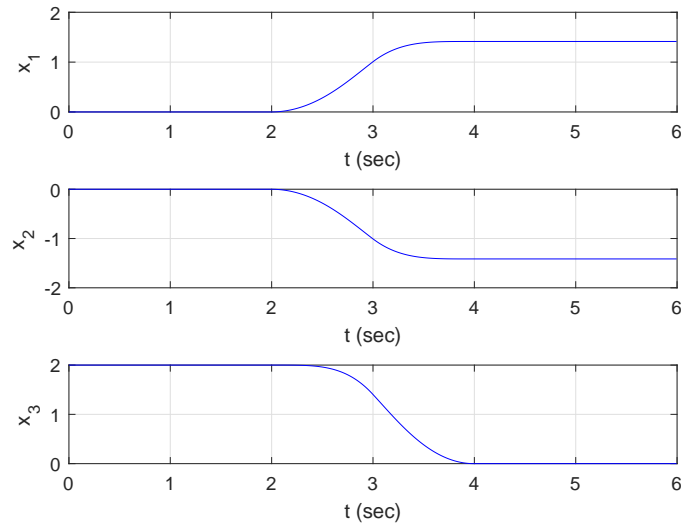
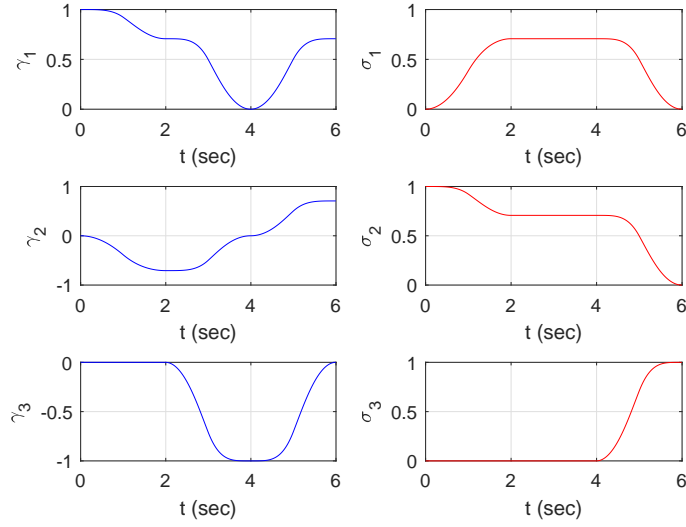
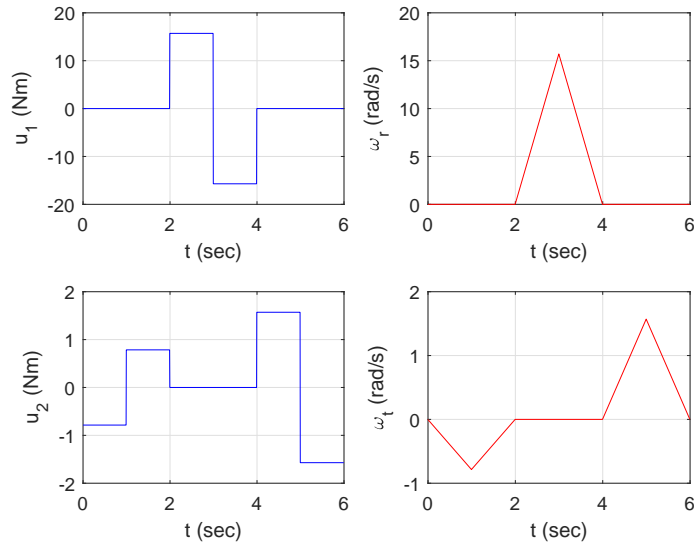


FIGURE 4.8: Position  $x$  (spherical surface case).

FIGURE 4.9: Vectors  $\gamma$  and  $\sigma$  (spherical surface case).FIGURE 4.10: Controls  $(u_1, u_2)$  and angular velocities  $(\omega_r, \omega_s)$  (spherical surface case).

## 4.6 Conclusions

The motion of a disk rolling on an arbitrary smooth surface has been studied. The results are based on new formulations of the dynamics equations that are globally defined on the surface. A motion planning algorithm is proposed for two different surfaces: flat surface and spherical surface. The motion planning algorithm can be extended to more complex geometric surfaces such as surfaces of torus, hyperboloid, and cone. The ideas presented in this chapter can also be extended to the trajectory tracking control of a disk rolling on an arbitrary smooth surface.

# Chapter 5

## Global Formulation and Motion Planning for a Sphere Rolling on a Smooth Surface

In this chapter, we study the motion of a rolling sphere on an arbitrary smooth manifold embedded in  $\mathbb{R}^3$ . The sphere is allowed to roll on the surface without slipping or twisting. A nonlinear control system model describing the kinematics of the sphere is developed in a geometric form so that the model is globally defined without singularities or ambiguities. An algorithm for constructing a path between specified initial and final configurations is presented. The algorithm utilizes the nonholonomic nature of the system. The theoretical results are specialized for two specific surfaces defined in  $\mathbb{R}^3$ , namely a flat surface and the surface of a stationary sphere.

### 5.1 Introduction

The rolling motion of a sphere on a smooth surface without slipping and twisting is an interesting problem in classical mechanics. The motion planning problem for the rolling sphere is categorized as nonholonomic control problem due to non-integrable velocity constraints. The literature on such nonholonomic control problems is large, both in terms of theoretical results and studies of specific physical examples in the context of robot manipulation, wheeled mobile robotic systems, and space robotic systems Murray et al (1994); Li et al (1990); Liu et al (2017); Cheng et al (2017); Petrinic et al (2017). An excellent reference that provides a geometric and control theoretical view of nonholonomic systems is the book by Bloch Bloch. (2003). A few representative control works include the study of controllability and stabilizability in Bloch et al (1992, 1991); motion planning in Reyhanoglu (1994); Murray et al (1993); and feedback stabilization and tracking in Astolfi (1996); Jiang et al (1999); Sordalen et al (1995); Zhao et al (2018).

The research on rolling sphere problem has evolved consistently for more than a

century and mathematicians, physicists and engineers from all around the world have studied various aspects of the problem. That certainly shows the richness and importance of the domain and its applications to science and technology. The theoretical problem has a large number of applications; for example, a spherical mobile robot moving on the surface of an asteroid to collect a sample, where precise control of both position and attitude are required.

The nonholonomic motion of the rolling sphere is explained in Johnson (2007). Geometric aspects for the control of position and orientation of the sphere rolling on a plane is discussed in Jurdjevic (1993); Bicchi et al (1995); Marigo et al (2000). Motion planning algorithms for spherical robots are studied in Minor et al (2002); Svinin et al (2008); Zheng et al (2011). The dynamics of a spherical robot are discussed in Camicia et al (2000), wherein a linear control law for the longitudinal dynamics of the robot is proposed. The rolling motion of a homogeneous ball on an arbitrary surface is studied in Borisov et al (2002). In Shen et al (2008), internal rotors and sliders are proposed as the mechanism for the control of spherical robots. The work in Morin et al (2008) considers a rolling sphere actuated by a moving plate and develops a control algorithm for the stabilization of admissible reference trajectories. In Borisov et al (2012), dynamics and control of a non-symmetric sphere (with rotors) on a plane are discussed and the controllability for the system is shown. Moreover, the influence of rolling friction on the control of the sphere is discussed. The work in Muralidharan et al (2015) derives the dynamics of a spherical robot on a plane in a geometric framework and studies strong accessibility and small-time local controllability for the system. A smooth global tracking controller is proposed for the position trajectories. In Kleinstauber et al (2006), the motion of the rolling sphere on a flat plane is studied and the ideas of slip and twist maneuvers are presented. In the slip maneuver, the sphere moves from a given position to the desired position without changing the attitude. While in the twist maneuver, the sphere rolls in a closed path trajectory to produce a desired twist about the surface normal.

In this chapter, we study the kinematics of a rolling sphere on an arbitrary smooth surface (smooth embedded manifold) using geometric mechanics. The development follows the new formulation introduced in our recent work McClamroch et al (2017) for a simple nonholonomic system. A nonlinear system model is derived that is globally defined on the manifold without singularities or ambiguities. The theoretical results are specialized for two specific surfaces defined in  $\mathbb{R}^3$ , namely a flat surface and the surface of a stationary sphere. A motion planning scheme is proposed that incorporates the slip and twist maneuvers described in Kleinstauber et al (2006).



## 5.2 Kinematics of a sphere rolling on a smooth surface

Consider a Euclidean frame in  $\mathbb{R}^3$  with standard basis vectors  $e_1, e_2, e_3$ . A fixed surface is defined by the two-dimensional connected manifold

$$M = \{x \in \mathbb{R}^3 : \phi(x) = 0\},$$

where  $\phi : \mathbb{R}^3 \rightarrow \mathbb{R}^1$  is a differentiable function that satisfies  $\frac{\partial \phi(x)}{\partial x} \neq 0, x \in M$ . The sphere is assumed to be rigid and have single point of contact with the surface  $M$ . Let  $x \in M \subset \mathbb{R}^3$  denote the position vector of the contact point of the sphere in the Euclidean frame. As usual, the notation  $T_x M$  denotes the tangent plane of the manifold at  $x \in M$ .

$$T_x M = \left\{ \xi \in \mathbb{R}^n : \frac{\partial \phi(x)}{\partial x} \cdot \xi = 0 \right\}.$$

It is assumed that the sphere can roll without slipping or twisting on the smooth surface defined by  $M$ . Consider an actuation plane that has single point of contact with the rolling sphere. Let  $\nu \in \mathbb{S}^2$  be the unit normal to the surface  $M$  at  $x$ , which is given by  $\nu = n(x)$ , where the vector function  $n(x) = \frac{\partial \phi(x)}{\partial x} / \left\| \frac{\partial \phi(x)}{\partial x} \right\|$ . Let  $\gamma$  and  $\sigma$  be two orthogonal basis vectors that span the tangent space  $T_x M$  such that  $\nu = \gamma \times \sigma$ . The actuation plane is always parallel to the tangent plane at the given position  $x \in M$  (see Figure 5.1).

Consider a body-fixed frame  $\{b_1, b_2, b_3\}$  whose origin is at the center of the sphere. The attitude of the sphere  $R \in SO(3)$  is defined by

$$R = \begin{bmatrix} e_1 \cdot b_1 & e_1 \cdot b_2 & e_1 \cdot b_3 \\ e_2 \cdot b_1 & e_2 \cdot b_2 & e_2 \cdot b_3 \\ e_3 \cdot b_1 & e_3 \cdot b_2 & e_3 \cdot b_3 \end{bmatrix}$$

The sphere can roll about a unit vector  $\chi \in T_x M$  with a rate  $\omega \in \mathbb{R}$ . The rolling angular velocity  $\omega \chi$  can be expressed as a linear combination of  $\gamma$  and  $\sigma$  as

$$\omega \chi = \omega_1 \gamma + \omega_2 \sigma.$$

The following result can now be stated:

**Proposition 5.1:** *The kinematics of a sphere of radius  $r_s$  controlled by its rolling*

rate  $\omega$  about an axis  $\chi \in T_x M$  are given by

$$\dot{x} = r_s(\omega_2\gamma - \omega_1\sigma), \quad (5.1)$$

$$\dot{R} = S(\Omega)R, \quad (5.2)$$

$$\dot{\gamma} = -r_s\gamma^T N(x)(\omega_2\gamma - \omega_1\sigma)n(x), \quad (5.3)$$

$$\dot{\sigma} = -r_s\sigma^T N(x)(\omega_2\gamma - \omega_1\sigma)n(x), \quad (5.4)$$

where  $\omega_1 = \omega\gamma^T\chi$ ,  $\omega_2 = \omega\sigma^T\chi$ ,  $N(x) = \frac{\partial n(x)}{\partial x}$ ,  $\Omega \in \mathbb{R}^3$  is the angular velocity of the rolling sphere in inertial frame of reference, and  $S : \mathbb{R}^3 \rightarrow \mathbb{R}^{3 \times 3}$  is the skew-symmetric matrix representing the cross product operator on  $\mathbb{R}^3$ .

**Proof:** Rolling without slipping about  $\gamma$  by  $\omega_1$  yields a velocity of  $-r_s\omega_1\sigma$  and about  $\sigma$  by  $\omega_2$  yields a velocity of  $r_s\omega_2\gamma$ . Thus, the sphere satisfies the nonholonomic constraint given by (5.1). Equation (5.2) describes the attitude kinematics of a rigid body whose angular velocity in the inertial frame is  $\Omega$ .

Since twisting is not allowed, the time rates of change of  $\gamma$  and  $\sigma$  along the normal to the tangent plane  $T_x M$  due to the translational motion should be of the form

$$\dot{\gamma} = h_1(x, \gamma, \sigma, \omega_1, \omega_2)n(x), \quad (5.5)$$

$$\dot{\sigma} = h_2(x, \gamma, \sigma, \omega_1, \omega_2)n(x), \quad (5.6)$$

where  $h_i$ ,  $i = 1, 2$ , are scalar functions to be determined using the geometric properties of the configuration manifold. Clearly,  $\nu^T \dot{\gamma} = h_1$  and  $\nu^T \dot{\sigma} = h_2$ . Since

$$\nu^T \gamma = 0 \Rightarrow \nu^T \dot{\gamma} + \dot{\nu}^T \gamma = 0,$$

it follows that

$$\nu^T \dot{\gamma} = -\gamma^T \dot{\nu} = -\gamma^T N(x)\dot{x}.$$

Therefore,  $h_1 = -r_s\gamma^T N(x)(\omega_2\gamma - \omega_1\sigma)$ , and thus the equation (5.3) follows. Similarly, since

$$\nu^T \sigma = 0 \Rightarrow \nu^T \dot{\sigma} + \dot{\nu}^T \sigma = 0,$$

we have

$$\nu^T \dot{\sigma} = -\sigma^T \dot{\nu} = -\sigma^T N(x)\dot{x}.$$

Therefore,  $h_2 = -r_s\sigma^T N(x)(\omega_2\gamma - \omega_1\sigma)$ , and thus the equation (5.4) follows.  $\blacksquare$

The equations (5.1) and (5.2) describe the coupled translational and rotational kinematics of the sphere rolling on an arbitrary smooth surface. They represent a kinematic control system with the configuration (or state) vector  $q = (x, R) \in M \times SO(3)$  and the control vector  $u = (\omega_1, \omega_2)$ . Note that equations (5.3) and (5.4) describe the actuation condition that there is no twisting. Since  $M$  is a two dimensional manifold and the rotation manifold  $SO(3)$  is a three dimensional Lie

group, it is possible to describe the kinematics using five local coordinates as has been shown in [2].

### 5.3 Sphere rolling on a flat plane

Consider a sphere rolling on a flat horizontal plane defined as

$$M = \{x \in \mathbb{R}^3 : e_3^T x = 0.\}$$

The surface normal for the flat plane is  $\nu = e_3$ , and thus  $N(x) = 0$ . The velocity of the rolling sphere lies in the tangent plane at  $x$ . Let  $\gamma = e_1$  and  $\sigma = e_2$ . Then, the kinematics equations (5.1)-(5.2) simplify to

$$\dot{x} = r_s(\omega_2\gamma - \omega_1\sigma), \quad (5.7)$$

$$\dot{R} = S(\Omega)R, \quad (5.8)$$

and  $\dot{\gamma} = \dot{\sigma} = 0$ . Thus, the configuration vector for the flat surface case is  $q = (x, R) \in M \times SO(3)$ . Here  $\Omega \in \mathbb{R}^3$  is the angular velocity of the rolling sphere, which is given in the inertial frame by

$$\Omega = \omega \begin{bmatrix} \chi \cdot e_1 \\ \chi \cdot e_2 \\ 0 \end{bmatrix}. \quad (5.9)$$

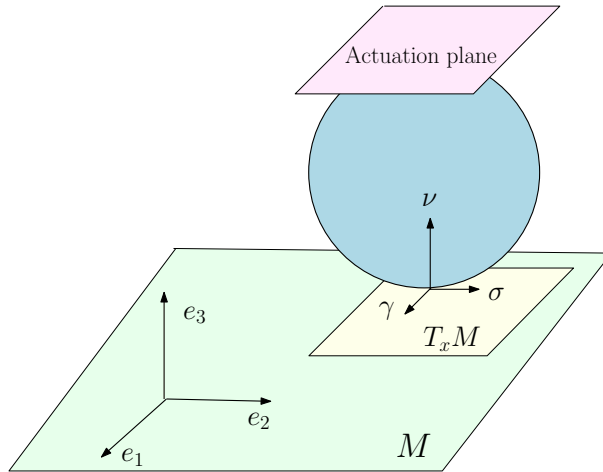


FIGURE 5.1: Sphere rolling on a flat surface.

### 5.3.1 Motion planning

Assume that the initial and final position and attitudes are given by  $(x^0, R^0)$  and  $(x^f, R^f)$ , respectively. A natural approach for solving the rolling sphere maneuver problem is to construct a path in  $M \times SO(3)$  that connects  $(x^0, R^0) \in M \times SO(3)$  and  $(x^f, R^f) \in M \times SO(3)$ . The initial and final attitudes can be expressed as  $R^0 = [b_1^0, b_2^0, b_3^0]$  and  $R^f = [b_1^f, b_2^f, b_3^f]$ .

Without loss of generality, assume that  $x^f \neq x^0$  and  $R^f \neq R^0$ . Also, for simplicity, let  $t_i = iT$ ,  $i = 1, \dots, 10$ ,  $T > 0$ , denote the time instants switching is performed. We now describe a 10-Step solution of the maneuver problem. In Step 1, the sphere is rolled along the shortest path from  $(x^0, R^0)$  to  $(x^f, R^1)$ . In Step 2, a pre-slip maneuver is performed to roll the sphere from  $(x^f, R^1)$  to  $(x^2, R^2)$ , where  $b_3^2$  is aligned with the surface normal  $e_3$ . Slip maneuver is accomplished in Steps 3 and 4. As shown in Figure 5.2, the maneuver starts and ends at positions  $x^2$  and  $x^4$ , respectively, and  $x^3$  is an intermediate position that is equidistant to both  $x^2$  and  $x^4$ . To compute  $x^3$  and  $x^4$ , first define the auxiliary variables  $\omega^a$ ,  $\Omega^a$  and  $\chi^a$  as

$$\chi^a = \frac{S(b_3^f)e_3}{\|S(b_3^f)e_3\|}, \quad \omega^a = \frac{1}{T} \tan^{-1} \left( \frac{\|S(b_3^f)e_3\|}{b_3^f \cdot e_3} \right),$$

$$\Omega^a = \omega^a \begin{bmatrix} \chi^a \cdot e_1 \\ \chi^a \cdot e_2 \\ 0 \end{bmatrix},$$

and then compute

$$x^4 = x^f + r_s \omega^a T S(\chi^a) e_3, \quad R^a = e^{S(\Omega^a)T} R^f.$$

Choose the smallest integer value of  $l$  that satisfy

$$l > \frac{\|x^4 - x^2\|}{2\pi r_s} \quad (5.10)$$

and solve the following equations simultaneously for  $x^3$  using Symbolic Math Toolbox of Matlab :

$$\|x^3 - x^2\| - \|x^4 - x^3\| = 0, \quad (5.11)$$

$$\|x^3 - x^2\| = 2\pi r_s l. \quad (5.12)$$

In Steps 5-9, a twist maneuver is performed. As shown in Figure 5.3, the maneuver starts and ends at position  $x^4$  producing a twist of angle  $\Phi$  (about the surface normal

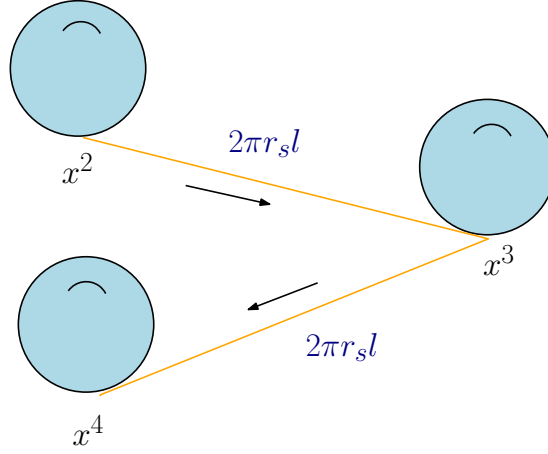


FIGURE 5.2: Slip maneuver; the position changes but the attitude remains the same.

at  $x^4$ ) given by

$$\Phi = \tan^{-1} \left( \frac{e_3 \cdot (S(b_2^4) b_2^a)}{b_2^4 \cdot b_2^a} \right).$$

Finally, Step 10 accomplishes the motion planning goal of reaching  $(x^f, R^f)$ .

**Remark:** Note that  $R^a = [b_1^a, b_2^a, b_3^a]$  can be determined by using Rodrigues' formula given by

$$e^{S(\Omega^a)T} = I + \frac{S(\Omega^a)}{\|\Omega^a\|} \sin(\|\Omega^a\| T) + \frac{S^2(\Omega^a)}{\|\Omega^a\|^2} (1 - \cos(\|\Omega^a\| T)).$$

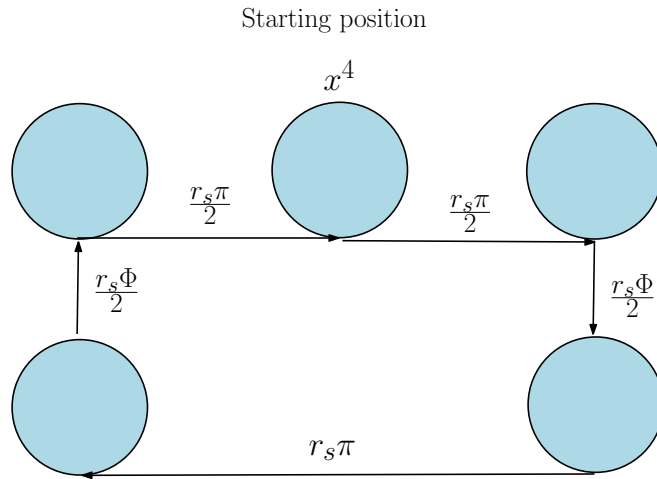


FIGURE 5.3: Twist maneuver; the attitude changes but the position remains the same.

We now describe the 10-Step motion planning algorithm for the flat surface case.

**Step 1:** Compute

$$\chi^1 = \frac{S(e_3)(x^f - x^0)}{\|x^f - x^0\|}, \quad \omega^1 = \frac{\|x^f - x^0\|}{Tr_s}$$

and then roll the sphere about  $\chi^1$  with the angular speed  $\omega^1$ . At the end of this step, the position and attitude of the sphere are  $x^f$  and  $R^1 = [b_1^1, b_2^1, b_3^1]$ , respectively.

**Step 2:** Compute

$$\chi^2 = \frac{S(b_3^1)e_3}{\|S(b_3^1)e_3\|}, \quad \omega^2 = \frac{1}{T} \tan^{-1} \left( \frac{\|S(b_3^1)e_3\|}{b_3^1 \cdot e_3} \right)$$

and then roll the sphere about  $\chi^2$  with the angular speed  $\omega^2$ . At the end of this step, the position and attitude of the sphere are  $x^2$  and  $R^2 = [b_1^2, b_2^2, b_3^2]$ , respectively, where  $b_3^2$  is aligned with the surface normal  $e_3$ .

**Step 3:** Compute

$$\chi^3 = \frac{S(e_3)(x^3 - x^2)}{\|x^3 - x^2\|}, \quad \omega^3 = \frac{\|x^3 - x^2\|}{Tr_s}$$

and then roll the sphere about  $\chi^3$  with angular speed  $\omega^3$ . At the end of this step, the position and attitude of the sphere are  $x^3$  and  $R^3 = [b_1^3, b_2^3, b_3^3]$ , respectively.

**Step 4:** Compute

$$\chi^4 = \frac{S(e_3)(x^4 - x^3)}{\|x^4 - x^3\|}, \quad \omega^4 = \frac{\|x^4 - x^3\|}{Tr_s}$$

and then roll the sphere about  $\chi^4$  with the angular speed  $\omega^4$ . At the end of this step, the position and attitude of the sphere are  $x^4$  and  $R^4 = [b_1^4, b_2^4, b_3^4]$ , respectively.

**Step 5:** Compute

$$\chi^5 = \sigma, \quad \omega^5 = \frac{\pi}{2T}$$

and then roll the sphere about  $\chi^5$  with the angular speed  $\omega^5$ . At the end of this step, the position and attitude of the sphere are  $x^5$  and  $R^5 = [b_1^5, b_2^5, b_3^5]$ , respectively.

**Step 6:** Compute

$$\chi^6 = \gamma, \quad \omega^6 = \frac{\Phi}{2T}$$

and then roll the sphere about  $\chi^6$  with the angular speed  $\omega^6$ . At the end of this step, the position and attitude of the sphere are  $x^5$  and  $R^6 = [b_1^6, b_2^6, b_3^6]$ , respectively.

**Step 7:** Compute

$$\chi^7 = -\sigma, \omega^7 = \frac{\pi}{T}$$

and then roll the sphere about  $\chi^7$  with the angular speed  $\omega^7$ . At the end of this step, the position and attitude of the sphere are  $x^7$  and  $R^7 = [b_1^7, b_2^7, b_3^7]$ , respectively.

**Step 8:** Compute

$$\chi^8 = -\gamma, \omega^8 = \frac{\Phi}{2T}$$

and then roll the sphere about  $\chi^8$  with the angular speed  $\omega^8$ . At the end of this step, the position and attitude of the sphere are  $x^8$  and  $R^8 = [b_1^8, b_2^8, b_3^8]$ , respectively.

**Step 9:** Compute

$$\chi^9 = \sigma, \omega^9 = \frac{\pi}{2T}$$

and then roll the sphere about  $\chi^9$  with the angular speed  $\omega^9$ . At the end of this step, the position and attitude of the sphere are  $x^9$ , where  $x^9 = x^4$ , and  $R^9 = [b_1^9, b_2^9, b_3^9]$ , respectively.

**Step 10:** Compute

$$\chi^{10} = \frac{S(e_3)b_3^f}{\|S(e_3)b_3^f\|}, \omega^{10} = \frac{1}{T} \tan^{-1} \left( \frac{\|S(e_3)b_3^f\|}{e_3 \cdot b_3^f} \right)$$

and then roll the sphere about  $\chi^{10}$  with the angular speed  $\omega^{10}$ . At the end of this step, the position and attitude of the sphere will be  $x^f$  and  $R^f = [b_1^f, b_2^f, b_3^f]$ , respectively, thereby accomplishing the motion planning goal.

### 5.3.2 An example controlled maneuver

We now illustrate the ideas developed in the previous section through computer simulations of a sphere of radius  $r_s = 2$  on a surface with  $T = 2$ . We implement the 10-step algorithm described in the previous section for the following initial and final conditions:

$$x^0 = (0, 0, 0), R^0 = \begin{bmatrix} 0 & 1/\sqrt{2} & 1/\sqrt{2} \\ 0 & 1/\sqrt{2} & -1/\sqrt{2} \\ -1 & 0 & 0 \end{bmatrix},$$

$$x^f = (5, 8, 0), \quad R^f = \begin{bmatrix} -1/\sqrt{2} & 0 & 1/\sqrt{2} \\ -1/\sqrt{2} & 0 & -1/\sqrt{2} \\ 0 & -1 & 0 \end{bmatrix}.$$

Figures 5.4-5.6 show the results of the simulation. Figure 5.4 shows the time response of position  $x$ . The time responses of  $\omega_1$  and  $\omega_2$  are shown in Figure 5.5. Figure 5.6 shows the path of the contact point of the rolling sphere on the flat surface.

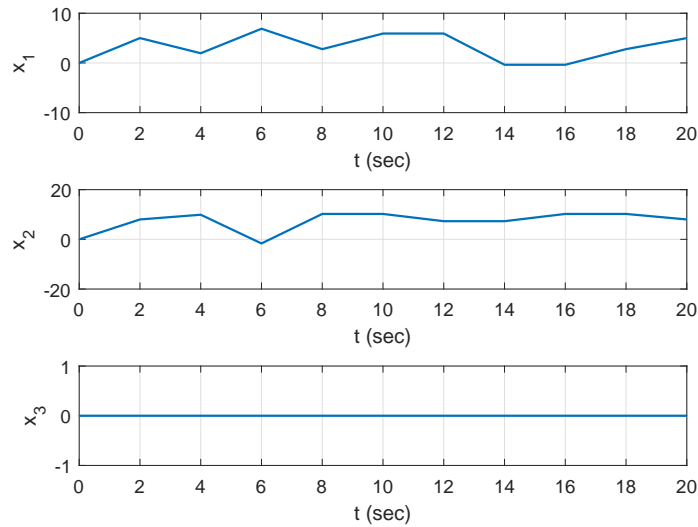


FIGURE 5.4: Position  $x$  (flat surface case).

## 5.4 Kinematics of a sphere rolling on a stationary sphere

Consider a sphere rolling on a stationary sphere of radius  $R_s$  defined as

$$M = \mathbb{S}_{R_s}^2 = \{x \in \mathbb{R}^3 : \|x\|^2 - R_s^2 = 0\}. \quad (5.13)$$

The surface normal is  $\nu = \frac{x}{R_s}$ , and thus  $N(x) = \frac{I_{3 \times 3}}{R_s}$ . The velocity of the rolling sphere lies in the tangent plane at  $x$ . As shown in Figure 5.7,  $\sigma, \gamma \in T_x M$  are two orthogonal basis vectors that span the tangent plane at  $x$ . The kinematics of the



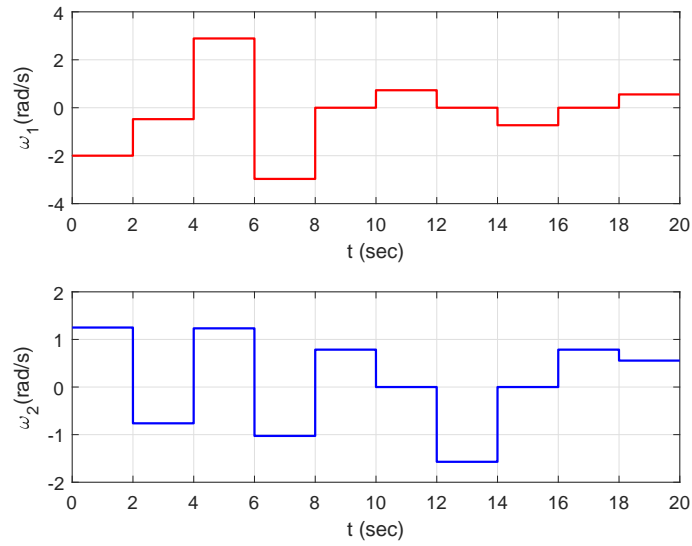


FIGURE 5.5: Controls  $\omega_1$  and  $\omega_2$  (flat surface case).

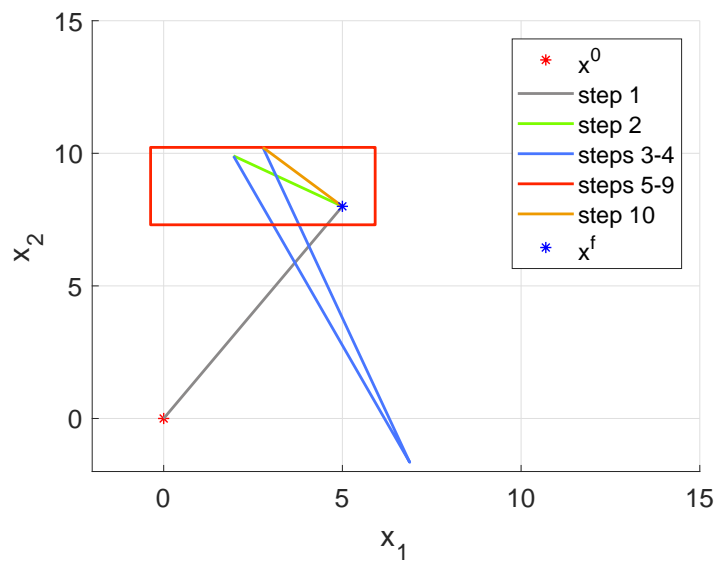


FIGURE 5.6: The path of the contact point of the rolling sphere (flat surface case).

sphere of radius  $r_s$  are obtained using (5.1)-(5.2) as

$$\dot{x} = r_s(\omega_2\gamma - \omega_1\sigma), \quad (5.14)$$

$$\dot{R} = S(\Omega)R, \quad (5.15)$$

$$\dot{\gamma} = -\frac{r_s}{R_s^2}\omega_2x, \quad (5.16)$$

$$\dot{\sigma} = \frac{r_s}{R_s^2}\omega_1x, \quad (5.17)$$

$$(5.18)$$

Thus, the configuration vector for the spherical surface case is  $q = (x, \gamma, \sigma, R) \in M \times (\mathbb{S}^2)^2 \times SO(3)$ . Here  $\Omega \in \mathbb{R}^3$  is the angular velocity of the rolling sphere, which is given in the inertial frame by

$$\Omega = \left(1 + \frac{r_s}{R_s}\right)\omega \begin{bmatrix} \chi \cdot e_1 \\ \chi \cdot e_2 \\ \chi \cdot e_3 \end{bmatrix}.$$

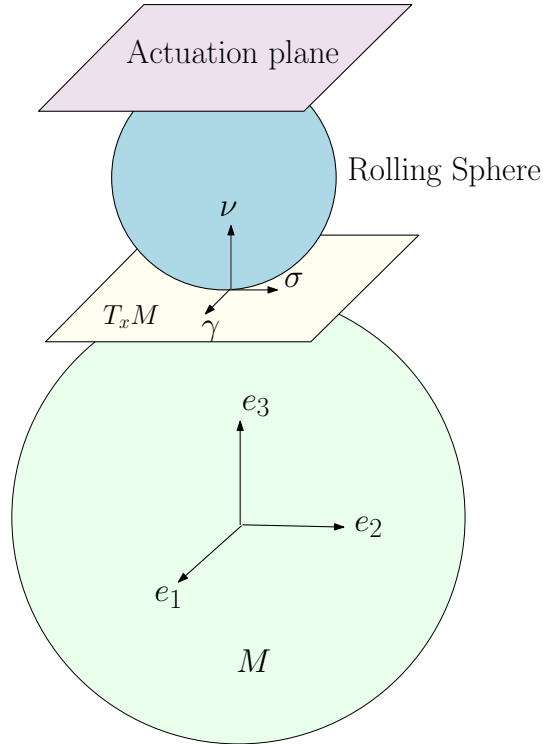


FIGURE 5.7: Sphere rolling on a stationary sphere.

### 5.4.1 Motion planning

Assume that the initial and final position and attitudes are given by  $(x^0, R^0)$  and  $(x^f, R^f)$ , respectively. A natural approach for solving the rolling sphere maneuver problem is to construct a path on  $M \times SO(3)$  that connects  $(x^0, R^0) \in M \times SO(3)$  and  $(x^f, R^f) \in M \times SO(3)$ . The initial and final attitudes can be expressed as  $R^0 = [b_1^0, b_2^0, b_3^0]$  and  $R^f = [b_1^f, b_2^f, b_3^f]$ . The initial values of  $\gamma$  and  $\sigma$  can be computed as

$$\sigma^0 = \frac{S(x^0)x^f}{\|S(x^0)x^f\|}, \quad \gamma^0 = S(\sigma^0)\nu^0,$$

Without loss of generality, assume that  $x^f \neq x^0$  and  $R^f \neq R^0$ . Also, for simplicity, let  $t_i = iT$ ,  $i = 1, \dots, 10$ ,  $T > 0$  denote the time instants switching is performed. We now describe a 10-Step solution of the maneuver problem. In Step 1, the sphere is rolled along the shortest path (geodesic) from  $(x^0, R^0)$  to  $(x^f, R^1)$ . In Step 2, a pre-slip maneuver is performed to roll the sphere from  $(x^f, R^1)$  to  $(x^2, R^2)$ , where  $b_3^2$  is aligned with the surface normal at  $x^2$ . Slip maneuver is accomplished in Steps 3 and 4. As shown in Figure 5.2, the maneuver starts and ends at positions  $x^2$  and  $x^4$ , respectively, and  $x^3$  is an intermediate position that is equidistant to both  $x^2$  and  $x^4$ . To compute  $x^3$  and  $x^4$ , first define the auxiliary variables  $\omega^a$ ,  $\Omega^a$  and  $\chi^a$  as

$$\chi^a = \frac{S(b_3^f)\nu^f}{\|S(b_3^f)\nu^f\|}, \quad \omega^a = \frac{1}{T} \tan^{-1} \left( \frac{\|S(b_3^f)\nu^f\|}{b_3^f \cdot \nu^f} \right),$$

$$\Omega^a = \left(1 + \frac{r_s}{R_s}\right) \omega^a \begin{bmatrix} \chi^a \cdot e_1 \\ \chi^a \cdot e_2 \\ \chi^a \cdot e_3 \end{bmatrix},$$

and then compute

$$x^4 = e^{S(\chi^a)\bar{V}^a T} x^f, \quad R^a = e^{S(\Omega^a)T} R^f,$$

where  $\bar{V}^a = \frac{r_s \omega^a}{R_s}$ . Choose the smallest integer value of  $l$  that satisfy

$$l > \frac{R_s}{2\pi r_s} \tan^{-1} \left( \frac{\|S(x_1)x_4\|}{x_1 \cdot x_4} \right) \quad (5.19)$$

and solve the following equations simultaneously for  $x^3$  using Symbolic Math Toolbox of Matlab:

$$\|x^3\| = R_s, \quad (5.20)$$

$$R_s \tan^{-1} \left( \frac{n^1 \cdot S(x^2)x^3}{x^2 \cdot x^3} \right) = 2\pi r_s l, \quad (5.21)$$

$$R_s \tan^{-1} \left( \frac{n^2 \cdot S(x^3)x^4}{x^3 \cdot x^4} \right) = 2\pi r_s l, \quad (5.22)$$

where

$$n^1 = \frac{S(x^2)x^3}{\|x^2 \cdot x^3\|}, \quad n^2 = \frac{S(x^3)x^4}{\|x^3 \cdot x^4\|}.$$

In Steps 5-9, a twist maneuver is performed. As shown in Figure 5.3, the maneuver starts and ends at position  $x^4$  producing a twist of angle  $\Phi$  (about the surface normal at  $x^4$ ) given by

$$\Phi = \tan^{-1} \left( \frac{\nu^4 \cdot (S(b_2^4)b_2^a)}{b_2^4 \cdot b_2^a} \right).$$

Finally, Step 10 accomplishes the motion planning goal of reaching  $(x^f, R^f)$ .

We now describe the 10-Step motion planning algorithm for the spherical surface case.

**Step 1:** Compute

$$\chi^1 = \sigma^0, \quad \omega^1 = \frac{R_s}{r_s T} \tan^{-1} \left( \frac{\|S(x^0)x^f\|}{x^0 \cdot x^f} \right)$$

and then roll the sphere about  $\chi^1$  with angular speed  $\omega^1$ . At the end of this step, the position and attitude of the sphere are  $x^f$  and  $R^1 = [b_1^1, b_2^1, b_3^1]$ , respectively.

**Step 2:** Compute

$$\chi^2 = \frac{S(b_3^1)\nu^f}{\|S(b_3^1)\nu^f\|}, \quad \omega^2 = \frac{1}{T} \tan^{-1} \left( \frac{\|S(b_3^1)\nu^f\|}{b_3^1 \cdot \nu^f} \right)$$

and then roll the sphere about  $\chi^2$  with angular speed  $\omega^2$ . At the end of this step, the position and attitude of the sphere are  $x^2$  and  $R^2 = [b_1^2, b_2^2, b_3^2]$ , respectively, where  $b_3^2$  is aligned with the surface normal at  $x^2$ .

**Step 3:** Compute

$$\chi^3 = \frac{S(x^2)x^3}{\|x^2 \cdot x^3\|}, \quad \omega_3 = \frac{R_s}{r_s T} \tan^{-1} \left( \frac{\|S(x^2)x^3\|}{x^2 \cdot x^3} \right)$$

and then roll the sphere about  $\chi^3$  with angular speed  $\omega^3$ . At the end of this step, the position and attitude of the sphere are  $x^3$  and  $R^3 = [b_1^3, b_2^3, b_3^3]$ , respectively.

**Step 4:** Compute

$$\chi^4 = \frac{S(x^3)x^4}{\|x^3 \cdot x^4\|}, \quad \omega_4 = \frac{R_s}{r_s T} \tan^{-1} \left( \frac{\|S(x^3)x^4\|}{x^3 \cdot x^4} \right).$$

and then roll the sphere about  $\chi^4$  with angular speed  $\omega^4$ . At the end of this step, the position and attitude of the sphere are  $x^4$  and  $R^4 = [b_1^4, b_2^4, b_3^4]$ , respectively.

**Step 5:** Compute

$$\chi^5 = \sigma, \quad \omega^5 = \frac{\pi}{2T}$$

and then roll the sphere about  $\chi^5$  with angular speed  $\omega^5$ . At the end of this step, the position and attitude of the sphere are  $x^5$  and  $R^5 = [b_1^5, b_2^5, b_3^5]$ , respectively.

**Step 6:** Compute

$$\chi^6 = \gamma, \quad \omega^6 = \frac{\Phi}{2T}$$

and then roll the sphere about  $\chi^6$  with angular speed  $\omega^6$ . At the end of this step, the position and attitude of the sphere are  $x^6$  and  $R^6 = [b_1^6, b_2^6, b_3^6]$ , respectively.

**Step 7:** Compute

$$\chi^7 = -\sigma, \quad \omega^7 = \frac{\pi}{T}$$

and then roll the sphere about  $\chi^7$  with angular speed  $\omega^7$ . At the end of this step, the position and attitude of the sphere are  $x^7$  and  $R^7 = [b_1^7, b_2^7, b_3^7]$ , respectively.

**Step 8:** Compute

$$\chi^8 = -\gamma, \quad \omega^8 = \frac{\Phi}{2T}$$

and then roll the sphere about  $\chi^8$  with angular speed  $\omega^8$ . At the end of this step, the position and attitude of the sphere are  $x^8$  and  $R^8 = [b_1^8, b_2^8, b_3^8]$ , respectively.

**Step 9:** Compute

$$\chi^9 = \sigma, \quad \omega^9 = \frac{\pi}{2T}$$

and then roll the sphere about  $\chi^9$  with angular speed  $\omega^9$ . At the end of this step, the position and attitude of the sphere are  $x^9$  and  $R^9 = [b_1^9, b_2^9, b_3^9]$ , respectively.

**Step 10:** Compute

$$\chi^{10} = \frac{S(\nu^f)b_3^f}{\|S(\nu^f)b_3^f\|}, \quad \omega^{10} = \frac{1}{T} \tan^{-1} \left( \frac{\|S(\nu^f)b_3^f\|}{\nu^f \cdot b_3^f} \right)$$

and then roll the sphere about  $\chi^{10}$  with angular speed  $\omega^{10}$ . At the end of this step, the position and attitude of the sphere are  $x^f$  and  $R^f = [b_1^f, b_2^f, b_3^f]$ , respectively, thereby accomplishing the motion planning goal.

### 5.4.2 An example controlled maneuver

We now illustrate the ideas developed in the previous section through computer simulations of a sphere of radius  $r_s = 2$  rolling on a stationary sphere of radius  $R_s = 10$ . We implement the 10-step algorithm described in the previous section with  $T = 2$  for the following initial and final conditions:

$$x^0 = (10, 0, 0), \quad R^0 = \begin{bmatrix} 1/\sqrt{2} & 1/\sqrt{2} & 0 \\ -1/\sqrt{2} & 1/\sqrt{2} & 0 \\ 0 & 0 & 1 \end{bmatrix},$$

$$x^f = (10, 10, 10)/\sqrt{3}, \quad R^f = \begin{bmatrix} 1 & 0 & 0 \\ 0 & 1 & 0 \\ 0 & 0 & 1 \end{bmatrix}.$$

Figures 5.8-5.11 show the results of the simulation. Figures 5.8 and 5.9 show the time responses of position  $x$  and basis vectors  $(\gamma, \sigma)$ , respectively. The time responses of  $\omega_1$  and  $\omega_2$  are shown in Figure 5.10. Figure 5.11 shows the path of the contact point of the rolling sphere on the spherical surface.

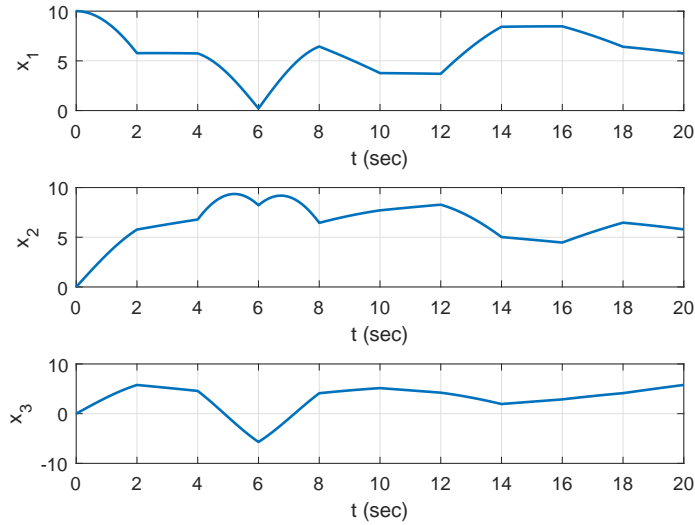


FIGURE 5.8: Position  $x$  (spherical surface case).

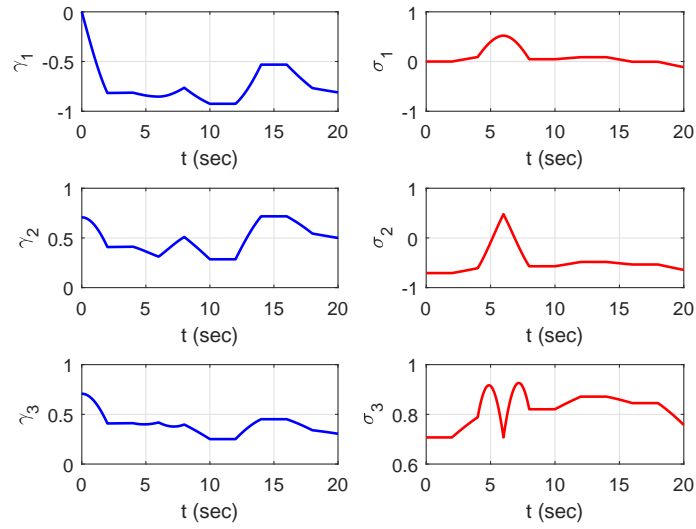


FIGURE 5.9: Basis vectors of the actuation plane (spherical surface case).

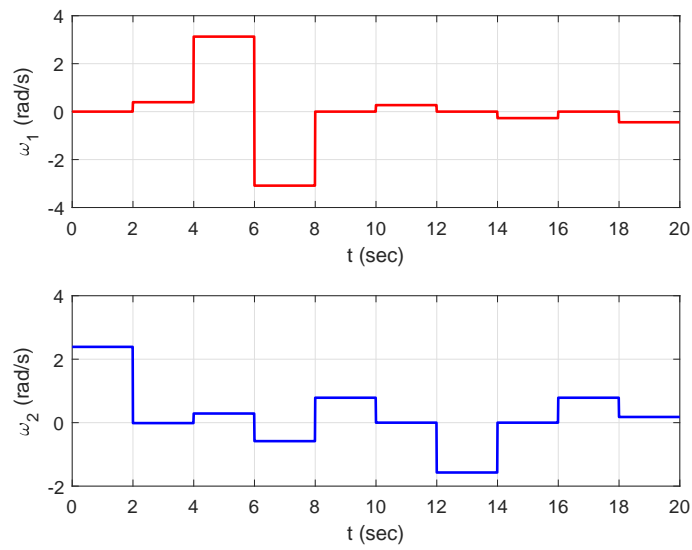


FIGURE 5.10: Controls  $\omega_1$  and  $\omega_2$  (spherical surface case).

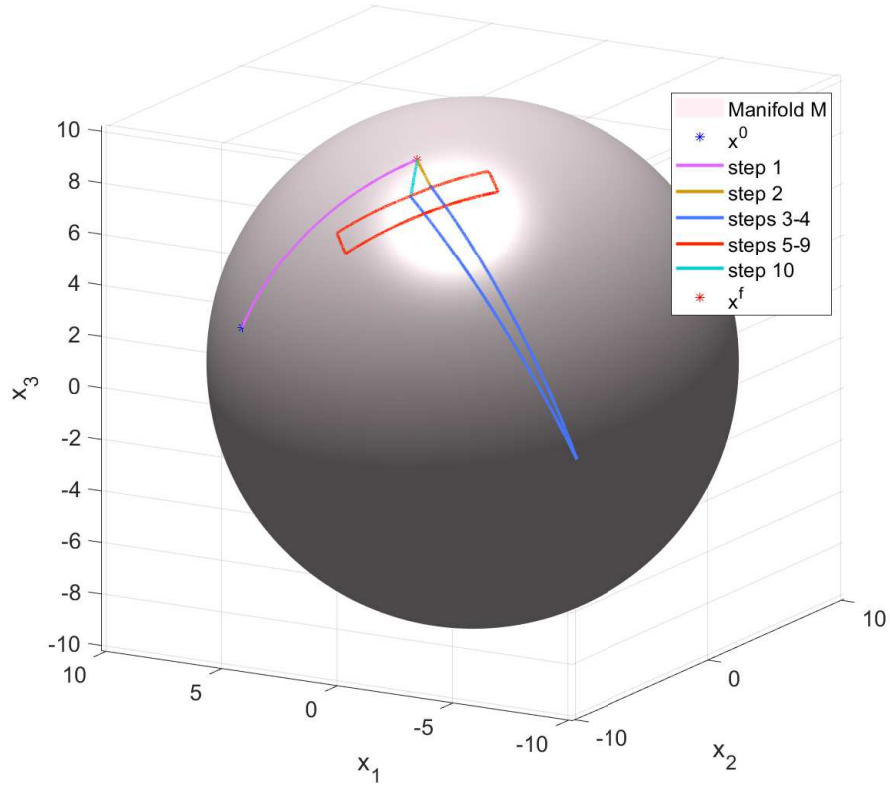


FIGURE 5.11: The path of the contact point of the rolling sphere (spherical surface case).

## 5.5 Conclusion and future work

The motion of a sphere rolling on an arbitrary smooth surface has been studied. The results are based on new formulations of the kinematics equations that are globally defined on the surface. A motion planning algorithm is proposed for two different surfaces: flat surface and spherical surface. The geometries of the flat surface and the sphere allow development of analytical expressions for the rolling sphere in the proposed maneuvers. The motion planning algorithm can be extended to more complex geometric surfaces such as surfaces of torus, hyperboloid, and cone. The ideas presented in this chapter can also be extended to the trajectory tracking control of a sphere rolling on an arbitrary smooth surface.

The focus in this chapter has been on the rolling sphere kinematics. It is possible to formulate the rolling sphere dynamics, using methods of dynamic extension, and to develop associated control results for such nonholonomic dynamics. In other words, the development in Lee et al (2017) can be utilized to obtain a globally defined



---

geometric formulation of rolling sphere dynamics, and develop motion planning results following the methods used in this chapter.

# Bibliography

- A. Astolfi (1996). Discontinuous Control of Nonholonomic Systems, *Systems and Control Letters*, Vol. 27, pp. 37-45.
- A. M. Bloch. (2003). Nonholonomic Mechanics and Control *Springer*.
- A. M. Bloch, M. Reyhanoglu and N. H. McClamroch (1992). Control and Stabilization of Nonholonomic Dynamic Systems *IEEE Transactions on Automatic Control*, Vol. 37, No. 11, pp. 1746-1757.
- A. M. Bloch, M. Reyhanoglu and N. H. McClamroch (1991). Control and Stabilization of Čaplygin Nonholonomic Dynamic Systems, *Proceedings of IEEE Conference on Decision and Control*, pp. 1127-1132.
- A. Bicchi, D. Prattichizzo, and S. S. Sastry (1995). The Nonholonomy of the Rolling Sphere, *Proceedings of IEEE Conference on Decision and Control*, pp. 2812-2817.
- A. V. Borisov, I. S. Mamaev, and A. A. Kilin (2002). The Rolling Motion of a Ball on a Surface. New Integrals and Hierarchy of Dynamics, *Regular and Chaotic Dynamics*, Vol. 7, pp. 201-218.
- A. V. Borisov, A. A. Kilin, and I. S. Mamaev (2012). How To Control Chaplygin's Sphere Using Rotors, *Regular and Chaotic Dynamics*, Vol. 13, pp. 144-158.
- C. Camicia, F. Conticelli, and A. Bicchi (2000). Nonholonomic Kinematics and Dynamics of the Sphericle, *Proceedings of the IEEE/RSJ International Conference on Intelligent Robots and Systems*, pp. 805-810.
- J. Cheng, B. Wang, Y. Zhang, and Z. Wang (2017). Backward Orientation Tracking Control of Mobile Robot with N Trailers, *International Journal of Control, Automation and Systems*, Vol. 15, No. 2, pp. 867-874.
- J.-M. Coron (1995). On the Stabilization in Finite Time of Locally Controllable Systems by Means of Continuous Time-varying Feedback Law, *SIAM Journal on Control and Optimization*, Vol. 33, pp. 804-833.

- Ebrahimi, Arezoo (2015). Design, Manufacturing and Control of an Advanced High-Precision Robotic System for Microsurgery *Electronic Thesis and Dissertations*, 2378.
- N. E. Leonard and P. S. Krishnaprasad (1995). Motion Control of Drift-Free, Left-Invariant Systems on Lie Groups, *IEEE Transactions on Automatic Control*, Vol. 40, No. 9, pp. 1539-1554.
- D. Hilbert and S. Cohn-Vossen (1999). Geometry and the Imagination. New York, *Chelsea House Pub.*.
- M. Ishikawa and A. Astolfi (2008). Finite-time Control of Cross-chained Nonholonomic Systems by Switched State Feedback, *Proceedings of IEEE Conference on Decision and Control*, pp. 304-309.
- M. Ito (2015). Holonomy-based Motion Planning of a Second-order Chained Form System by Using Sinusoidal Functions, *Proceedings of International Workshop on Robot Motion and Control*, , pp. 283-287.
- Z.P. Jiang and H. Nijmeijer (1999). A Recursive Technique for Tracking Control of Nonholonomic Systems in Chained Form, *IEEE Transactions on Automatic Control*, Vol. 44, No. 2, pp. 265-279.
- I. Kolmanovsky and N. H. McClamroch (1995). Developments in Nonholonomic Control Problems, *Control Systems Magazine*, Vol. 15, pp. 20-36.
- B. D. Johnson (2007). The Nonholonomy of the Rolling Sphere, *American Mathematical Monthly*, Vol. 114, No. 6, pp. 500-508, 2007.
- V. Jurdjevic (1993). The Geometry of the Plate-Ball Problem, *Archive for Rational Mechanics and Analysis*, Vol. 124, No. 4, pp. 305-328.
- M. Kleinstaubert, K. Huper, and F. Silva Leite (2006). Complete Controllability of the Rolling n-Sphere - A Constructive Proof, *Department of Mathematics, University of Coimbra, Portugal*.
- T. Lee, M. Leok, and N. H. McClamroch (2017). Global Formulations of Lagrangian and Hamiltonian Dynamics on Manifolds: A Geometric Approach to Modeling and Analysis, *Springer*.
- T. Lee, M. Leok, and N. H. McClamroch (2009). Lagrangian Mechanics and Variational Integrators on Two-Spheres, *International Journal for Numerical Methods in Engineering*, Vol. 79, No. 9, pp. 1147-1174.
- Z. Li and J. Canny (1990). Motion of Two Rigid Bodies with Rolling Constraints, *IEEE Transactions on Automatic Control*, Vol. 6, No. 1, pp. 62-72.

- Z. Li and J. Canny (1999). Stabilization and Control of the Motion of a Rolling Disk, *Mathematical and Computer Modelling*, 29 45-54.
- C. Liu, J. Gao, and D. Xu (2017). Lyapunov-based Model Predictive Control for Tracking of Nonholonomic Mobile Robots under Input Constraints, *International Journal of Control, Automation and Systems*, Vol. 15, No. 5, pp. 2313-2319.
- A. Marigo and A. Bicchi (2000). Rolling Bodies with Regular Surface: Controllability Theory and Applications, *IEEE Transactions on Automatic Control*, Vol. 45, No. 9, pp. 1586-1599..
- N. H. McClamroch, M. Reyhanoglu, and M. Rehan (2017). Knife-Edge Motion on a Surface as a Nonholonomic Control Problem, *IEEE Control Systems Letters*, Vol. 1, No. 1, pp. 26-31.
- M. Minor, and J. Pukrushpan (2002). Motion Planning for a Spherical Mobile Robot: Revisiting the Classical Ball-Plate Problem, *ASME Journal of Dynamic Systems, Measurement, and Control*, Vol. 124, No. 4, pp. 502-511.
- P. Morin and C. Samson (2003). Practical Stabilization of Driftless Systems on Lie Groups: the Transverse Function Approach, *IEEE Transactions on Automatic Control*, Vol. 48, No. 9, pp. 1496-1508.
- P. Morin and C. Samson (2008). Stabilization of Trajectories for Systems on Lie Groups, *Proceedings of the 17th IFAC World Congress*, pp. 508-513.
- V. Muralidharan and A. Mahindrakar(2015). Geometric Controllability and Stabilization of Spherical Robot Dynamics, *IEEE Transactions on Automatic Control*, Vol. 60, No. 10, pp. 2762-2767 .
- R. M. Murray and S. S. Sastry (1993). Nonholonomic motion planning: Steering using sinusoids, *IEEE Transactions on Automatic Control*, vol. 38, No. 5, pp. 700-716.
- R. M. Murray, Z. Li, and S. S. Sastry (1994). Control and Stabilization of Čaplygin Nonholonomic Dynamic Systems, *A Mathematical Introduction to Robotic Manipulation*, CRC Press.
- Ju. I. Neimark and F. A. Fufaev (1972). Dynamics of Nonholonomic Systems, *A.M.S. Translations of Mathematical Monographs*, Providence, RI: AMS.
- P. Morin and C. Samson (2008). Stabilization of Trajectories for Systems on Lie Groups. Application to the Rolling Sphere, *IFAC Proceedings*, pp. 508-513.
- J. M. Osborne and D. V. Zenkov (2005). DSteering the Chaplygin Sleigh by a Moving Mass, *Proceedings of IEEE Conference on Decision and Control*, pp.1114-1118.

- T. Petrinic, M. Brezak, and I. Petrovic (2017). Time-optimal Velocity Planning Along Predefined Path for Static Formations of Mobile Robots, *International Journal of Control, Automation and Systems*, Vol. 15, No. 1, pp. 293-302.
- M. Rehan, M. Reyhanoglu, and N. Harris McClamroch (2007). Motion Planning for a Knife-Edge on the Surface of a Hyperboloid, *Proceedings of Asian Control Conference*, pp. 1326-1330.
- M. Reyhanoglu (1994). A General Nonholonomic Motion Planning Strategy for Čaplygin Systems, *Proceedings of IEEE Conference on Decision and Control*, pp. 2964-2966.
- S. Salinic, A. Obradovic, and Z. Mirovic (2013). On the Brachistochronic Motion of the Chaplygin Sleigh, *Acta Mechanica*, Vol. 224, pp. 2127-2141.
- J. Shen, D. A. Schneider, and A. M. Bloch (2008). Controllability and Motion Planning of Multibody Chaplygin's Sphere and Chaplygin's Top, *International Journal on Robust and Nonlinear Control*, Vol. 18, pp. 905-945.
- O.J. Sordalen and O. Egeland (1995). Exponential Stabilization of Nonholonomic Chained Systems, *IEEE Transactions on Automatic Control*, Vol. 40, No. 1, pp. 35-49.
- H.J. Sussmann (1987). A General Theorem on Local Controllability, *SIAM Journal on Control and Optimization*, Vol. 25, No. 1, pp. 158-194.
- H.J. Sussmann (1979). Subanalytic Sets and Feedback Control, *J. Differential Equations*, Vol. 31, pp. 31-52.
- M. Svinin and S. Hosoe (2008). Motion Planning Algorithms for a Rolling Sphere with Limited Contact Area, *IEEE Transactions on Robotics*, Vol. 24, No. 3, pp. 612-625.
- Y. Yavin (1999). Stabilization and Control of the Motion of a Rolling Disk, *Mathematical and Computer Modelling*, Vol. 29, pp. 45-54.
- B. J. Young, J. R. Lawton, and R. W. Beard (2000). Two Hybrid Control Schemes for Nonholonomic Robots, *Proceedings of IEEE International Conference on Robotics and Automation*, pp. 1824-1829.
- Y. Zhao, C. Wang, and J. Yu (2018). Partial-state Feedback Stabilization for a Class of Generalized Nonholonomic Systems with ISS Dynamic Uncertainties, *International Journal of Control, Automation and Systems*, Vol. 16, No. 1, pp. 79-86.
- M. Zheng, Q. Zhan, J. Liu, and Y. Cai (2011). Control of a Spherical Robot: Path Following Based on Nonholonomic Kinematics and Dynamics, *Chinese Journal of Aeronautics*, Vol. 24, pp. 337-345..